Origin, structure and evolution of submarine canyons on central and southern continental slopes of Okinawa Trough and its potential genetic mechanism related to methane seepage

Deyong Li[1], Jie Liang[2], Honggang Cheng[3], Gang Dong[2], Xiting Liu[4], Shujuan Xu[3], Chaoyang Li[5], and Xiaodian Jiang[1]

[1]Ocean University of China
[2]Qingdao Institute of Marine Geology
[3]Research Institute of Petroleum Exploration & Development
[4]College of Marine Geosciences, Ocean University of China
[5]Shandong University of Science and Technology

November 23, 2022

Abstract

Submarine canyons are of great significance to understand the transport mechanism of terrigenous clastic materials to deep sea and the deep-sea sedimentary dynamic process. In this study, the spatiotemporal framework of stratigraphic sequence in the central and southern slopes of the Okinawa Trough was established, and the geomorphological and erosional-depositional features of submarine canyons were analyzed detailedly. The submarine canyons on the continental slope of Okinawa Trough began to develop in the early Pleistocene (< 1.8 Ma), and continued to develop even today. The canyons could be divided into three parts along the axial direction: head, upstream, and downstream. The head of the canyon was mostly inherited from the ancient incised valley developed on the outer continental shelf during the last glacial maximum (LGM). The canyon channel was filled with multi-stage turbidites and mass transport deposits (MTDs). The seismogeologic characteristics, such as the MTDs associated with the bottom simulating reflectors (BSRs), the imbricated, twisty or chaotic seismic reflections, the liquefaction deformation structures, the fluid transport channels, and the gaps that indicate methane escaping on the side walls, and the truncated relationship between the BSRs and the submarine canyons all indicate that there is a complex relationship between the submarine canyons and the methane seepage associated with gas hydrate in the Okinawa Trough. Finally, a coupled model with four evolutional stages for the submarine canyons was established.

Origin, structure and evolution of submarine canyons on central and southern continental slopes of Okinawa Trough and its potential genetic mechanism related to methane seepage

Deyong Li[1], Jie Liang[2],Honggang Cheng[3], Gang Dong[2],Xiting Liu[1], Shujuan Xu[3], Chaoyang Li[4], Xiaodian Jiang[1]

[1]Key Laboratory of Submarine Geosciences and Prospecting Techniques, MOE, Laboratory for Marine Mineral Resources, Qingdao National Laboratory for Marine Science and Technology, College of Marine Geosciences, Ocean University of China, Qingdao 266100, China.

[2]Key laboratory of Marine Hydrocarbon Resources and Environment Geology, Ministry of Natural Resources, Laboratory for Marine Mineral Resources, Qingdao National Laboratory for Marine Science and Technology, Qingdao Institute of Marine Geology, Qingdao 266071, China.

[3]Research Institute of Petroleum Exploration & Development, Beijing 100083, China.

[4]College of Earth Science and Enginering, Shandong University of Science and Technology, Qingdao, Shandong 266590, China.

Corresponding author: Deyong Li (*ldyc411@ouc.edu.cn)* , Jie Liang (*cgsljie@mail.cgs.gov.cn*)

Key Points:

- The submarine canyons on the continental slope of Okinawa Trough began to develop in the early Pleistocene (< 1.8 Ma), and continued to develop even today.
- The canyons are mainly related to the gravity flow, syngenetic fault, sea-level eustacy, and methane seepage associated with hydrate dynamic accumulation.
- A coupled model with four evolutional stages for submarine canyons associated with methane seepage related to gas hydrate dynamic accumulation was established..

Abstract

Submarine canyons are of great significance to understand the transport mechanism of terrigenous clastic materials to deep sea and the deep-sea sedimentary dynamic process. In this study, the spatiotemporal framework of stratigraphic sequence in the central and southern slopes of the Okinawa Trough was established, and the geomorphological and erosional-depositional features of submarine canyons were analyzed detailedly. The submarine canyons on the continental slope of Okinawa Trough began to develop in the early Pleistocene (< 1.8 Ma), and continued to develop even today. The canyons could be divided into three parts along the axial direction: head, upstream, and downstream. The head of the canyon was mostly inherited from the ancient incised valley developed on the outer continental shelf during the last glacial maximum (LGM). The canyon channel was filled with multi-stage turbidites and mass transport deposits (MTDs). The seismogeologic characteristics, such as the MTDs associated with the bottom simulating reflectors (BSRs), the imbricated, twisty or chaotic seismic reflections, the liquefaction deformation structures, the fluid transport channels, and the gaps that indicate methane escaping on the side walls, and the truncated relationship between the BSRs and the submarine canyons all indicate that there is a complex relationship between the submarine canyons and the methane seepage associated with gas hydrate in the Okinawa Trough. Finally, a coupled model with four evolutional stages for the submarine canyons was established.

1 Introduction

Submarine canyons are an important transport channel for sediments from source to sink (de Stigter et al., 2011; Xu, 2013; Xu et al., 2014; Su et al., 2014; Tubau, et al., 2015; Bozzano et al., 2020; Liu et al., 2020), which control the transport and accumulation of terrigenous clastic material from land to deep sea (Shepard, 1981; Wu & Sakamoto, 2001; Harris & Whiteway, 2011). As an important part of deep-water sedimentary system, the formation and evolution of submarine canyons also record crucial geological information about the regional sea-level eustacy, climate change, and tectonic activities (Wang et al., 2011, 2015a; Xie et al., 2012; Voigt et al., 2013; Gao & Collins, 2014; Han et al., 2017). Meanwhile, due to the vibrant hydrodynamic conditions of turbidity currents, submarine canyons have become an important carrier and potential inducer of submarine landslide hazard (Webster et al., 2012; He et al., 2014; Sun et al., 2018; Nazarian et al., 2021).

The formation of submarine canyon often undergoes a long evolutionary process and influenced by many factors (Han et al., 2010; Gong et al., 2011; Su et al., 2014), such as tectonic activity (earthquake, volcanism, fault, and diapir; Wu & Sakamoto, 2001; Chiang & Yu, 2006; Yu & Hong, 2006; Ding et al., 2013; Yang & Van Loon, 2016; Han et al., 2017), climate change (sea-level eustacy, typhoon, and sediment supply; Huh et al., 2009; Ding et al., 2013; Xu, 2013; Tubau et al., 2015), and deep-sea sedimentary process (gravity flow and contour current; Xie et al., 2008; Han et al., 2010; Xu, 2013). Tectonic dynamic shapes the topography of continental margins from shelf to slope, and provides favorable topographic conditions for the development of submarine canyons (Normandeau et al., 2015). Especially, the faults break the bedrock and induce gravity flow to preferentially erode the fractured zone, which ultimately affects the canyon path (Chiang & Yu, 2006; Xu et al., 2014). Although accidental earthquakes and volcanic activities cannot exert continuous influence on submarine canyons, they provide abundant pyroclastic sources for gravity flow and are one of the main factors that induce mass flow and turbidity erosion in the canyon (Wu & Sakamoto, 2001; de Stigter et al., 2011). The erosion of mass-flow or turbidity current on shelf and slope are considered as the most important mechanisms for the formation and evolution of submarine canyons (Xu, & Noble, 2009; Harris & Whiteway, 2011; Xu et al., 2013; Lo Iacono et al., 2014; Su et al., 2014). Additionally, the numerical simulation also proves that the headward erosion of gravity flow plays a key role in the formation of submarine canyons (Harris & Whiteway, 2011; Xu, 2013; Lo Iacono et al., 2014). Notably, the global sea-level fall caused by the Quaternary glacial cycle is of great significance to the development of submarine canyons (Harris & Whiteway, 2011; Gong et al., 2011; Su et al., 2014; Xu et al., 2014; Tubau et al., 2015). For example, along with the ancient sea level dropped to the current water depth of 120–150 m during the LGM (Lambeck & Chappell, 2001; Li et al., 2014), the East China Sea continental shelf was exposed and eroded extensively, and subsequently, terrestrial rivers extended and carried a large amount of sediment directly to the shelf edge (Li et al., 2004, 2014). The rapid supply of sediment induced mass instability and formed an erosive turbidity flow downward along the continental slope, which caused canyon downcutting (Gao & Collins, 2014; Lo Iacono et al., 2014; Li et al., 2014; Xu et al., 2014; Yin et al., 2015). However, for the slope rich in gas hydrates, it is more important that the changes of temperature and pressure caused by sea-level fall will induce the large-scale decomposition of hydrates (Song et al., 2003; Wu et al., 2009; Nakajima et al., 2014). And the subsequent escape and leakage of methane-bearing fluid to the seabed can trigger slope instability and induce turbidity currents, which promotes the formation of submarine canyons, even leading to large-scale submarine landslides (Wu et al., 2011; Nakajima et al., 2014; Li et al., 2016). Some researchers believe that methane fluid leakage is the main cause of the formation of blind canyons (Orange & Breen, 1992).

Submarine canyons and methane seepages associated with gas hydrates are the most important geological features of the Okinawa Trough (Luan & Qin, 2005; Liu et al., 2005; Li, 2008). The submarine canyons are mainly developed on the central and southern continental slopes of the Okinawa Trough, all of which are shelf-incising canyons (whose heads are not connected to a terrestrial river) or slope-confined canyons (blind or headless canyons) (Li, 2008; Zhao et al., 2011; Wu et al., 2014). Liu et al. (2005), Li (2008), and Zhao et al. (2011) believed that faults are the dominant factor that control the formation and distribution of submarine canyons on the continental slope of the Okinawa Trough, which explains the genesis of submarine canyons associated with fault. However, the submarine canyons unrelated to faults and the discovery of gravity flow deposition inside the canyons show that the role of gravity flow in the formation and evolution of submarine canyons cannot be ignored (Li et al., 2001; Liu et al., 2005; Zhao et al., 2009; Li et al., 2019). Many geological and geophysical indicators for methane-bearing fluid seepage related to gas hydrate in the Okinawa Trough have been reported, such as methane leakage and associated cold seep carbonate (Luan & Qin, 2005; Sun et al., 2015; Li et al., 2018a; Guan et al., 2019; Wang et al., 2019; Zhang et al., 2020; Cao et al., 2020; Li et al. 2021a, 2021b), mud diapir and volcano (Zhao et al., 2006; Xu et al., 2009), methane anomaly in pore water, water column and even sediments (Lu et al., 2003; Li, 2008; Wang et al., 2015b; Li et al. 2015; Xu et al., 2018, 2020; Zhang et al., 2020), and bottom simulating reflectors (BSRs; Luan et al., 2008; Xu et al., 2009, 2012; Chen, 2014; Li et al., 2019). Notably, some methane seep sites and associated cold seep carbonates had been successfully discovered on the northern slope of the Okinawa Trough using remotely operated underwater vehicle (ROV; Wang et al., 2019; Cao et al., 2020; Zhang et al., 2020; Li et al., 2021a). The extremely negative carbon isotopic and positive oxygen isotopic compositions of the cold seep carbonates suggest that the carbon in the carbonates was mainly derived from biogenic methane coupled with sulfate-dependent anaerobic oxidation of methane and the fluid flow from which carbonate precipitated is sourced from dissociation of gas hydrates (Wang et al., 2019; Cao et al., 2020). Cao et al. (2020) proposed that during sea level fall in the late Pleistocene (22.8–55.7 ka BP), gas hydrate decomposed and released extensive methane, resulting in the precipitation of cold seep carbonate. Nakajima et al. (2014) linked the origin of the Joetsu Knoll submarine canyon in the Sea of Japan to the pockmark formed by the decomposition of gas hydrates during the LGM and believed that the submarine canyon formation is the result of turbidity erosion caused by the overflow of methane-bearing sand or mud fluid during the formation of the pockmark. For the submarine canyons developed on the continent slope of the Okinawa Trough, which are far from the estuary of continental rivers, when and why they started to form will be the focus of this paper. Furthermore, whether the formation and evolution of submarine canyons are related to the methane-bearing fluid activity associated with gas hydrate, is also an issue that we attempt to clarify. However, so far, the lack of observation data and drilling sample are still the biggest obstacle to understand this scientific problem.

In this paper, we have carried out a detailed study of seismic stratigraphy, geomorphology, and seismosedimentology using reflection seismic profiles, well logging, and topographic data. The sequence stratigraphic framework in the continental slope of the Okinawa Trough was established, and consequently, the startup times of the submarine canyons was determined. Through the analysis of seismosedimentological characteristics and controlling factors of submarine canyons on the continental slope of the Okinawa Trough, we boldly gave a new and potential genetic model of submarine canyons related to gas hydrate dynamic accumulation due to the Quaternary glacial-interglacial cycle. Our work is not only useful for understanding the genetic mechanism of submarine canyons, but also of great significance to the prediction and exploitation of gas hydrate in the future.

2 Geological setting

The Okinawa Trough is located to the east of the continental shelf of East China Sea and in the west of the Ryukyu Island Arc. It connects with Yilan County of Taiwan in the southwest and Kyushu Islands of Japan in the northeast. The Okinawa Trough and East China Sea Shelf Basin (ECSSB) are separated by the Diaoyu Islands uplift-fold belt. The Okinawa Trough is an important part of the trench–arc–basin system in the western Pacific active continental margin and is still an active back-arc extensional basin (Figure 1). Separated by the NW-trending Tokara and Miyako faults, the trough is divided into three segments: northern, central, and southern parts, which show the "wide", "hot", and "deep" features, respectively (Hao et al., 2004; Luan & Qin, 2005; Xu et al., 2012; Wu et al., 2014). The northern section of the Okinawa Trough is NNE-trending, with a width of 230 km and water depth of 200–1000 m (Wu et al., 2014), and filled with thick Miocene–Quaternary strata (Li et al., 2004, 2019). The central section is NE-trending, with a water depth of 1000–2000 m (Wu et al., 2014), and is characterized by high heat flow, high geothermal gradient, and strong hydrothermal and earthquake activities (Luan et al., 2008; Xu et al., 2012). Its average heat flow is 590 mW/m^2 (Xu et al., 2009, 2012). The southern section is NEE–EW-trending, with the deepest water depth over 2000 m (Wu et al., 2014), and has the highest degree of crust extension, with crust thickness of only 15 km in the Yaeyama Graben (Hao et al., 2004; Zhang & Shang, 2014). Submarine magnetic anomaly belts and polarity events, such as the Brunhes, Jaramillo, and Olduvai polarity reversals, indicate that the southern trough has entered the stage of sea-floor spreading and oceanic crust forming (Zhang & Shang, 2014).

For the East China Sea Shelf Basin with abundant hydrocarbon resources, petroleum geologists had determined the stratigraphic sequence of the basin (formations of Yueguifeng, Lingfeng, Mingyuefeng, Oujiang, Wenzhou, Pinghu, Huagang, Longjing, Yuquan, Liulang, Santan, and Donghai; Figure 2; Zhang et al., 2014; Zhang & Zhang, 2015; Liu et al., 2020) and defined the corresponding seismic reflection interfaces (T_0, T_{10}, T_{12}, T_{16}, T_{20}, T_{30}, T_{40}, T_{50}, T_{80}, T_{85}, T_{90}, and T_{100}; Figure 2) among which T_0, T_{12}, T_{20}, T_{30}, T_{80}, T_{85}, and T_{100} were all regional unconformities (Zhang et al., 2014; Zhang & Zhang, 2015; Liu et al., 2020), comprehensively using seismic and well data. This provided an important basis for stratigraphic tracking in the continental slope of the Okinawa Trough (Li et al., 2019). Li et al. (2004) and Li (2008) identified two regional unconformities (equivalent to the Quaternary bottom boundary (T_0) and the Pliocene bottom boundary (T_{10}) in the East China Sea Shelf, respectively) and divided five seismic sequences (Ua, Ub, Uc, Ud, and Ue) in the Okinawa Trough using seismic and shallow seismic profiles. Moreover, they interpreted the sedimentary strata from top to bottom as: the argillaceous silt, semi-deep-sea turbidite, and clay of Holocene; shallow marine terrigenous sand, semi-deep-sea mud, and tuffaceous mud of Pleistocene; dolomitic mudstone, sandstone, and volcanic rocks of Pliocene; and transitional sandstone, mudstone, and tuff of Miocene (Li et al., 2004; Li, 2008). However, Luan et al. (2008) only used reflection seismic to divide the sedimentary strata in the continental slope of the Okinawa Trough into five seismostratigraphic units (A–E) which were speculated as the sedimentary formations of Late Miocene–Quaternary (A), Oligocene–

Miocene (B–C), Eocene (D), and Paleocene (F), respectively. Li et al. (2019) tracked the stratigraphic distribution from the East China Sea Shelf Basin to the continental slope using sequence stratigraphic and well-seismic calibration technologies. They identified six sequence boundaries and finally determined that the oldest strata deposited in the continental slope of the Okinawa Trough was the Lower Miocene formation, or even earlier (Li et al., 2019).

The Okinawa Trough is the result of the interaction of subduction, collision, back-arc spreading between the Pacific–Philippine Sea Plate and the Eurasian Plate, and the far-field effect of convergence, collision, and wedging between the Indian–Australian plate and the Eurasian plate (Li et al., 2007, 2013; Hall, 2012). In the Late Cretaceous, the Pacific Plate subducted under the Eurasian Plate in the NNW- direction, and the subduction angle gradually increased to 80° (Li & Zhou, 1999). The high-angle subduction and rollback of the plate made the Pacific subduction zone retreat and jump eastward (Li et al., 2007, 2013; Hall, 2012). Then, the East China Sea Shelf rifted into a NE-trending half-graben (Liu et al., 2004; Zhang et al., 2014; Liu et al., 2020), forming the prototype of the ECSSB. In the Cenozoic, with the retreat of the Pacific Plate and the uplift of the Qinghai-Tibetan Plateau, the ECSSB continuously back-arc rifted until the end of Oligocene and was filled with thick Paleogene strata (Li et al., 2013; Zhang et al., 2014; Liu et al., 2020). After the formation of the Shikoku–Parece Vela Basin in the Middle Miocene, the Pacific subduction zone jumped from the Ryukyu Island Arc to the Izu–Bonin–Mariana Trench, and the Okinawa Trough began to back-arc spreading, which caused the Ryukyu Island Arc to break away from the East Asia continental margin (Li et al., 2013). At this time, the ECSSB had entered depression stage. Since then, the Okinawa Trough continuously back-arc rifted. The discovery of pillow basalt in the central and southern trough indicates that the mantle-derived material has been directly exposed to the seabed (Hao et al., 2004; Zhang & Shang, 2014).

3 Data set and method

Six 2D reflection seismic profiles (inline L1–L5 and crossline L6) across the continental shelf and slope of the East China Sea, logging data of Well A (located on the seismic line L1), digital elevation model (DEM), seabed temperature, heat flow, and paleontological chronostratigraphic data of the ECSSB constitute the data set of this study. The total length of 2D seismic lines is about 2390 km, and the dominant frequency ranges from 20 HZ to 30 HZ. The resolution of these seismic data used for submarine canyons is between 12–18 m. Well A is located in the ECSSB and reveals Oligocene–Quaternary strata sequence (Huagang, Longjing, Yuquan, Liulang, Santan, and Donghai formations, from bottom to top). Although we published the sequence stratigraphic results of seismic line L1 (Li et al., 2019), based on seismogram synthesizing and horizon calibrating, we further revised and tracked the sequence stratigraphic boundaries on seismic line L1–L5 from the East China Sea Shelf to the Okinawa Trough. Sequentially, we established the isochronous stratigraphic framework of the study area and determined the age of stratigraphic boundaries on the seismic profiles, based on the comparison and revision of the biostratigraphic data of the East China Sea Shelf Basin (Wu et al., 1998a, 1998b; Zhong et al., 2006), the 2009 geologic time scale (Walker & Geissman, 2009), the updated international chronostratigraphic chart (v2017/02; Cohen et al., 2013), and magnetostratigraphic–biostratigraphic–chronostratigraphic sequence stratigraphic results (Haq et al., 1987).

As the age and magnetic chronology of the stratigraphic boundaries were slightly different in the chronostratigraphic tables published in different years or by different researchers, and the international chronostratigraphic chart (v2017/02; Cohen et al., 2013) did not provide the magnetic chronology, we firstly assumed that the magnetic chronology in the 2009 geologic time scale (Walker & Geissman, 2009) is consistent with the stratigraphic division in the International Chronostratigraphic Chart (v2017/02; Cohen et al., 2013). Then, based on the sparse stratigraphic ages provided by the international chronostratigraphic chart (v2017/02; Cohen et al., 2013), the ages of magnetic polarity zones in the 2009 Geologic Time Scale (Walker & Geissman, 2009) were determined using interpolation method. Sequentially, the ages of stratigraphic boundaries, sequence boundaries, and biostratigraphic zones provided by Haq et al. (1987) were revised using the new ages of magnetic polarity zones calculated from the previous step. Finally, based on the paleontological and lithostratigraphic data of the ECSSB (Wu et al., 1998a, 1998b; Zhong et al., 2006; Xie et al., 2014) and its revision with the result of Haq et al. (1987), we established the Cenozoic chronostratigraphic table applicable to the East China Sea region (Figure 2). The ages of stratigraphic boundaries and sequence boundaries in Haq's eustatic curve were also determined.

The principle and method implemented for sequence stratigraphy analysis were as follows: (1) By comparing the lithostratigraphic, paleontological, and logging data of Well A with the chronostratigraphic table of the East China Sea, we firstly determined the ages of the stratigraphic boundaries of Well A; (2) Using the density and acoustic logging data of Well A, a synthetic seismogram that used for the seismic horizon calibration on line L1 was made. Then, based on our previous research results (Li et al., 2019) and the Cenozoic chronostratigraphic table (Figure 2), we further revised and redetermined the geological horizons and ages of the seismic reflection interfaces (e.g., seafloor, T_0, T_{10}, T_{12}, T_{16}, T_{20}, T_{30}) on the line L1. And finally, the isochronal seismic stratigraphic framework on line L1 was established (Figure 3). In addition, the T_{LGM} interface [the maximum regressive surface formed by the rapid sea level fall in the East China Sea during the LGM (23 kyr B.P.)] was determined by the identification of a set of regressive parasequence groups and a series of backstepping onlap points on the seismic profiles due to the sea level rise after the LGM (Figure 4); (3) The seafloor, T_{LGM}, T_0, T_{10}, T_{12}, T_{16}, T_{20}, T_{30}, and T_g on the inline L1 were tracked from shelf to slope by using seismic wave parameters, such as frequency, amplitude, seismic event continuity, reflection termination styles, internal structure, and external geometry of seismic reflection units. Then, the seismic horizons on the inline L1 were tracked to the L2, L3, L4, and L5 inlines through the crossline L6. And finally, the isochronal stratigraphic framework of the Okinawa Trough was established. Notably, the T_{12}, T_{16}, T_{20}, T_{30}, and T_g interfaces on the seismic profiles could not be tracked continuously from the shelf to the slope due to the Diaoyu Island Uplift. These seismic interfaces were identified based on the theory and method of sequence stratigraphy. They were comprehensively determined by identifying the unconformities (or its corresponding correlative conformities) and reflection termination symbols (onlap, downlap, toplap, truncation, offlap, progradation, retrogradation, incision, and marine erosion) of the 4^{th}-order sequence boundaries, such as maximum regressive surface, basal surface of forced regression, and maximum flooding surface, as well as the spatial characteristics and superimposed styles of lowstand systems tract (LST), transgressive systems tract (TST), highstand systems tract (HST), and falling stage systems tract (FSST; Figure 4). The terminology of sequence stratigraphy and sedimentology used in this study mainly refers to the concepts and principles of Haq et al. (1987), Hunt & Tucker (1995), and Catuneanu (2002).

The spatial resolution of DEM was 1'. The geomorphological factors, such as elevation, slope, and aspect ratio, were calculated using the ArcGIS software. Considering the low resolution of the DEM, the multi-beam sounding data and topographic maps obtained from Liu et al. (2005), Li (2008), and Wu et al. (2014) were referenced to analyze the geomorphological characteristics of submarine canyons on the slope of the Okinawa Trough. The sea floor heat flow and temperature data are derived from the global heat flow database (http://www.ihfc-iugg.org/products/global-heat-flow-database/data) issued by the International Heal Flow Commission. In addition, partial sea floor temperature data are derived from Luan et al. (2008) and Xu et al. (2012).

4 Results

4.1 Sequence stratigraphy

Based on previous research results (Li et al., 2004; 2019; Luan et al., 2008; Li, 2008) and the Cenozoic chronostratigraphic table of the East China Sea (Figure 2), nine unconformities and sequence boundaries, such as Seafloor, T_{LGM} (23 kyr B.P.; Mix et al., 2001; Li et al., 2014), T_0 (1.8 Ma), T_{10} (6.0 Ma), T_{12} (11.02 Ma), T_{16} (16.12 Ma), T_{20} (23.03 Ma), T_{30} (33.9 Ma), and T_g were finally determined on the seismic profiles (Figure 3) across the East China Sea Shelf and Slope comprehensively using the horizon calibration of a synthetic seismogram of Well A, seismic boundaries tracking, and identification of sequence structure style. Six sequence boundaries, such as Seafloor, T_{LGM}, T_0, T_{10}, T_{12}, and T_{16} were developed on the slope of the Okinawa Trough (Figures. 4a and 4b). The filling strata were divided into five 3^{rd}-order sequences (SQIII 1–SQIII 5). The sequence SQIII 4 consisted of four parasequence units (systems tract), such as LST, TST, HST, and FSST, while the SQIII 5 consisted of only LST and TST. The FSST at the top of SQIII 4 was characterized by a wedge-shaped and stepping-down progradation reflection unit towards the trough basin, which reflected the sedimentary migration stages controlled by sea-level fall. Thus, a regressive unconformity (T_{LGM}) which can be tracked in the whole region was formed (Figure 4). The lower Miocene strata may also have deposited on the slope, but its reflection characteristics were fuzzy, discontinuous, and difficult to track.

Tracking from L1 to L2, L3, L4, and L5 lines, we found that the Diaoyu Island fold-uplift had an increasing influence on the sedimentary structure of the slope from north to south. Only three unconformities and sequence boundaries, such as Seafloor, T_{LGM} (23 kyr B.P.), and T_0 (1.8 Ma) were effectively determined on the southernmost seismic line L5. The T_{10} (6.0 Ma), T_{12} (11.02 Ma), and T_{16} (16.12 Ma) surfaces were further determined using the sequence scale, grade, and growth cycle by compared with other seismic lines. Stratigraphic sequence tracking from north to south showed that the Okinawa Trough started to be rifted in the Early Miocene affected by the subduction of the Philippine Sea Plate (Li et al., 2013). The northern trough was firstly rifted and therefore, filled by thick Miocene–Quaternary strata. Until the Late Miocene–Pliocene, as the rifting center migrating to the southern trough, the Okinawa Trough evolved into a unified basin. The southern trough was only filled by the Pliocene and Quaternary strata (Li et al., 2004; Wu et al., 2014).

Seismic interpretation showed that line L2 extends across submarine canyon C4, which has developed since the Early Pleistocene (<1.8 Ma). Along with the progradation of the continental slope, the canyon channel gradually migrated to the SE (Figure 4b), and then, moved to the present location after the LGM. It can be inferred that, during the LGM, the ancient river channel on the East China Sea Shelf transported a large amount of clastic materials to the submarine canyon C4. Following the deposition of the clastic materials, the downcutting rate of the canyon decreased, resulting in channel filling.

The stratigraphic sequence of line L5 indicated that the submarine canyon C6 started to develop during the LGM (Figures 5a, 5b, 5e, and 5f). Its formation and evolution were mainly controlled by the syndepositional fault developed in the SE-wing wall of the canyon. Line L3 extends across the head of the submarine canyon C5 and its branch C5-1 (Figures 5c and 5d), while line L4 extends across the branch C5-2 (Figures 5g and 5h). The stratigraphic sequence of lines L3 and L4 shows that the canyon system C5 was formed during the LGM, or even earlier (Middle Pleistocene). In addition, two juvenile submarine canyons were seen on line L4 (Figure 5e) which are mainly controlled by the active faults that cut through the seafloor.

In conclusion, submarine canyons on the continental slopes of the central and southern Okinawa Trough began to develop in the Early Pleistocene (< 1.8 Ma) and further evolved after the LGM. The canyon survival time spans two sequence cycles of SQIII 4 (1.8–0.023 Ma) and SQIII 5 (0.023–0 Ma) (Figure 4). Some submarine canyons may have migrated or even disappeared due to the climate changes during the glacial-interglacial cycle.

4.2 Geomorphological features of submarine canyons

There are many submarine canyons and valleys of different scales and shapes on the central and southern slopes of the Okinawa Trough (Liu et al., 2005; Li, 2008; Li et al., 2019; Wu et al., 2014). As mentioned above, the canyons were mainly formed in the Quaternary period. During the LGM, the sea-level in the East China Sea dropped to the current water depth of 135–150 m, which caused the continental shelf to be completely exposed and denuded, and finally led to the formation of the regional unconformity interfaces (T_{LGM}). This also provided favorable provenance and hydrodynamic conditions for the development of submarine canyons (Gao & Collins, 2014; Li et al., 2014; Wu et al., 2014). The submarine canyon showed typical erosional–depositional structures, with obvious down-cutting truncation at the bottom on reflection seismic profiles. It was characterized by irregular V-shaped or U-shaped with different terrain height. Small secondary-sequence surfaces developed in the interior of these canyons (Wu et al., 2011; Su et al., 2015).

The slope gradient map extracted from the DEM (Figure 6) indicates that the average slope gradient of the Okinawa Trough gradually increases from north to south. The slope gradient of the northern slope ranged from 0.5deg to 2deg, and the slope gradient of the central slope was mainly between 0.5–10deg. The slope gradient of the transition zone between the central and the southern slopes increased to 2–15deg. However, the slope gradient of the southern slope decreased to 0.5–10deg. On the map, ten large-scale submarine canyons (C1–C10) was identified.

In this study, two large-scale submarine canyons (C5 and C6) in the central slope of the Okinawa Trough were selected for geomorphological analysis (Figure 7). The submarine canyons C5 and C6 were separated by a submarine plateau on the slope. The lengths of canyons C5 and C6 from the shelf break (water depth 180–200 m) to the bottom of the Okinawa Trough (water depth 1800 m) were about 90 km and 73 km, respectively. Their structures can be divided into three parts: head, upstream, and downstream (Figures 7c and 7e). From the head to downstream area, the canyon gradually changes from near SN-trending to NW-trending or NWW-trending. The submarine plateau partly affected the extension direction of submarine canyons. The canyon head is V-shaped and gradually transits to an irregular V-shaped or U-shaped structure with a wider canyon shoulder or a U-shaped structure with a wider canyon floor. The canyon downstream was mostly dish-shaped or dustpan-shaped (Figures 7d and 7f). The submarine canyons C5 and C6 are the meandering shelf-incising canyons not connected with a river whose heads have retrogressively eroded into the East China Sea Shelf. Branching channels were common at the head and upstream of the canyons (Figures 7a and 7b).

On the topographic profile along the thalweg of canyon C6, the bottom configuration slope presents two steps (Figure 7c). The maximum shoulder width of C6 ranged from 9 km–20 km (Figure 7d), and the maximum undercutting depth at the transition zone between the head and the upstream reached 900 m. The slope gradient of the side wall at the canyon head ranged from 0.5deg to 7.4deg, and the slope gradient of the upstream was between 1.5–9.1deg. The slope gradient of the downstream gradually decreased, mostly to less than 3deg. Notably, there was a long and narrow natural levee (of 35 km length) on the NE-side in the downstream channel of canyon C6. The topographic height difference was 100–170 m across the channel, and the slope gradient of the NE-side wall was higher than that of the SW-side wall (Figures 7b and 7d). The seismic profile indicated a parallel–subparallel reflection structure with medium–high continuity and medium–strong amplitude (Zhao et al., 2008), reflecting the characteristics of fine-grained overbank sediments at the end of the canyon. The reason that the overbank sediments formed on the NE-side of the channel is speculated to be the combined effects of Coriolis force and the Kuroshio movement from south to north (Li et al., 2014, 2019), which preserved the turbidity sediments effectively in the NE-side of the channel.

The submarine canyon C5 has many branches (e.g. C5-1 and C5-2). However, the connectivity between the branch channel and the main channel was still unclear (Figures 7a and 7b). The maximum shoulder width of canyon C5 was 7–19 km (Figure 7f), and the incised depth was 40–430 m. The slope gradient at the canyon head ranged from 0.1deg to 6.4deg. The slope gradient at the canyon upstream was 0.3deg–4.8deg, while the slope gradient at the canyon downstream was less than 2deg. The thalweg profile showed that the bottom configuration descended in three steps (water depths were 180–610 m, 610–1200 m, and 1200–1800 m, respectively; Figure 7e).

4.3 Erosional–depositional texture in submarine canyons

On the seismic line L4, the canyon head of C6 is V-shaped. The seismic reflection with medium amplitude and medium continuity at the canyon bottom represents turbidite channels, while the seismic reflection with weak amplitude, low continuity at the middle part represents the mass transport deposits (MTD) (Figures 5e and 5f). The ancient sea-level in the East China Sea dropped to the current water depth of 120–150 m during the LGM, which caused the East China Sea Shelf to be exposed and eroded. Affected by the rejuvenation of the rivers, many incised channels developed on the shelf edge (Li et al., 2004, 2019). According to the morphological structure of the canyon and its downcutting position, the head of the canyon C6 justly developed from these channels.

The seismic line L5 shows that the canyon C6 is dustpan-shaped, with steep SE-side-wall and gentle NW-side-wall. The morphological structure of the canyon is obviously controlled by a normal fault paralleling or obliquing to the canyon strike (Figures 5a and 5b). Within the canyon, only two complexes of turbidity current channels could be identified, which are mainly characterized by layered seismic reflections with medium–strong amplitude and medium continuity. The maximum downcutting depth of the canyon was found to be consistent with the T_{LGM} surface (Figures. 5a and 5b). However, five–six large-scale MTDs were identified in the canyon, which were characterized by layered or progradation reflections with weak amplitude and medium continuity. Besides, imbricated seismic reflections due to gravitational sliding and compressional deformation were also observed (Figures. 5a and 5b). The dustpan-shape and internal structure of the canyon C6 indicated that it was jointly controlled by gravity flow and seabed subsidence caused by the syndepositional fault dragging on the SE-wing (Liu et al., 2005; Li, 2008; Zhao et al., 2011). Therefore, the bottom boundary of the canyon C6 was not exactly the downcutting surface of the gravity flow. Based on the comprehensive interpretation and analysis of seismic stratigraphy, we believe that the maximum regressive surface (T_{LGM}) formed at the LGM is the bottom boundary of the submarine canyon C6.

The seismic line L3 extends across the head of the canyon C5 and its branch C5-1. The seismic profile shows that there are one or two ancient, incised valleys buried under the canyon C5 (Figures 5c and 5d). According to the superimposed relationship, it can be inferred that the rapid sea-level fall in the East China Sea during the LGM caused the continental shelf to be exposed and downcut due to river rejuvenation. The ancient, incised valleys now buried under the head of canyon C5 were thus formed. After LGM, the rivers gradually retreated to the continent due to sea-level rise, and the ancient channels on the continental shelf were filled and buried (Li et al., 2004). However, it still retained the negative topography which became the prototype of the canyon head.

The seismic profile showed that the channel of canyon C5-1 was about 6 km wide and undercut close to the surface T_0. Eroded by the mass flow transportation, the bottom surface of the canyon was undulating (Figures 5c and 5d). In the canyon, three MTD units are identified, which indicated that the submarine canyon has entered the shrinking and filling stage (Reading & Richards, 1994; Wu & Qin, 2009). The NW-side wall of the canyon is one MTD unit formed by slump, which presents chaotic or continuous reflection with medium–weak amplitude. The toe of the slump body was strongly folded. The sedimentary layer was broken to form an imbricated structure, in which many compressional deformation structures developed. All of these indicated that the side wall of the canyon may further slide or slump (Figures 5c and 5d). The SE-side wall of the canyon was composed of two MTD units. The interface between these two MTDs was interpreted as one detachment fault for sediment decoupling. The detachment surface formed the bottom boundary of the canyon. The lower part of the MTDs showed layered seismic reflection with medium amplitude and medium–weak continuity, while the upper part presented imbricated or chaotic reflections with medium–low amplitude and medium–low continuity (Figures 5c and 5d).

The seismic profile L4 indicated that the canyon C5-2 underwent obvious lateral migration and diversion (Figures 5g and 5h). We believe that the SE-migration of canyon C5-2 was mainly caused by the rapid sea-level fall and the rightward deflection of Coriolis force during the LGM (Li et al., 2014, 2019). The buried canyon channel was U-shaped, or even dish-shaped, with wide canyon floor. Its interior was characterized by progradational-filling reflections with weak amplitude and medium continuity. The canyon was mainly filled by multi-stage turbidite deposits characterized by the medium–strong amplitude, medium–high continuous, and layered-filling reflection complexes (Figures 5g and 5h).

Seismic profile L2 showed that the canyon C4 underwent 3–4 stages of SE-migration and diversion, during which two ancient channels now buried under the continental slope seabed were formed (Figure 4b). The first ancient channel presented an irregular U-shaped and undercut to the bottom of the Quaternary strata. Its channel was about 3 km wide. The lower channel presents waving reflection with weak-amplitude and medium–low continuity, which reflects the sedimentary characteristics of high-density debris flow. The central channel shows layered-filling reflection with strong amplitude and medium continuity, which represents turbidite channel deposits. The upper part is characterized by mounded or chaotic reflection with weak amplitude and medium–low continuity, which represent the MTDs (Figure 4b). The other ancient channel was U-shaped, with a channel width of 2.5 km, characterized by the layered reflection with medium–

strong amplitude and medium–low continuity (Figure 4b). The head of canyon C4 had two branches. The branch channel width ranged 2–2.5 km and represented an irregular U-shaped or V-shaped. The channels were filled by layered sediments characterized by weak amplitude and medium continuous reflections. The syndepositional deformation structures were also developed in the channels (Figure 4b).

In addition, on the seismic profile L3, eight ancient, incised channels were identified on the shelf edge (Figures 5c and 5d). These channels were small with widths of 0.7–1.5 km, respectively and presented chaotic-filling, onlap-filling, progradational-filling, or complex-filling reflections. The ancient channels were mainly distributed near the T_{LGM} and migrated frequently, indicating that its formation was closely related to the river rejuvenation during the LGM (Figure 5c). On one hand, these small-scale channel systems could carry turbidity sources for the erosion of submarine canyon, while on the other hand, under the action of the retrogressive erosion, they could connect with the slope-confined canyons (blind canyon or headless canyon) and transformed into the canyon head (Li et al., 2014; Wu et al., 2014).

4.4 Seismic reflection mark of methane-bearing fluid activity

Methane leakage and gas-bearing fluid activities at the bottom of the Okinawa Trough have been confirmed by the seabed gas leakage and associated cold seep carbonates (Luan & Qin 2005; Sun et al., 2015; Wang et al., 2019; Guan et al., 2019; Zhang et al., 2020; Cao et al., 2020; Li et al., 2018a, 2021b), pore water geochemistry in shallow sediments (Wang et al., 2015b, 2019; Li et al., 2015; Xu et al., 2018, 2020), mud diapir and volcano (Zhao et al., 2006; Xu et al., 2009) and abnormal methane flux in water column (Luan & Qin 2005; Zhang et al., 2020).

The arched, imbricated reflections on seismic profiles L3, L4, and L5 may indicate the upward escape and diffusion of methane-bearing fluids caused by gas hydrate decomposition (Figures 4d, 5a, 5c and 5e; Wu et al., 2011; Davies, et al., 2012; Su et al., 2015). On the SE- and NW-side walls of canyon C6, well preserved fluid migration channels had been found and identified (Figure 5a). The gas-bearing fluid leakage through these channels only cut the seismic events and formed gaps on the seabed, which did not cause large-scale stratigraphic disturbance. Therefore, the intact escape channels were preserved on the seismic profiles (Figure 5a). The location of canyon C6 is exactly close to the mud volcano or diapir associated with gas hydrate reported by Xu et al. (2009), which confirms the judgment that fluid escape and leakage has occurred and participated in the evolution of canyon C6.

The gap on the side wall of canyon C5-1 and the adjacent slope indicated the traces left by the escaping gas after hydrate decomposition (Figures 5c and 5d). We believed that the detachment fault on the SE-side wall of canyon C5-1 was also further shaped by MTD sliding from the fluid escape channel. However, when the fluid could not be effectively discharged, the liquefied deformation of sediments will present distorted, chaotic or twisty reflections on the seismic profiles (Figures 4d, 5a, and 5c). The ridge of canyon C5-1 are composed of several wedgy or triangular slope fans which are characterized by weak amplitude, chaotic-filling reflections or medium amplitude, medium–low continuous, oblique-filling reflections. The liquefaction-induced deformation exactly developed at the fan end (Figure 5c). Therefore, we believed that the SE-wing of canyon C5-1 was an active methane seep area, which could be confirmed by methane flux observation (Zhang et al., 2020). Coincidentally, the gaps, imbricated structures, and internal chaotic-twisty reflection marks caused by strong methane-bearing fluid seepage were also identified at the end of seismic line L3 (Figure 8c).

On the seismic line L4, we identified a cold seep site which is exactly close to the seabed gas spring (Luan & Qin 2005; Zhang et al., 2020) and an active CH_4 emission area (Xu et al., 2018; Zhang et al., 2020). We believed that the liquefaction deformation due to strong methane-bearing fluid leakage and disturbance caused some gap structures and arched, imbricated reflection units on the seismic profile (Figure 4d). The interior units were characterized by chaotic or twisty reflections (Figure 4d). The reflection seismic, seabed gas spring (Luan & Qin 2005), pore water geochemistry in sediments (Xu et al., 2018), and the highest sea-to-air flux of methane (Zhang et al., 2020) all confirmed the universality of methane-bearing fluid activity in this area of Okinawa Trough.

5 Discussion

5.1 Dynamic accumulation of hydrate indicated by BSRs and its relationship with methane seepage

Since the discovery of the BSRs (Yang et al., 2004; Luan et al., 2008; Xu et al., 2009; Xu et al., 2012; Chen et al., 2014; Li et al., 2019), many evidences for gas hydrate, such as seabed methane seepage and associated carbonate (Luan & Qin, 2005; Sun et al., 2015; Li et al., 2018a; Guan et al., 2019; Wang et al., 2019; Zhang et al., 2020; Cao et al., 2020; Li et al. 2021a, 2021b), pyrite associated with methane leakage (Wang et al., 2015b), mud diapir or volcanoes (Zhao et al., 2006; Xu et al., 2009), and methane anomaly in pore water, water column and even sediments (Lu et al., 2003; Li, 2008; Wang et al., 2015b; Li et al. 2015; Xu et al., 2018, 2020; Zhang et al., 2020), were revealed in the Okinawa Trough (Figure 1). The hydrate phase equilibrium simulation showed that the hydrate resource in the Okinawa Trough can be as high as 24×10^{12} m^3 (Chen, 2014). In this study, based on the measured temperature–depth (pressure) data in the Okinawa Trough (Xu et al., 2012; Li et al., 2019), the phase equilibrium model of gas hydrates was also established, according to the 4^{th}-order equation of temperature-pressure (depth) proposed for the stable existence of gas hydrates (Miles, 1995; Xu et al., 2009). The results show that the minimum pressure required for gas hydrate formation in the Okinawa Trough is 630 m in water depth, which is very close to the result of 500–600 m calculated by Fan & Yang (2004), and the results of 600 m calculated by Luan et al. (2008). All this show that the continental slope of the Okinawa Trough has favorable thermodynamic geological conditions for gas hydrate accumulation.

On the seismic profile L5, two intermittent BSRs with different buried depth were found on the NW-side wall of the canyon C6 (Figure 8a). The distribution horizon of the lower BSR was consistent with the T_{LGM}, distributed across or parallel to the sedimentary strata. The reflection polarity of the BSR was opposite to that of the seafloor, showing strong amplitude and negative seismic polarity clamped by positive polarity (Figure 8a). The blank reflection unit above the lower BSR indicated that the hydrate reservoir thickness was about 150–300 ms (two-way reflection time). The residual discontinuous reflections inside the seismic unit reflected the spatial heterogeneity of the gas hydrates. The upper BSR was distributed intermittently from the side wall slope to the canyon floor, with a cumulative extended distance of 10 km. The BSR trend was basically consistent with the seabed topography (Figure 8a). The thickness of the blank reflection zone above the BSRs on the side wall was about 50–150 ms (two-way reflection time). At the canyon floor, the thickness of the blank reflection zone above the BSR was 100–300 ms (two-way reflection time). Therefore, we believe that there were already gas hydrates in the submarine sediments of the East China Sea Slope during the Pleistocene.

On the seismic profile L4 (Figure 8b), the BSR was located under the NW-side wall of canyon C5-2. The blank reflection zone was characterized by weak amplitude, chaotic-filling or low continuous, oblique-filling reflections, with thickness of 50–150 ms (two-way reflection time). The BSR extended about 4.5 km in the SE-direction and was cut off by the canyon channel, indicating that the submarine canyon has an important influence on the GHSZ (Figure 8b). In the maturity stage, the canyon underwent strong erosion, and the seafloor was downcut into V-shaped or U-shaped structures. Influenced by the cooling effects of seawater (Bangs et al., 2010; Davies et al., 2012), the GHSZ under the canyon floor will gradually migrate deeper. While in the old stage, the submarine canyons are strongly filled, and the MTDs and turbidite channel sand in these canyons can become gas hydrate reservoirs again.

After the last glacial period, owing to the pressure release and rise in the seafloor temperature caused by the rapid sea-level fall, the gas hydrate stable zone (GHSZ) gradually drifted upward and moved towards the seafloor during the LGM, resulting in the overlapping of the lower BSR and the T_{LGM} surface. The leakage of methane-bearing fluid released from hydrate decomposition due to GHSZ migration caused gap structures and fluid escape channels on the seismic profile (Figure 5a). During this period, jointly controlled by sediment slumping (Figure 8a; large wedge-shaped and blank reflection unit above the lower BSR) induced by gas hydrate decomposition and seafloor subsidence caused by contemporaneous faulting on the SE-side wall, the submarine canyon C6 grew rapidly and suffered turbidity flow erosion, which ended the SE-extension of the lower BSR. After the LGM, along with the sea-level rose, the turbidity sediments filled in the canyon once again hosted gas hydrates, forming a 10-km long BSR across the side wall and subchannel floor in the canyon C6 (Figure 8a). Mass flow sediments constituted the main body of the blank reflection zone above the BSR (Figure 8a), indicating that deep water turbidites, such as canyon channel and MTD, were the dominant gas hydrate reservoirs in these canyons (Noguchi et al., 2011; Boswell et al., 2012; Wu et al., 2011; Su et al., 2015; Suzuki et al., 2015). The detachment surface of the shallow MTDs inside the canyon C6 completely coincided with the BSRs (Figure 8a), indicating an inseparable connection between gas hydrate decomposition and the erosive turbidity current that dominates the development of the canyon.

Although we did not identify enough BSRs on the seismic profiles, a lot of gap structures and fluid transport channels caused by gas escaping, and imbricated, chaotic or twisty seismic reflections caused by gas-bearing fluid liquefaction associated with methane leakage were found (Figures 4d, 5a, 5c, and 8c). Notably, the petrological, mineralogical, and geochemical analysis of carbonate associated with methane seepage in the Okinawa Trough, show that the leakage of biogenic methane and intense anaerobic oxidation of methane (AOM) resulted in the formation of abundant authigenic carbonates, which represented extremely negative carbon isotopic and positive oxygen isotopic compositions (Wang et al., 2019; Cao et al., 2020). Moreover, isotopes have confirmed that the fluid required for carbonates precipitation in the Okinawa Trough comes from decomposition of gas hydrate (Cao et al., 2020), which just approves our understanding that the methane-bearing fluid activity caused by hydrate dynamic decomposition affects the origin and evolution of submarine canyons.

5.2 Factors controlling the formation and evolution of submarine canyons

The submarine canyons on the continental slope of Okinawa Trough began to form in the early Pleistocene (<1.8 Ma), which was strongly controlled by the climate and environment changes due to the glacial-interglacial cycle in the Quaternary (Gao & Collins, 2014). The origin and evolution of these submarine canyons are mainly related to the gravity transportation (small-scale landslides and sediment gravity flows; Li et al., 2001; Liu et al., 2005; Zhao et al., 2009; Li et al., 2019), the rifting settlement of syndepositional faults (Liu et al., 2005; Li, 2008; Zhao et al., 2011), and the sea-level eustacy, river rejuvenation and methane-bearing fluid leakage due to dynamic evolution of GHSZ caused by climate change in the Quaternary glacial-interglacial cycles (Li et al., 2019; Cao et al., 2020). In addition, the strong submarine volcanic activities in the Okinawa Trough may also affect the development of submarine canyons.

The seabed topography shows that the trend of the submarine canyons on the continental slope of Okinawa Trough is basically perpendicular to the isobaths, reflecting that the extension of canyons is controlled by gravitational process. The MTDs associated with slide or slump and characterized by imbricated, twisty or chaotic seismic reflections, the channel-lag deposits (high density debris flow) characterized by chaotic-filling reflections, and turbidity channel deposits characterized by progradational-filling, parallel onlap-filling or divergent-filling reflections indicate that gravity flow plays a key role in shaping the submarine canyons (Wu & Sakamoto, 2001; Wu et al., 2011; Xu et al., 2014; Su et al., 2014, 2015; Yin et al., 2015). Published cases of submarine fans outside the canyon mouths and the natural levees and fine-grained overflow deposits of the Chiwei canyon-fan system also illustrate the frequent turbidity current activities in the Okinawa Trough (Li et al., 2001; Liu et al., 2005; Li, 2008; Zhao et al., 2009, 2011). Especially since the Holocene, after the Kuroshio warm current strengthened (Xiang et al., 2003; Gao & Collins, 2014), it intruded into the Okinawa Trough again and would induce the frequent activities of seabed turbidity current to a certain extent.

The dustpan-shaped structure with NE-wing faulting and SW-wing overlapping and its associated relationship with syndepositional faults show that some submarine canyons on the continental slope of Okinawa Trough are dominated by active faults. Canyon embryos controlled by these syndepositional faults were also found on the seismic line L4. The dragging subsidence of active faults can not only form canyon negative topography, but also induce erosive activities of turbidity current, and instability and slump of canyon side-walls, thus leading the evolution process of this kind of submarine canyons. Since the late Miocene, under the control of back-arc tension, two groups of NE-SW trending (approximately E-W trending in the southern part of the trough) and NW-SE trending fault systems have developed in the Okinawa Trough (Liu et al., 2005; Li, 2008; Zhao et al., 2011). The NE-SW trending faults control the topographic division from continental shelf to slope. While the secondary NW-SE trending faults and its branch faults cut the continental shelf and slope from west to east and break the bedrocks providing good geological conditions for the formation of submarine canyons.

The formation time of the submarine canyons (< 1.8 Ma) on the continental slope of the Okinawa Trough is equivalent to the starting time of the oldest glacial epoch (Shishapangma epoch) in China, the Eburonian epoch recorded in the European Alps, and pre-Illinoian H epoch recorded in the Great Lakes (Shi & Liu, 1964; Zhang et al., 2002; Mutton et al., 2003; Ehlers & Gibbard, 2007; Cui et al., 2011) reflecting that the formation of submarine canyons is closely related to the Quaternary glacial-interglacial cycle (Nakajima et al., 2014; Xu et al., 2014; Su et al., 2014, 2015; Yin et al., 2015; Li et al., 2019; Cao et al., 2020). During the LGM, the sea-level of the East China Sea dropped to the present-day water depth of 120–150 m (Lambeck & Chappell, 2001; Li et al., 2014) and the continental shelf was exposed. The terrestrial rivers advanced rapidly toward the ocean and eroded the shelf margin, thus forming many incised channels (Li et al., 2004, 2014). The heads of submarine canyons C5 and C6 was inherited from these ancient incised channels. At the same time, these ancient channels also transported a large amount of clastic materials for the downcutting of canyons due to gravity flow. For the Okinawa Trough, another important influence of the Quaternary sea-level eustacy was the variation of the temperature and pressure conditions of gas hydrate (Song, 2003; Yu et al., 2014; Maslin et al., 2004). The periodic decomposition of hydrate and methane leakage caused by GHSZ migration due to the temperature and pressure change, weakened the stability of seabed sediments on the continental slope, which had seriously affected the development and evolution of submarine canyons in the forms of landslides and sediment gravity flows. In return, the continuously downcutting and lateral erosion of canyons would also cause the spatial migration of GHSZ (Bangs et al., 2010; Davies et al., 2012; Su et al., 2015). The MTDs characterized by imbricated, twisty or chaotic seismic reflections, the gaps that indicate gas escaping on the canyon side-walls, the liquefaction deformation structures on the canyon ridge, and the truncated relationship between BSRs' reflectors and canyon channels on the seismic profiles all proved the interaction between gas hydrate and submarine canyons. In addition to the gravity flow, the sea-level and climate changes caused by the Quaternary glacial-interglacial cycle are the main factors for the origin and evolution of submarine canyons in the Okinawa Trough.

5.3 Submarine canyon evolution model coupling with methane seepage associated with hydrate

The temperature and pressure conditions of the GHSZ can be destroyed by the alternating cold and warm events caused by climate change or sea-level eustacy (Song, 2003; Maslin et al., 2004; Wu et al., 2009; Bangs et al., 2010; Nakajima et al., 2014). The most remarkable is the global sea-level fluctuation caused by glacial-interglacial cycle in the Quaternary controlled by the Milankovich cycle. For example, during the LGM, the sea level of the East China Sea dropped to the present-day water depth of 120–150 m and reached the continental slope edge of the Okinawa Trough (Lambeck & Chappell, 2001; Li et al., 2014; Gao & Collins, 2014). During this period, the intense climate change and sea-level fall played a key role in the formation, decomposition, and accumulation of gas hydrates in the Okinawa Trough. In turn, the methane released from hydrate decomposition could also contributed to climate change (Maslin et al., 2004; Wang et al., 2015a).

Many submarine canyons have developed on the central and southern slope of the Okinawa Trough (Li et al., 2001; Liu et al., 2005; Liu et al., 2005; Li, 2008; Wu et al., 2014). The formation of these canyons began in the early Pleistocene (< 1.8 Ma), and they continue to develop even today. During this period, the submarine canyons underwent multi-stages of channel migration and erosional–depositional evolution. Some submarine canyons had even disappeared and were buried. The submarine canyons on the slope of the Okinawa Trough were formed earlier than the oldest Shishapangma Glaciation (1.17–0.8 Ma) discovered in Western China (Shi & Liu, 1964; Zhang et al., 2002; Cui et al., 2011) and the age of the seep carbonates [31.54–34.1 ka B.P. from Sun et al. (2015) and 22.8–55.7 ka B.P. from Cao et al. (2020), respectively] in the Okinawa Trough. However, its formation time is consistent with the starting time of the Eburonian epoch in and pre-Illinoian H epoch (Mutton et al., 2003; Ehlers & Gibbard, 2007; Cui et al., 2011). Moreover, the rapid sea-level fall during the LGM in the East China Sea Shelf are confirmed by many sedimentary records (Gao & Collins, 2014; Li et al., 2014, 2019). Therefore, the formation, development, and evolution of submarine canyon in the study area are closely related to the global glacial–interglacial cycle during the Quaternary period (Nakajima et al., 2014; Xu et al., 2014; Su et al., 2014, 2015; Yin et al., 2015).

Since the LGM, the coupling evolution process of submarine canyon and gas hydrate system in the Okinawa Trough were clearly preserved in the canyon sediment records, such as the MTD characterized by imbricated, twisty or chaotic seismic reflections, fluid transport channels and the gaps that indicate gas escaping on the side walls of the C6 and C5-1 submarine canyons (Figures 5a and 5c). Additionally, a truncated relationship between the BSRs reflector and the submarine canyon on seismic lines L5 and L4 (Figure 8) was also observed. All these indicate that there is a complex relationship between the erosional–depositional evolution of submarine canyons and the development of gas hydrates on the continental slope of the Okinawa Trough. On one hand, strong downcutting and retrogressive erosion of submarine canyons will steepen the canyon sidewall, which can easily induce sediments instability on the canyon sidewall. The channel downcutting and sediment instability will destroy the GHSZ. Therefore, the methane released by hydrate decomposition will leak out through the gap formed by the sediment instability on the side walls and seabed gas seepage (Luan & Qin, 2005; Wu et al., 2011; Davies et al., 2012; Su et al., 2015; Cao et al., 2020); On the other hand, the sea-level eustacy caused by the glacial–interglacial cycles will lead to frequent changes of temperature and pressure in the GHSZ. Therefore, the hydrates can form or decompose dynamically and repeatedly, that promotes the escape and leakage of methane-bearing fluids. This methane-bearing fluid activity can, in turn, induce sediment instability and deformation, and then, influence the formation and erosion processes of the submarine canyon (Nakajima et al., 2014; He et al., 2014; Li et al., 2017, 2018b) and even cause the occurrence of submarine landslide. However, the channel sand inside the submarine canyon and the submarine fan outside the canyon mouth can often be used as the high-quality reservoirs for hydrate. We believe that erosion and deposition in the submarine canyon and the dynamic accumulation of gas hydrate are interdependent and reciprocal.

Based on the influence of sea-level fall caused by Quaternary glaciation on the gas hydrate dynamic accumulation system in the continental slope of the Okinawa Trough and the interaction between the gas hydrate decomposition and the formation of submarine canyons, a coupling evolution model of submarine canyon erosion and gas hydrate dynamic accumulation on the continental slope of the Okinawa Trough was established (Figure 9): The stage of sea-level fall, hydrate decomposition, and submarine canyon forming. The formation time (<1.8 Ma) of submarine canyon on the continental slope of the Okinawa Trough is consistent with the glacier onset time in the Northern Europe and Northern America (Mutton et al., 2003; Ehlers & Gibbard, 2007; Cui et al., 2011), which indirectly proves the genetic relationship between submarine canyons and the sea-level fall during the glacial epoch. During the glacial epoch in the Middle Pleistocene, the sea-level fall led to pressure release and seabed temperature rise and the upward migration of GHSZ resulted in the decomposition of hydrate layers between the old and new stable zones (Wu et al., 2011; Nakajima et al., 2014; He et al., 2014). The released methane migrated and seeped rapidly upward to the seabed and accumulated beneath the seafloor, forming hydrate mounds on the continental slope. With the continuous hydrate accumulation, the stress reached the critical condition, which resulted in the collapse of the hydrate mound. The scarp formed by the instability of hydrate mounds became the rudiment of the valley, which opened the development process of the submarine canyon (Figures 9a and 9b). Notably, the formation of submarine canyon C6 is also controlled by contemporaneous faulting (Figure 5a). In other words, faulting is also one factor affecting the initiation of submarine canyons. Active faults break the bedrocks of the seabed to form a negative terrain, inducing gravity flow to preferentially erode the broken strata and ultimately, affected the canyon path. Faulting can be combined with the decomposition of gas hydrate to control the development and evolution of the submarine canyon; The stage of submarine canyon continuously downcutting, canyon retrogressive erosion, and gas hydrate stable zone (GHSZ) dynamic migrating. After the rudiment formation of the submarine canyons, the scour and retrogressive erosion of gravity flow (e.g., MTDs and turbidity flow) became the main factor to shape the canyon structure. In this stage, the seabed continuously suffered downcutting and erosion, forming V-shaped or U-shaped canyon channels. Affected by the cooling effects of seawater (Bangs et al., 2010; Davies et al., 2012), the GHSZ under the canyon floor gradually migrated deeper (Figure 9c). The free methane under the previous GHSZ then combined with water molecules to form new gas hydrates (Sun et al., 2017). The BSRs were truncated by the MTDs on the side wall of the submarine canyons C6 and C5-2, which proved the influence of canyon downcutting on the GHSZ migration. At the same time, the reason why multiple BSRs have developed in the canyon development area is explained reasonably (Wu et al., 2009; Davies et al., 2012; Su et al., 2015). The mutual promotion stage of sediment instability and the collapse of the canyon wall, along with methane leakage. The gap from which the gas escaped, imbricated deformation structures on the side wall of the C6 and C5-1 canyons, and the liquefaction deformation structures on the canyon ridge (Figure 5) all indicated that, in the trough, gas escape interacted with mass sliding. When the slope gradient of the canyon wall increased to the critical conditions under the erosion of turbidity flow, the sediments on the head and flank of the canyon channel became instable and collapsed. Thus, the hydrate layers on the canyon wall decomposed, resulting in the methane escaping and a gap was formed where the gas seeped through. Similarly, the escape of methane-bearing fluid will also aggravate the sediment deformation and induce new mass sliding events. With the retrogressive erosion of the canyon, the ancient, incised channels formed on the edge of the outer shelf during the LGM may be connected to the canyon, forming the head of the current submarine canyon (Figure 9d). The stage of the wakening of canyon erosion, filling of the sandy channel, and hydrate reaccumulating. With the weakening of canyon downcutting, the submarine canyon entered the main filling stage (Wu & Qin, 2009; Walsh et al., 2007). The coarse-grained channel sand with high porosity and permeability or re-transported MTDs started to develop in the canyon. If the methane supply is enough, the hydrates will be reaccumulated in these high-quality reservoirs. Of course, most of the submarine canyons on the continental slope of the Okinawa Trough are in their youth. It is possible that only a few submarine canyons filled and buried by clastic sediments have experienced this stage.

6 Conclusions

According to the theory of sequence stratigraphy, six seismic sequence boundaries have been identified on the central and southern slopes of the Okinawa Trough. Their geological ages have been determined as Seafloor (0 Ma), T_{LGM} (23kyr B. P.), T_0(1.8 Ma), T_{10} (6.0 Ma), T_{12} (11.02 Ma), and T_{16} (16.12 Ma). The isochronous chronostratigraphic framework in the central and southern slopes of the Okinawa Trough was established and the sedimentary strata were divided into five 3rd-order sequences. The central and northern slopes of the Okinawa Trough were characterized by thick Miocene–Quaternary strata, while the southern slope was mainly filled with Pliocene–Quaternary strata. The submarine canyons on the central and southern slopes of the Okinawa Trough began to develop in the early Pleistocene (< 1.8 Ma) and continued to develop even today.

The geomorphological features of submarine canyons on the central and slopes of the Okinawa Trough (e.g., C5 and C6) were found to be segmented: The head was V-shaped; the upstream was gradually transformed into V-shaped or U-shaped with wider shoulder and deeper downcutting depth; and the downstream region consisted as dish-shaped or dustpan-shaped structure with a wide canyon floor. These canyons were meandering canyons not connected to a river. The heads of the C5 and C6 submarine canyons were evolved from the ancient, incised channels formed in the LGM. The canyon C5-1 was filled by three MTD units related to side-wall sliding. The canyon C5-2 migrated southeastward, and the interior was mainly filled by turbidite channel complex. There were two turbidite scouring–depositional layers and five–six MTDs in the canyon C6. The maximum downcutting position of the C6 coincided with the T_{LGM} surface. The dustpan-shape and internal filling structures of the canyon C6 indicated that it was formed by turbidity current erosion and unstable collapse of the canyon walls under the control of the seabed subsidence caused by the SE-wing synsedimentary faulting.

The gas hydrate phase equilibrium simulation predicts that the minimum water depth required for gas hydrate is 630 m, which shows that the Okinawa Trough has favorable thermodynamic geological conditions for gas hydrate accumulation. Three BSRs were identified on the seismic profiles L5 and L4, of which the profile L5 had double-BSRs structure. The trend of the BSRs was consistent with the seabed topography, which was inclined across or parallel to the sedimentary strata, showing strong amplitude, negative polarity, and continuous reflections. The blank reflection zone above the BSRs showed that the thickness of the GHSZ ranged between 50 ms and 300 ms (two-way reflection time).(4) The origin and evolution of submarine canyons on the continental slope of Okinawa Trough are mainly related to the gravity transportation of continental slope, the rifting settlement of syndepositional faults, and the sea-level eustacy, river rejuvenation and methane seepage due to dynamic evolution of GHSZ caused by climate change due in the Quaternary glacial-interglacial cycle. The formation time of submarine canyons on the continental slope of the Okinawa Trough was found to overlap with the start of the Eburonian epoch in North Europe and pre-Illinoian H epoch in North America. Especially, the seismogeologic characteristics, including MTDs associated with the BSRs, the gaps and fluid channels on the side-walls (through which gas could escape), the liquefaction deformation structures and the truncated relationship between the BSRs reflector and the submarine canyons all indicate that there is a complex relationship between the submarine canyons and the methane seepage associated with hydrate dynamic decomposition on the continental slope of the Okinawa Trough. Finally, a coupled model with four evolutional stages for the submarine canyons associated with gas hydrate was established.

Acknowledgments

This work is supported by the National Natural Science Foundation of China (Grant No. 41806073), the Fundamental Research Funds for the Central Universities (Grant No. 201964016), the Opening Foundation of Key Lab of Submarine Geosciences and Prospecting Techniques, MOE, Ocean University of China (Grant No. SGPT-2020OF-06) and the Natural Science Foundation of Shandong Province (Grant No. ZR2017BD014). We would like to thank professors San-Zhong Li of Ocean University of China and Zheng-Xiang Li of Curtin University, Australia for their scientific guidance and help during the article preparing process.

Data Availability

Datasets related to this article can be found at https://www.bodc.ac.uk/data//hosted_data_systems/gebco_gridded_bathymetry_data/ and http://www.ihfc-iugg.org/products/global-heat-flow-database/data, the open-source online data repositories hosted by British Oceanographic Data Centre and the International Heat Flow Commission, respectively. The original seismic images are included in the article.

References

Bangs, N.L., Hornbach, M.J., Moore, G.F., & Park, J.D. (2010). Massive methane release triggered by seafloor erosion offshore southwest Japan.*Geology* , *38* , 1019-1022.

Boswell, R. Frye, M., Shelander, D., Shedd, W., McConnell, D., & Cook, A. (2012). Architecture of gas-hydrate-bearing sands from Walker Ridge 313, Green Canyon 955, and Alaminos Canyon 21: Northern deepwater Gulf of Mexico. *Marine and Petroleum Geology* , *34* , 134-149.

Bozzano, G., Cerredo, M.E., Remesal, M., Steinmann, L., Hanebuth, T.J.J., Schwenk, T., Baques, M., Hebbeln, D., Spoltore, D., Silvestri, O., Acevedo, R.D., Spiess, V., Violante, R.A., & Kasten, S. (2020). Dropstones in the Mar del Plata Canyon area (SW Atlantic): evidence for provenance, transport, distribution, and oceanographic implications.*Geochemistry* , *Geophysics* , *Geosystems* , *22* , e2020GC009333. https://doi.org/10.1029/2020GC009333

Cao, H., Sun, Z.L., Wu, N.Y., Liu, W.L., Liu, C.L., Jiang, Z.K., Geng, W., Zhang, X.L., Wang, L.B., Zhai, B., Jiang, X.J., Liu, L.P., & Li, X. (2020). Mineralogical and geochemical records of seafloor cold seepage history in the northern Okinawa Trough, East China Sea. *Deep-Sea Research I* , *155* , 103165.

Catuneanu, O. (2002). Sequence stragraphy of clastic systems: concepts merits, and pitfalls. *Journal of African Earth Sciences* ,*35* , 1-43.

Chen, J. W. (2014). Formation Conditions and Resources Potential of Gas Hydrate in the Okinawa Trough of the East China. *Acta Geoscientica Sinica* , *35(6)* , 726-732.

Cohen, K.M., Finney, S.C., Gibbard, P.L., & Fan, J.X. (2013). The ICS International Chronostratigraphic Chart. *Episodes* , *36* , 199-204.

Cui, Z.J., Chen, Y.X., Zhang, W., Zhou, S.Z., Zhou, L.P., Zhang, M., & Li, C.C. (2011). Research history, glacial chronology and origins of Quaternary glaciations in China. *Quaternary Sciences* ,*31(5)* , 749-764.

Chiang, C. S., & Yu, H.S. (2006). Morphotectonics and incision of the Kaoping submarine canyon, SW Taiwan orogenic wedge.*Geomorphology* , *80* , 199-213.

Davies, R.J., Thatcher, K.E., Mathisa, S.A., & Yang, J. (2012). Deepwater canyons: An escape route for methane sealed by methane hydrate. *Earth and Planetary Science Letters* , *323-324* , 72-78.

de Stigter, H.C., Jesus, C.C., Boer, W., Richter, T.O., Costa, A., & van Weering, T.C.E. (2011). Recent sediment transport and deposition in the Lisbon-Setubal and Cascais submarine canyons, Portuguese continental margin. *Deep-Sea Research II* , *58* , 2321-2344.

Ding, W. W., Li, J.B., Li J., & Han, X. B. (2013). Formation process and controlling factors of the Pearl River Canyon in the South China Sea. *Journal of Tropical Oceanography* , *32(6)* , 63-72.

Ehlers, J., & Gibbard, P.L. (2007). The extent and chronology of Cenozoic global glaciation. *Quaternary International* ,*164-165* , 6-20.

Fan, D.J., & Yang, Z.S. (2004). Development and distribution of natural gas hydrate in the Okinawa trough. *Acta Petrolei Sinica* ,*25(3)* , 11-18.

Gao, S., & Collins, M.B. (2014). Holocene sedimentary systems on continental shelves. *Marine Geology* , *352* , 268-294.

Gong, C.L., Wang, Y.M., Zhu, W.L., Li, W.G., Xu, Qiang, & Zhang, J.M. (2011). The Central Submarine Canyon in the Qiongdongnan Basin, northwestern South China Sea: Architecture, sequence stratigraphy, and depositional process. *Marine and Petroleum Geology* , *28* , 1690-1702.

Gong, C.L., Steel, R.J., & Wang, Y.M. (2020). Channel-levee evolution in combined contour current-turbidity current flows from flume-tank experiments: Comment. *Geology* , DOI: 10.1130/G47508C.1.

Guan, H.X., Sun, Z.L., Mao, S.Y., Xu, L.F., Cao, H., Geng, W., Xu, C.L., Zhang, X.R., & Wu, N.Y. (2019). Authigenic carbonate formation revealed by lipid biomarker inventory at hydrocarbon seeps: a case study from the Okinawa Trough. *Marine and Petroleum Geology* , *101* , 502-511.

Hall, R. (2012). Late Jurassic-Cenozoic reconstructions of Indonesian region and the Indian Ocean. *Tectonopyhsics* , *570-571* , 1-41.

Han, W.C., Liu, C.S., Chi, W.C., Chen, L.W., Lin, C.C., & Chen, S.C. (2017). Westward advance of the deformation front and evolution of submarine canyons offshore of southwestern Taiwan. *Journal of Asian Earth Sciences* , *149* , 6-19.

Han, X.B., Li, J.B., Long, J.P., Chu, F.Y., Ding, W.W., Zhang, S.Y., Xu, D., & Yang, H.L. (2010). Development of research on submarine canyon in China. *Marine Geology Letters* , *26(2)* , 41-48.

Hao, T.Y., Liu, J.H., Guo, F., Huang, Z.X., Xu, Y., Dai, M.G., Li, A.C., & Fu, Y.T. (2004). Research on crustal structure and lithosphere property in the Okinawa Trough area. *Chinese Journal of Geophysics* , *47(3)* , 462-468.

Haq, B.U., Hardenbol, J., & Vail, P.R. (1987). Chronology of fluctuating sea levels since the Triassic. *Science* , *235* , 1156-1166.

Harris, P.T., & Whiteway, T. (2011). Global distribution of large submarine canyons: Geomorphic differences between active and passive continental margins. *Marine Geology* , *285* , 69-86.

He, Y., Zhong, G.F., Wang, L.L., & Kuang, Z.G. (2014). Characteristics and occurrence of submarine canyon-associated landslides in the middle of the northern continental slope, South China Sea. *Marine and Petroleum Geology* , *57* , 546-560.

Huh, C.A., Liu, J.T., Lin, H.L., & Xu, J.P. (2009). Tidal and flood signatures of settling particles in the Gaoping submarine canyon (SW Taiwan) revealed from radionuclide and flow measurements. *Marine Geology* , *267* , 8-17.

Hunt, D., & Tucker, M.E. (1995). Stranded parasequences and the forced regressive wedge systems tract: deposition during base-level fall-reply.*Sedimentary Geology* , *95* , 147-160.

Kopper, A.A.P., & Staudigel, H. (2005). Asynchronous bends in Pacific seamont trails: a case for extensional volcanism. *Science* ,*307* , 904-907.

Lambeck, K., & Chappell, J. (2001). Sea level change through the last glacial cycle. *Science* , *292* , 679-686.

Li, A., Davies, R., & Yang, J.S. (2016). Gas trapped below hydrate as a primer for submarine slope failures. *Marine Geology* , *380* , 264-271.

Li, A., Li, Q., Xu, C.L., Cai, F., & Wang, H.B. (2021a). Review of Methane Seepages in the Okinawa Trough: Progress and Outlook.*Geofluids* ,*https://doi.org/10.1155/2021/5539893*.

Li, A., Cai, F., Wu, N.Y., Li, Q., Yan, G.J., Sun, Y.B., Dong, G., Luo, D., & Wang, X.X. (2021b). Gas emissions in a transtensile regime along the western slope of the Mid-Okinawa Trough. *Frontiers in Earth Science* , *9* , 557634.

Li, D.Y., Chen, H.Y., Xu, S.J., Xing, J.H., Cheng, H.G., & Wang, J.K. (2019). Stratigraphic sequence and sedimentary systems in the Middle-Southern Continental Slope of the East China Sea from seismic reflection data: exploration prospects of gas hydrate. *Journal of Ocean University of China* , *18* , 1302-1316.

Li, G.X., Lin, P., Liu, Y., Qiao, L.L., Ma, Y.Y., Xu, J.S., & Yang, Z.G. (2014). Sedimentary system response to the global sea level change in the East China Seas since the last glacial maximum.*Earth-Science Reviews* , *139* , 390-405.

Li, G.X., Liu, Y., Yang, Z.G., Yue, S.H., Yang, W.D., & Han, X.B. (2004). Ancient Changjiang channel system in the East China Sea continental shelf during the last glaciation. *Science China D* ,*35 (3)* , 284-289.

Li, J.B. (2008). *East China Sea regional geology* . Beijing: Ocean Press,

Li, J.W., Peng, X.T., Bai, S.J., Chen, Z.Y., & Nostrand, J.D.V. (2018a). Biogeochemical processes controlling authigenic carbonate formation within the sediment column from the Okinawa Trough.*Geochimica et Cosmochimica Acta* , *222* , 363-382.

Li, J.Z., Liu, S.S., Zhang, J.L., Fan, Z.L., Sun, Z.Q., Zhang, M., Yuan, Y., & Zhang, P.H. (2015). Architecture and facies model in a non-marine to shallow-marine setting with continuous base-level rise: An example from the Cretaceous Denglouku Formation in the Changling Depression, Songliao Basin, China. *Marine & Petroleum Geology* , *68* , 381-393.

Li, Q., Cai, F., Liang, J., Shao, H.B., Dong, G., Wang, F., Yang, C.S., & Hu, G.W. 2015. Geochemical sonstraints on the methane seep activity in western slope of the middle Okinawa Trough, the East China Sea.*Science China: Earth Sciences* , *45(5)* , 676-687.

Li, S.Z., Yu, S., Zhao, S.J., Liu, X., Gong, S.Y., Suo, Y.H., Dai, L.M., Ma, Y., Xu, L.Q., Cao, X.Z., Wang, P.C., Sun, W.J., Yang, C., & Zhu, J.J. (2013). Tectonic transition and plate reconstructions of the East Asian continental margin. *Marine Geology and Quaternary Geology* ,*33* , 65-94.

Li, W., Alves, T.M., Urlaub, M., Georgiopoulou, A., Klaucke, I., Wynn, R.B., Gross, F., Meyer, M., Repschager, J., Berndt, C., & Krastel, S. (2017). Morphology, age and sediment dynamics of the upper headwall of the Sahara Slide Complex, Northwest Africa: Evidence for a large Late Holocene failure. *Marine Geology* , *393* , 109-123.

Li, W., Krastel, S., Alves, T.M., Urlaub, M., Mehringer, L., Schurer, A., Feldens, P., Gross, F., Stevenson, C.J., & Wynn, R.B. (2018b). The Agadir Slide offshore NW Africa: Morphology, emplacement dynamics, and potential contribution to the Moroccan Turbidite System. *Earth and Planetary Science Letters* , *498* , 436-449.

Li, W.R., Yang, Z.S., Wang, Q., Cao, L.H., Wang, Y.J., & Wang, X.L. (2001). Sedimentation of submarine fan in the Okinawa Trough.*Oceanologia et Limnologia Sinica* , *32(4)* , 371-380.

Li, W.X., & Zhou, X.M. (1999_. Late Mesozoic subduction zone of Southeastern China. *Geological Journal of China Universities* ,*5* , 164-169.

Li, X.S., Liu, B.H., Wu, J.L., Zhao, Y.X., & Wang, K.Y. (2004). Seismic reflection facies and deposit systems in the west slope of the Okinawa Trough. *Oceanologia et Limnologia Sinica* , *35(2)* , 120-129.

Li, Z.X., & Li, X.H. (2007). Formation of the 1300-km-wide intracontinental orogen and postorogenic magmatic province in Mesozoic South China: A flat-slab subduction model. *Geology* , *35* , 179-182.

Liu, M., Cui X.J., & Liu F.T. (2004). Cenozoic rifting and volcanism in eastern China: a mantle dynamic link to the Indo–Asian collision?*Tectonophysics* , *393* , 29-42.

Liu, B.H., Li, X.S., Zhao, Y.X., Zheng, Y.P., & Wu, J.L. (2005). Debris transport on the western continental slope of the Okinawa Trough: slumping and gravity flowing. *Oceanologia et Limnologia Sinica* ,*36(1)* , 1-9.

Liu, J.P., Kuehl, S.A., Pierce, A.C., Williams, J., Blair, N.E., Harris, C., Aung, D.W., Aye, Y.Y. (2020). Fate of Ayeyarwady and Thanlwin rivers sediments in the Andaman Sea and Bay of Bengal. *Marine Geology* ,*423* , 106137.

Liu, J.P., DeMaster, D.J., Nittrouer, C.A., Eidam, E.F., Nguyen, T.T. (2017). A sesmic study of the Mekong subaqueous delta: Proximal versus distal sediment accumulation. *Continental Shelf Research* ,*147* , 197-212.

Liu, J.S., Xu, H.Z., Jiang, Y.M., Wang, J., & He, X.J. (2020). Mesozoic and Cenozoic basin structure and tectonic evolution in the East China Sea basin. *Acta Geologica Sinica* , *94(3)* , 675-691.

Liu, Z.C., Liu, B.H., Huang, Z.Z., Zhu, B.D., Fu, M.Z., Yan, J., Zhang, X.H., & Zheng, Y.P. (2005). *Topography of China offshore and adjacent Sea* . Beijing: Ocean Press.

Lo Iacono, C., Sulli, A., & Agate, M. (2014). Submarine canyons of north-western Sicily (Southern Tyrrhenian Sea): Variability in morphology, sedimentary processes and evolution on a tectonically active margin. *Deep-Sea Research II* , *104* , 93-105.

Lu, Z.Q., Gong, J.M., Wu, B.H., Chen, J.W., & Deng, J. (2003). Geochemical perspective of gas hydrate in the East China Sea.*Marine Geology and Quaternary Geology* , *23(3)* , 77-81.

Luan, X.W., Lu, Y.T., Zhao, K.B., Sun, D.S., & Li, J. (2008). Geological factors for the development and newly advance in exploration of gas hydrate in East China Sea Slope and Okinawa Trough.*Geoscience* , *22(3)* , 342-355.

Luan, X.W., & Qin, Y.S. (2005). Discovery of the gas spring at the seabed of the Miyako segment in the Okinawa Trough. *Chinese Science Bulletin* , *50(8)* , 802-810.

Maslin, M., Owen, M., Day, S. & Long, D. (2004). Linking continental-slope failures and climate change: testing the clathrate gun hypothesis. *Geology* , *32* , 53-56.

Miles, P.R. (1995). Potential distribution of methane hydrate beneath the European continental margin. *Geophysical Research Letters* ,*22* , 3179-3182.

Mix, A.C., Bard, E., & Schneider, R. (2001). Environmental processes of the ice age: Land, oceans, glaciers (EPILOG). *Quaternary Science Reviews* , *20* , 627-657.

Muttoni, G., Carcano, C., Garzanti, E., Ghielmi, M., Piccin, A., Pini, R., Rogledi, S., & Sciunnach, D. (2003). Onset of major Pleistocene glaciations in the Alps. *Geology* , *31(11)* , 1574-1578.

Nakajima, T., Kakuwa, Y., Yasudomi, Y., Itaki, T., Motoyama, I., Tomiyama, T., Machiyama, H., Katayama, H., Okitsu, O., Morita, S., Tanahashi, M., & Matsumoto, R. (2014). Formation of pockmarks and submarine canyons associated with dissociation of gas hydrates on the Joetsu Knoll, eastern margin of the Sea of Japan. *Journal of Asian Earth Sciences* , *90* , 228-242.

Nazarian, R.H., Burns, C.M., Legg, S., Buijsman, M.C., Kaur, H., & Arbic, B.K. (2021). On the Magnitude of Canyon-Induced Mixing.*Journal of Geophysical Research: Oceans* , *126* , e2021JC017671. https://doi.org/10.1029/2021JC017671

Noguchi, S., Shimoda, N., Takano, O., Oikawa, N., Inamorim, T., Saeki, T., & Fujii,T. (2011). 3-D internal architecture of methane hydrate-bearing turbidite channels in the Eastern Nankai Trough, Japan.*Marine and Petroleum Geology* , *28* , 1817-1828.

Normandeau, A., Lajeunesse, P., & St-Onge, G. (2015). Submarine canyons and channels in the Lower St.Lawrence Estuary (Eastern Canada): Morphology, classification and recent sediment dynamics.*Geomorphology* , *241* , 1-18.

Orange, D.L., & Breen, N.A. (1992). The effects of fluid escape on accretionary wedges 2: Seepage force, slope failure, headless submarine canyons, and vents. *Journal of Geophysical Research* , *97* , 9277–9295.

Reading, H.G., & Richards, M. (1994). Turbidite systems in deep-water basin margins classified by grain size and feeder system. *AAPG Bulletin* , *78* , 792-822.

Shepard, F.P. (1981). Submarine canyons: Multiple causes and long-time persistence. *AAPG Bulletin* , *65* , 1062-1077.

Song, H.B. (2003). Researches on dynamic evolution of gas hydrate system (I): Its development in geological history. *Progress in Geophysics* , *18(2)* , 188-196.

Shi, Y.F., & Liu, D.S. (1964). Preliminary report of scientific expedition in the region of Mount Shishapangma. *Chinese Science Bulletin* , *10* , 928-938.

Su, M., Sha, Z.B., Kuang, Z.G., Qiao, S.H., Liang, J.Q., Yang, R., Wu, N.Y., & Cong, X.R. (2015). Erosion and sedimentation of the submarine canyons and the relationship with gas hydrate accumulation.*Geoscience* , *29(1)* , 155-162.

Su, M., Zhang, C., Xie, X.N., Wang, Z.F., Jiang, T., He, Y.L, & Zhang, C.M. (2014). Controlling factors on the submarine canyon systems: a case study of the central canyon system in the Qiongdongnan Basin, northern South China Sea. *Science China: Earth Sciences* , *44(8)* , 1807-1820.

Sun, Q.L., Alves T., Xie, X.N., He, J.X., Li, W., & Ni, X.L. (2017). Free gas accumulations in basal shear zones of mass-transport deposits (Pearl River Mouth Basin, South China Sea): An important geohazard on continental slope basins. *Marine and Petroleum Geology* ,*81* , 17-32.

Sun, Q.L., Cartwright, J., Xie, X.N., Lu, X.Y., Yuan, S.Q., & Chen, C.X. (2018). Reconstruction of repeated Quaternary slope failures in the northern South China Sea. *Marine Geology* , *401* , 17-35.

Sun, Z.L., Wei, H.L., Zhang, X.H., Shang, L.N., Yin, X.J., Sun, Y.B., Xu, L., Huang, W., Zhang, X.R., 2015. A unique Fe-rich carbonate chimney associated with cold seeps in the Northern Okinawa Trough, East China Sea. *Deep-Sea Research Part I* , *95* , 37-53.

Suzuki, K., Schultheiss, P., Nakatsuka, Y., Ito, T., Egawa, K., Holland, M., & Yamamoto, K. (2015). Physical properties and sedimentological features of hydrate-bearing samples recovered from the first gas hydrate production test site on Daini-Atsumi Knoll around eastern Nankai Trough. *Marine and Petroleum Geology* , *66* , 346-375.

Tubau, X., Paull, C.K., Lastras, G., Caress, D.W., Canals, M., Lundsten, E., Anderson, K., Gwiazda, R., & Amblas, D. (2015). Submarine canyons of Santa Monica Bay, Southern California: Variability in morphology and sedimentary processes. *Marine Geology* , *365* , 61-79.

Voigt, I., Henrich, R., Preu, B.M., Piola, A.R., Hanebuth, T.J.J., Schwenk, T., & Chiessi, C.M., (2013). A submarine canyon as a climate archive-Interaction of the Antarctic Intermediate Water with the Mar del Plata Canyon (Southwest Atlantic). *Marine Geology* , *341* , 46-57.

Walker, J.D., & Geissman, J.W., compilers, (2009). Geologic Time Scale: Geological Society of America, doi: 10.1130/2009.CTS004R2C

Walsh, J.P., Alexander, C.R., Gerber, T., Orpin, A.R., & Sumners, B.W. (2007). Demise of a submarine canyon? Evidence for highstand infilling on the Waipaoa River continental margin, New Zealand. *Geophysical Research Letters* , *34* , L20606. doi:10.1029/2007GL031142, 2007

Wang, D.W., Wu, S.G., Yao, G.S., & Wang, W.W., (2015a). Architecture and evolution of deep-water cyclic deposits in the Qiongdongnan Basin, South China Sea: Relationship with the Pleistocene climate events. *Marine Geology* , *370* , 43-54.

Wang, M., Cai, F., Li, Q., Liang, J., Yan, H.J., Dong, G., Wang, F., Shao, H.B., & Hu, G.W. (2015b). Characteristics of authigenic pyrite and its sulfur isotopes influenced by methane seep at core A, site 79 of the middle Okinawa Trough. *Science China: Earth Sciences* ,*45(12)* , 1819-1828.

Wang, M., Li, Q., Cai, F., Liang, J., Yan, G.J., Wang, Z., Sun, Y.B., Luo, D., Dong, G., & Cao, Y.M. (2019). Formation of authigenic carbonates at a methane seep site in the middle Okinawa Trough, East China Sea. *Journal of Asian Earth Sciences* , *185* , 104028.

Wang, Y.M., Xu, Q., Li, D., Han, J.H., Lv, M., Wang, Y.F., Li, W.G., & Wang, H.R. (2011). Late Miocene Red River submarine fan, northwestern South China Sea. *Chinese Science Bulletin* , *56(10)* , 781-787.

Webster, J.M., Beaman, R.J., Bernabeu, A. P., Ludman, D., Renema, W., Wust, R.A.J., George, N.P.J., Reimer, P.J., Jacobsen, G.E., & Moss, P. (2012). Late Pleistocene history of turbidite sedimentation in a submarine canyon off the northern Great Barrier Reef, Australia. *Palaeogeography* , *Palaeoclimatology* , *Palaeoecology* ,*331-332* , 75-89.

Wu, F.D., Li, S.T., Lu, Y.C., Li, P.L., Zhou, P., & Zhao, J.H. (1998a). The Tertiary sea-level changes in the East China Sea Shelf Basin. *Scientia Geologica Sinica* , *33(2)* , 214-221.

Wu, F.D., Lu, Y.C., Li, S.T., Xie, X.n., Li, P.L., Zhou, P., & Zhao, J.H. (1998b). Tertiary sequence stratigraphic framework and sea-level changes in the East China Sea Shelf Basin. *Earth Science-Journal of China University of Geosciences* , *23(1)* , 13-20.

Wu, S.G., & Qin, Y.S. (2009). The research of deepwater depositional system in the northern South China Sea. *Acta Sedimentologica Sinica* , *27(5)* , 922-930.

Wu, S.G., Dong, D.D., Yang, S.X., Zhang, G.X., Wang, Z.J., Li, Q.P., Liang, J.Q., Gong, Y.H., & Sun, Y.B. (2009). Genetic model of the hydrate system in the fine grain sediments in the northern continental slope of South China Sea. *Chinese Journal of Geophysics* ,*52(7)* , 1849-1857.

Wu, S.G., Qin, Z.L., Wang, D.W., Peng, X.C., Wang, Z.J., & Yao, G.S. (2011). Seismic characteristics and triggering mechanism analysis of mass transport deposits in the northern slope of the South China Sea. *Chinese Journal of Geophysics* , *54(12)* , 3181-3195.

Wu, S.G., & Sakamoto. (2001). Sedimentation and development of the Qianzhou Deep Sea Canyon in Philippines Sea. *Chinese Science Bulletin* , *46(supplement)* , 84-88.

Wu, Z.Y., Li, J.B., Jin, X.L., Shang, J.H., Li, S.J., & Jin, X.B. (2014). Distribution, features, and influence of the submarine topographic boundaries of the Okinawa Trough. *Science China: Earth Sciences* , *44(7)* , 1477-1487.

Xiang, R., Li, T.G., Yang, Z.S., Li, A.C., Jiang, F.Q., Yan, J., & Cao, Q.Y. (2003). Geological records of marine environmental changes in the southern Okinawa Trough. *Chinese Science Bulletin* , *48(1)* , 78-82.

Xie, H., Zhou, D., Li, Y.P., Pang, X., Li, P.C., Chen, G.H., Li, F.C., & Cao, J.H. (2014). Cenozoic tectonic subsidence in deepwater sags in the Pearl River Mouth Basin, northern South China Sea.*Tectonophysics* , *615-616* , 182-198.

Xie, X.N., Chen, Z.H., Sun, Z.P., Jiang, T., & He, Y.L. (2012). Depositional architecture characteristics of deepwater depositional systems on the continental margins of northwestern South China Sea.*Earth Science-Journal of China Univeristy of Geosciences* ,*37(4)* , 627-634.

Xie, X.N., Muller, R.D., Ren, J.Y., Jiang, T., & Zhang, C. (2008). Stratigraphic architecture and evolution of the continental slope system in offshore Hainan, northern South China Sea. *Marine Geology* ,*247* , 129-144.

Xu, C.L., Wu, N.Y., Sun, Z.L., Zhang, X.R., Geng, W., Cao, H., Wang, L.B., Zhang, X.L., & Xu, G.Q. (2018). Methane seepage inferred from pore water geochemistry in shallow sediments in the western slope of the Mid-Okinawa Trough. *Marine and Petroleum Geology* , *98* , 306-315.

Xu, C.L., Wu, N.Y., Sun, Z.L., Zhang, X.R., Geng, W., Cao, H., Wang, L.B., Zhang, X.L., & Zhai, B. (2020). Assessing methane cycling in the seep sediments of the mid-Okinawa Trough: insights from pore-water geochemistry and numerical modeling. *Ore Geology Reviews* ,*129* , 103909.

Xu, H., Cai, Y., Sun, H.Q., Yan, G.J., Wei, K., Zhao, X.W., Zhu, Y.R., Shi, J., Dong, G., & Li, Q. (2012). The survey status and geological conditions of accumulation of gas hydrate resource in the East China Sea. *Journal of Tropical Oceanography* , *32(4)* , 22-29.

Xu, J.P. (2013). Accomplishments and challenges in measuring turbidity currents in submarine canyons. *Advances in Earth Science* ,*28(5)* , 552-558.

Xu, J.P., & Noble, M.A. (2009). Currents in Monterey Submarine Canyon.*Journal of Geophysical Research* , *114* , C03004. doi:10.1029/2008JC004992

Xu, N., Wu, S.G., Shi, B.Q., Lu, B., Xue, L.Q., Wang, X.J., & Jia, Y. (2009). Gas hydrate associated with mud diapirs in southern Okinawa Trough. *Marine and Petroleum Geology* , *26* , 1413-1418.

Xu, S., Wang, Y.M., Peng, X.C., Zhou, H.Y., Qiu, Y., Gong, C.L., & Zuo H.T. (2014). Origin of Taiwan Canyon and its effects on deepwater sediment. *Science China: Earth Sciences* , *44(9)* , 1913-1924.

Yang, R.C., & Van Loon, A.J. (2016). Early Cretaceous slumps and turbidites with peculiar soft-sedimentart deformation structures on Lingshan Island (Qingdao, China) indicating a tensional tectonic regime.*Journal of Asian Earth Sciences* , *129* , 206-219.

Yang, W.D., Zeng, J.L., & Wang, Z.Y. (2004). Prospect of gas hydrate resources in the continental slope of the East China Sea. *Offshore Oil* , *24(2)* , 1-8.

Yin, S.R., Wang, L.L., Guo, Y.Q., & Zhong, G.F. (2015). Morphology, sedimentary characteristics, and origin of the Dongsha submarine canyon in the northeastern continental slope of the South China Sea.*Science China: Earth Sciences* , *45(3)* , 275-289.

Yu, H.S., & Hong, E. (2006). Shifting submarine canyons and development of a foreland basin in SW Taiwan: Controls of foreland sedimentation and longitudinal sediment transport. *Journal of Asian Earth Sciences* ,*27* , 922-932.

Zhang, B.X., Xu, Q.Q., & Shen, Y.P. (2002). The relationship between climate change and Quaternary glacial cycles on the Qinghai-Tibetan Plateau: review and speculation. *Quaternary International* ,*97-98* , 93-101.

Zhang, G.H., & Zhang, J.P. (2015). A discussion on the tectonic inversion and its genetic mechanism in the East China Sea Shelf Basin.*Earth Science Frontiers* , *22(1)* , 260-270.

Zhang, J.P., Zhang, T., & Tang, X.J. (2014). Basin type and dynamic environment in the East China Sea Shelf Basin. *Acta Geologica Sinica* , *88(11)* , 2033-2042.

Zhang, X.H., & Shang, L.N. (2014). Study on crustal structure and nature of the Okinawa Trough. *Periodical of Ocean University of China* , *44(6)* , 72-80.

Zhang, X.R., Sun, Z.L., Wang, L.B., Zhang, X.L., Zhai, B., Xu, C.L., Geng, W., Cao, H., Yin, X.J., & Wu, N.Y. (2020). Distribution and discharge of dissolved methane in the middle Okinawa Trough, East China Sea. *Frontiers in Earth Science* , *8* , 333.

Zhao, H.Q., Wu, S.G., Xu, N., Wang, X.J., & Zhang, G.X. (2006). The elementary research of gas hydrate associated with mud diapir structure in the East China Sea. *Geoscience* , *20(1)* , 115-122.

Zhao, Y.X., Liu, B.H., Li, X.S., Cui, A.J., Han, G.Z., Hua, Q.F., & Hu, G.H. (2011). Sedimentary characters and material transportation of submarine canyon-fan systems in slope of the East China Sea.*Journal of Palaeogeography* , *13(1)* , 119-126.

Zhao, Y.X., Liu, B.H., Li, X.S., Liu, C.G., Pei, Y.L., Wu, J.L., & Zheng, Y.P. (2009). Distributions of different submarine canyon on the East China Sea Slope and their tectonic response. *Advances in Marine Science* , *27(4)* , 460-468.

Zhong, S.L., Jiang, L., Li, B.H., & Wang, J.P. (2006). *Paleogene high-resolution biostratigraphy and sequence stratigraphy of the Taibei Depression in the East China Sea Shelf* . Beijing: Petroleum Industry Press.

Figure 1. Geographic location of the study area and the distribution of seismic reflection lines and well and heat flow stations. Seafloor temperature and heat flow data are from the global heal flow database (http://www.ihfc-iugg.org/products/global-heat-flow-database/data) published by the International Heal Flow Commission. Location of methane seeping points is derived from Wang et al. (2015b) and Li et al. (2015). Location of bottom simulating reflectors (BSRs) is derived from Luan et al. (2008). Location of mud diapirs associated with hydrates is derived from Xu et al. (2009). Location of submarine gas seepage is from Luan & Qi (2005). Location of methane seepages are from Sun et al. (2015), Li et al. (2015), Wang et al. (2015, 2019), Li et al. (2018a), Xu et al. (2018, 2020), Guan et al. (2019), Zhang et al. (2020), Cao et al. (2020), and Li et al. (2021b)

Figure 2. Cenozoic stratigraphic sequence in the East China Sea (Wu et al., 1998a, 1998b; Zhong et al., 2006; Xie et al., 2014; Zhang et al., 2014; Zhang & Zhang, 2015; Liu et al., 2020) and its sequence boundary age. The magnetostratigraphic data is derived from the 2009 Geologic Time Scale (Walker & Geissman, 2009). The global sea level curve and biostratigraphic data are modified from Haq et al. (1987), where the sequence boundary and biostratigraphic zone age are revised using the International Chronostratigraphic Chart (v2017/02; Cohen et al., 2013) and the 2009 Geologic Time Scale (Walker & Geissman, 2009).

Figure 3. Cenozoic stratigraphic sequence framework in the East China Sea established by reflection seismic line

Figure 4. Chronostratigraphic framework, stratigraphic structure, and surface identification marks of lines L1 (a) and L2 (b) on the central and southern slope of the Okinawa Trough (see Figure 1 for seismic line location). (c) and (d) provide zoomed images of the regressive unconformity and backstepped onlap formed by sea-level fall at the Last Glacial Maximum (LGM). The gap structures and chaotic, twisty, or imbricated reflections in (d) also indicate the leakage of methane-bearing fluid. LST: Lowstand systems tract; TST: Transgressive systems tract; HST: Highstand systems tract; and FSST: Falling stage systems tract.

Figure 5. Morphological structure, growth time, and erosional–depositional characteristics of submarine canyons in the central and southern slopes of the Okinawa Trough (see Figure 1. for seismic line location

and Figure 4. for legend). MTD:Mass transport deposit; BSRs:Bottom simulating reflections.

Figure 6. Topographic slope map of Okinawa Trough and its adjacent area based on the digital elevation model (https://www.bodc.ac.uk/data//hosted_data_systems/gebco_gridded_bathymetry_data/) and submarine canyons identification.

Figure 7. Submarine topographic map (a; modified from Wu et al., 2014) and multi-beam geomorphologic map (b; modified from Li, 2008) of submarine canyons C5 and C6 in the Okinawa Trough continental slope (see Figure 1 for location). (c) and (d) are thalweg and transverse topographic profiles based on digital elevation model (DEM) of submarine canyon C6, respectively. (e) and (f) are thalweg and transverse topographic profiles based on digital elevation model (DEM) of submarine canyons C5, respectively.

Figure 8. Seismic reflection characteristics of Bottom Simulating Reflectors (BSRs) and methane leakage on variable density and variable area profiles (see Figure 5 and Figure 1 for seismic line location).

Figure 9. Coupling evolution model of submarine canyon and gas hydrate in Okinawa Trough slope. BGHSZ: bottom of gas hydrate stability zone. (a) During the interglacial period in the Quaternary, the sea level was at a high-water stage. Under suitable temperature and pressure in the continental slope of the Okinawa Trough, the thermogenic or biogenic methane combined with water molecules to form hydrates. Of course, methane can also be leaked to the seabed through a fault. (b) Entering the glacial epoch, the sea level fell rapidly. With the change of seafloor temperature and pressure due to the sea level fall, the original hydrates decomposed and released extensive methane. Due to the rapid accumulation of methane-bearing fluid under the seabed, the sediments on the slope lost stability and slumped to form the prototype of the submarine canyons. (c) As the continuously sea level fall, under the influence of scour and retrogressive erosion of gravity flow that partly associated with hydrate decomposition, the submarine canyons strongly downcut the slope to form V-shaped or U-shaped channels. The gas hydrate stability zone also migrated to the deep. (d) During the low sea level stage, although the gas hydrate stability zone remained relatively stable, the canyon sidewalls continued to slump due to the erosion of turbidity current and the methane continuously leaked. The submarine canyons can even be connected to the channels formed by syndepositional faults or the ancient incised valleys to form a new canyon system.

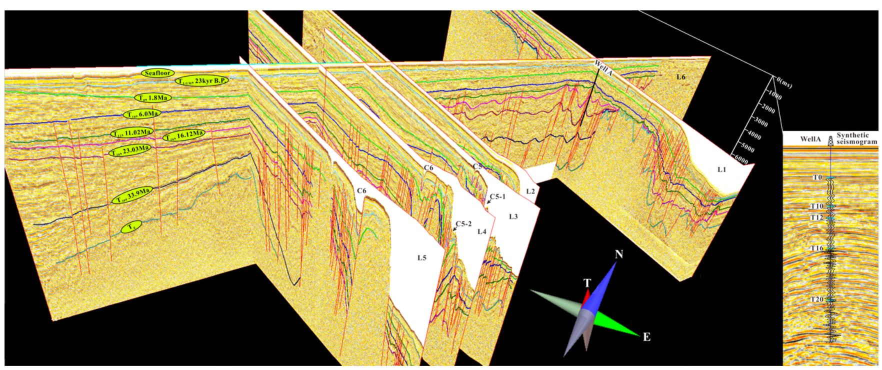

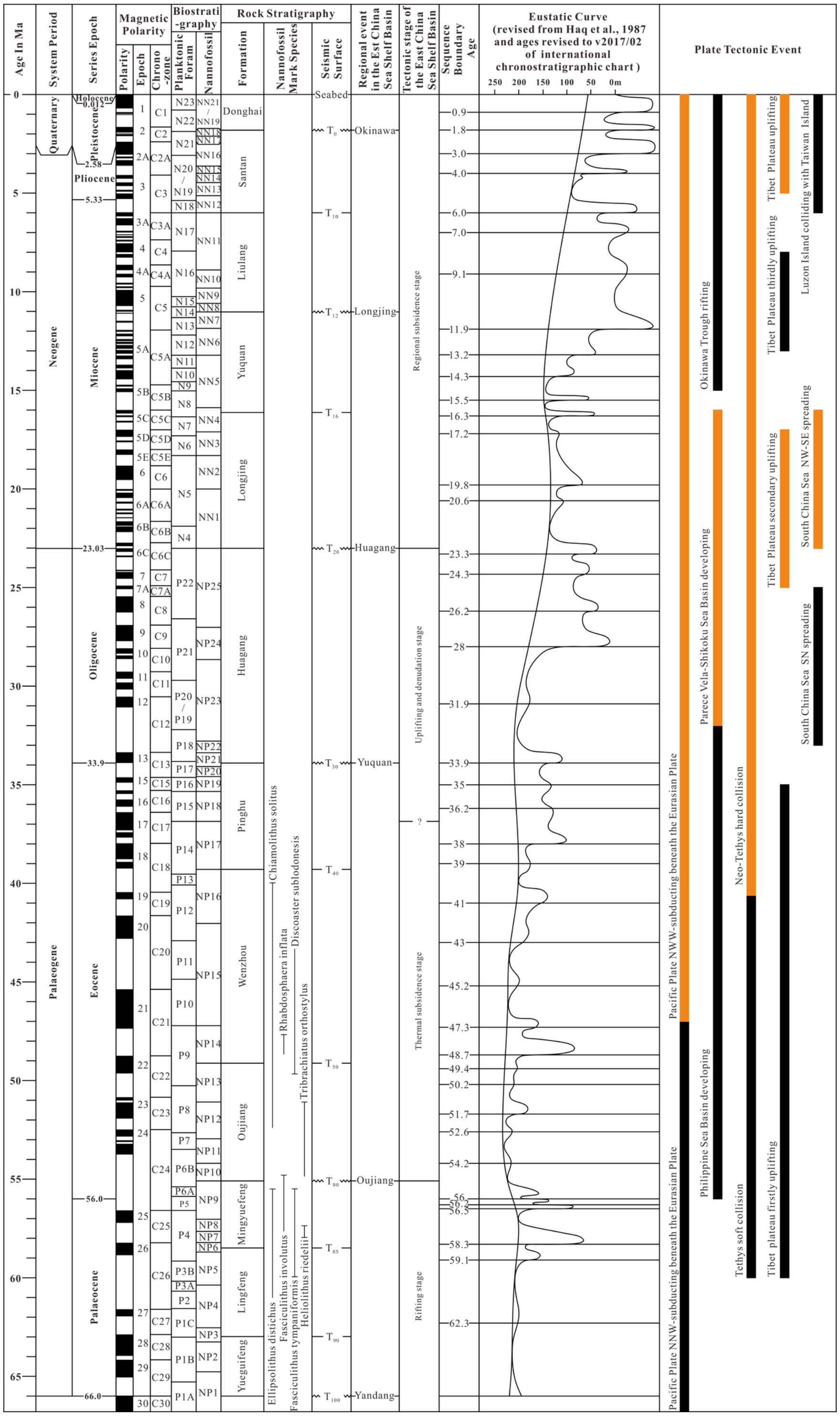
Age In Ma
System Period
Series Epoch
Magnetic Polarity
Polarity
Epoch
Chrono -zone
Biostrati -graphy
Planktonic Foram
Nannofossil
Rock Stratigraphy
Formation
Nannofossil Mark Species
Seismic Surface
Regional event in the Est China Sea Shelf Basin
Tectonic stage of the East China Sea Shelf Basin
Sequence Boundary Age
Eustatic Curve (revised from Haq et al., 1987 and ages revised to v2017/02 of international chronostratigraphic chart)
Plate Tectonic Event
Quaternary
Neogene
Palaeogene
Holocene
Pleistocene
Pliocene
Miocene
Oligocene
Eocene
Palaeocene
Donghai
Santan
Liulang
Yuquan
Longjing
Huagang
Pinghu
Wenzhou
Oujiang
Mingyuefeng
Lingfeng
Yueguifeng
Seabed
Okinawa
Longjing
Huagang
Yuquan
Oujiang
Yandang
Regional subsidence stage
Uplifting and denudation stage
Thermal subsidence stage
Rifting stage
Pacific Plate NNW-subducting beneath the Eurasian Plate
Okinawa Trough rifting
Parece Vela-Shikoku Sea Basin developing
Philippine Sea Basin developing
Neo-Tethys hard collision
Tethys soft collision
Tibet Plateau uplifting
Tibet Plateau thirdly uplifting
Tibet Plateau secondary uplifting
Tibet plateau firstly uplifting
Luzon Island colliding with Taiwan Island
South China Sea NW-SE spreading
South China Sea SN spreading

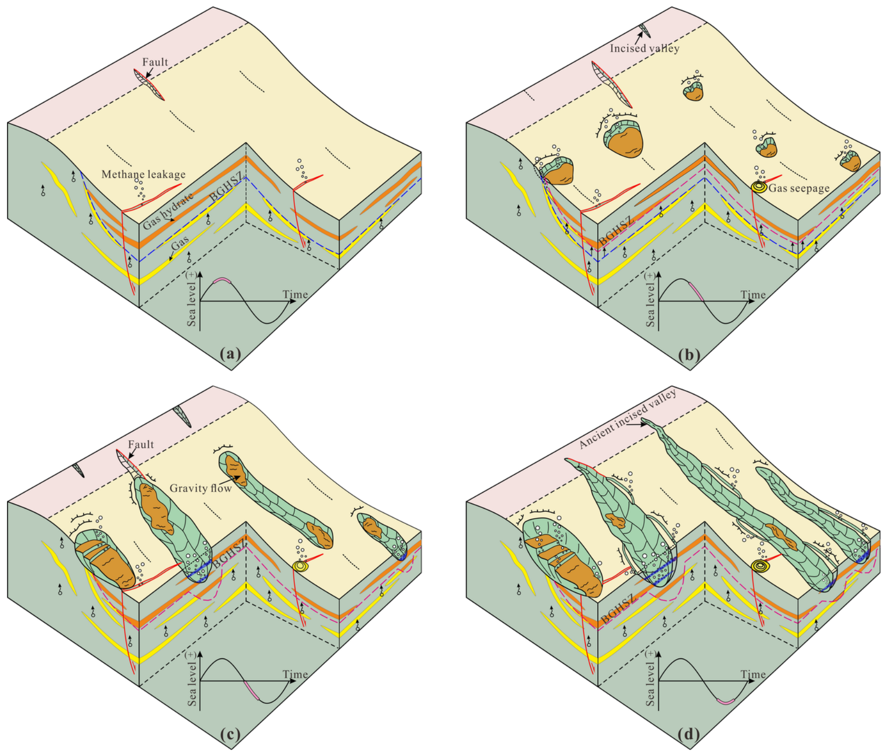
Fault
Methane leakage
Gas hydrate
BGHSZ
Gas
Sea level (+)
Time
(a)
Incised valley
Gas seepage
BGHSZ
Sea level (+)
Time
(b)
Fault
Gravity flow
BGHSZ
Sea level (+)
Time
(c)
Ancient incised valley
BGHSZ
Sea level (+)
Time
(d)

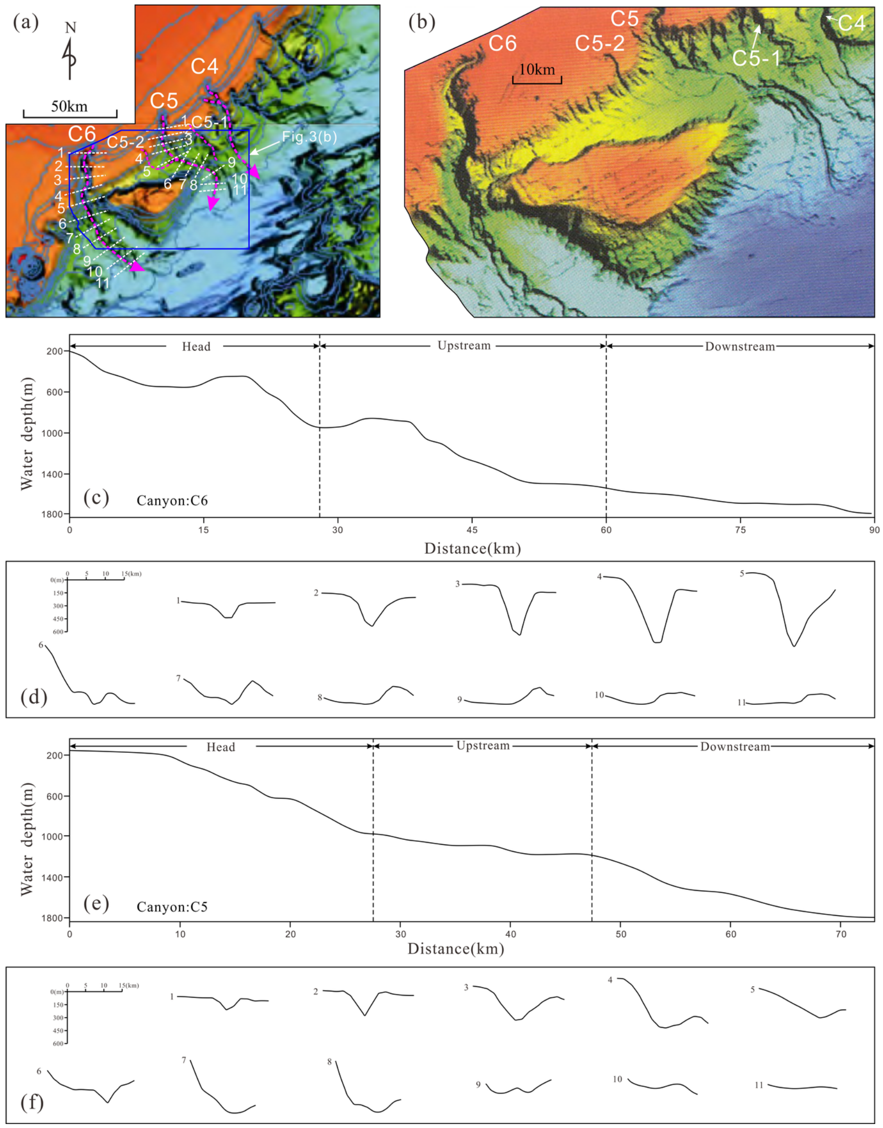
(a)
N
50km
C4
C5
C6
C5-1
C5-2
Fig.3(b)
(b)
C6
C5-2
C5
C5-1
C4
10km
(c)
Canyon:C6
Head
Upstream
Downstream
Water depth(m)
Distance(km)
(d)
(e)
Canyon:C5
Head
Upstream
Downstream
Water depth(m)
Distance(km)
(f)

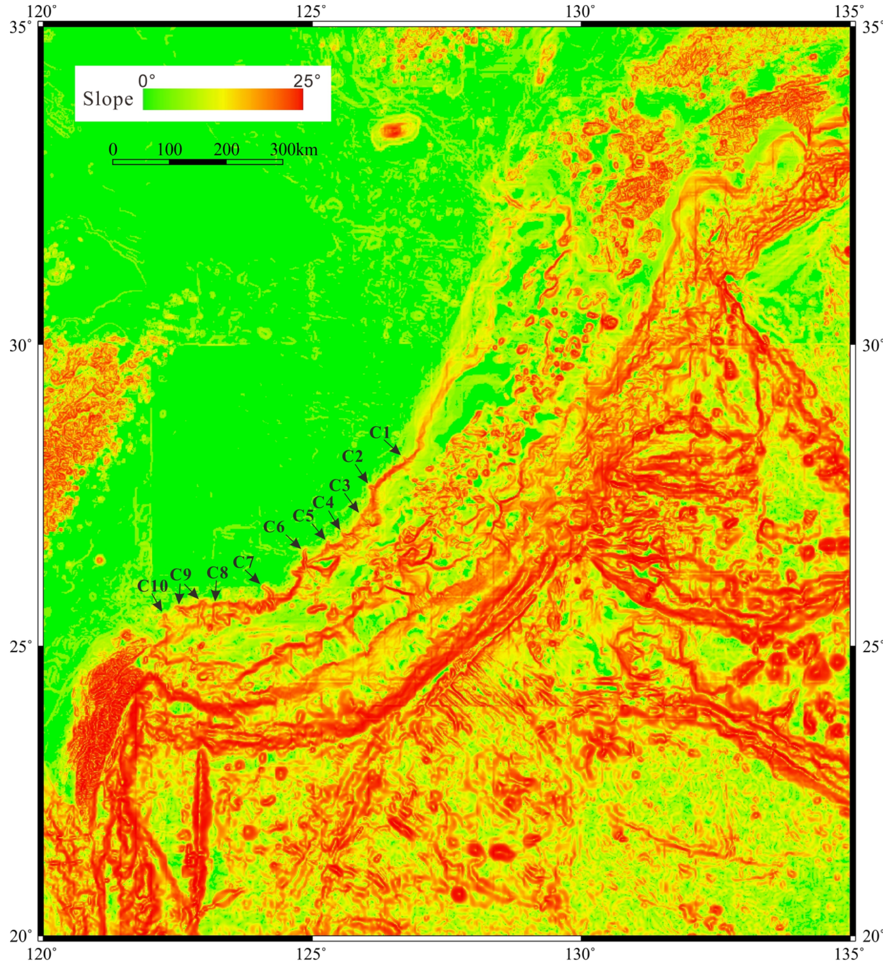
Slope
0°
25°
0
100
200
300km
C1
C2
C3
C4
C5
C6
C7
C8
C9
C10
120°
125°
130°
135°
35°
30°
25°
20°

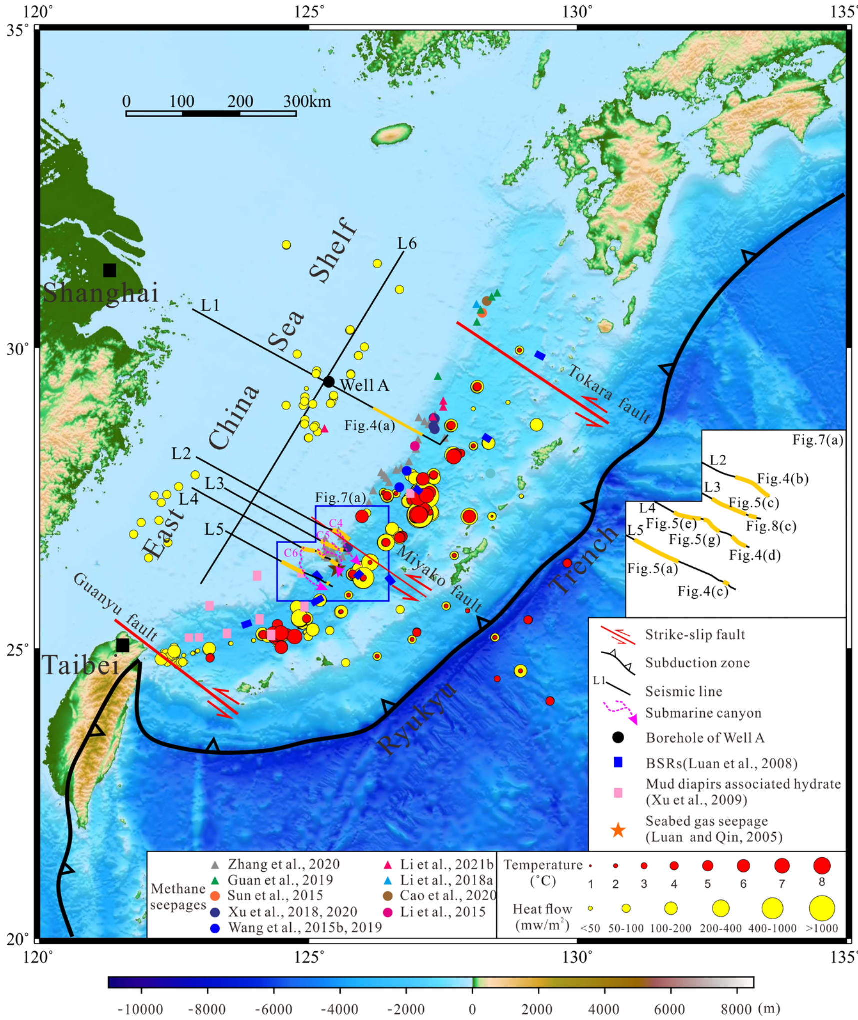

Shanghai
Taibei
East China Sea Shelf
Well A
L1
L2
L3
L4
L5
L6
Fig.4(a)
Fig.7(a)
Tokara fault
Miyako fault
Guanyu fault
Ryukyu Trench
0 100 200 300km
Fig.4(b)
Fig.5(c)
Fig.8(c)
Fig.5(e)
Fig.5(g)
Fig.4(d)
Fig.5(a)
Fig.4(c)
Strike-slip fault
Subduction zone
Seismic line
Submarine canyon
Borehole of Well A
BSRs(Luan et al., 2008)
Mud diapirs associated hydrate (Xu et al., 2009)
Seabed gas seepage (Luan and Qin, 2005)
Methane seepages
Zhang et al., 2020
Guan et al., 2019
Sun et al., 2015
Xu et al., 2018, 2020
Wang et al., 2015b, 2019
Li et al., 2021b
Li et al., 2018a
Cao et al., 2020
Li et al., 2015
Temperature (°C)
Heat flow (mw/m²)
<50 50-100 100-200 200-400 400-1000 >1000
120° 125° 130° 135°
35° 30° 25° 20°
-10000 -8000 -6000 -4000 -2000 0 2000 4000 6000 8000 (m)

Deyong Li[1], Jie Liang[2] Honggang Cheng[3], Gang Dong[2] Xiting Liu[1], Shujuan Xu[3], Chaoyang Li[4], Xiaodian Jiang[1]

[1]Key Laboratory of Submarine Geosciences and Prospecting Techniques, MOE, Laboratory for Marine Mineral Resources, Qingdao National Laboratory for Marine Science and Technology, College of Marine Geosciences, Ocean University of China, Qingdao 266100, China.

[2]Key laboratory of Marine Hydrocarbon Resources and Environment Geology, Ministry of Natural Resources, Laboratory for Marine Mineral Resources, Qingdao National Laboratory for Marine Science and Technology, Qingdao Institute of Marine Geology, Qingdao 266071, China.

[3]Research Institute of Petroleum Exploration & Development, Beijing 100083, China.

[4]College of Earth Science and Enginering, Shandong University of Science and Technology, Qingdao, Shandong 266590, China.

Corresponding author: Deyong Li (ldyc411@ouc.edu.cn) , Jie Liang (cgsljie@mail.cgs.gov.cn)

Key Points:

- The submarine canyons on the continental slope of Okinawa Trough began to develop in the early Pleistocene (< 1.8 Ma), and continued to develop even today.
- The canyons are mainly related to the gravity flow, syngenetic fault, sea-level eustacy, and methane seepage associated with hydrate dynamic accumulation.
- A coupled model with four evolutional stages for submarine canyons associated with methane seepage related to gas hydrate dynamic accumulation was established..

Abstract

Submarine canyons are of great significance to understand the transport mechanism of terrigenous clastic materials to deep sea and the deep-sea sedimentary dynamic process. In this study, the spatiotemporal framework of stratigraphic sequence in the central and southern slopes of the Okinawa Trough was established, and the geomorphological and erosional-depositional features of submarine canyons were analyzed detailedly. The submarine canyons on the continental slope of Okinawa Trough began to develop in the early Pleistocene (< 1.8 Ma), and continued to develop even today. The canyons could be divided into three parts along the axial direction: head, upstream, and downstream. The head of the canyon was mostly inherited from the ancient incised valley developed on the outer continental shelf during the last glacial maximum (LGM). The canyon channel was filled with multi-stage turbidites and mass transport deposits (MTDs). The seismogeologic characteristics, such as the MTDs associated with the bottom simulating reflectors (BSRs), the imbricated, twisty or chaotic seismic reflections, the liquefaction deformation structures, the fluid transport channels, and the gaps that indicate methane escaping on the side walls, and the truncated relationship between the BSRs and the submarine canyons all indicate that there is a complex relationship between the submarine canyons and the methane seepage associated with gas hydrate in the Okinawa Trough. Finally, a coupled model with four evolutional stages for the submarine canyons was established.

1 Introduction

Submarine canyons are an important transport channel for sediments from source to sink (de Stigter et al., 2011; Xu, 2013; Xu et al., 2014; Su et al., 2014; Tubau, et al., 2015; Bozzano et al., 2020; Liu et al., 2020), which control the transport and accumulation of terrigenous clastic material from land to deep sea (Shepard, 1981; Wu & Sakamoto, 2001; Harris & Whiteway, 2011). As an important part of deep-water sedimentary system, the formation and evolution of submarine canyons also record crucial geological information about the regional sea-level eustacy, climate change, and tectonic activities (Wang et al., 2011, 2015a; Xie et al., 2012; Voigt et al., 2013; Gao & Collins, 2014; Han et al., 2017). Meanwhile, due to the vibrant hydrodynamic conditions of turbidity currents, submarine canyons have become an important carrier and potential inducer of submarine landslide hazard (Webster et al., 2012; He et al., 2014; Sun et al., 2018; Nazarian et al., 2021).

The formation of submarine canyon often undergoes a long evolutionary process and influenced by many factors (Han et al., 2010; Gong et al., 2011; Su et al., 2014), such as tectonic activity (earthquake, volcanism, fault, and diapir; Wu & Sakamoto, 2001; Chiang & Yu, 2006; Yu & Hong, 2006; Ding et al., 2013; Yang & Van Loon, 2016; Han et al., 2017), climate change (sea-level eustacy, typhoon, and sediment supply; Huh et al., 2009; Ding et al., 2013; Xu, 2013; Tubau et al., 2015), and deep-sea sedimentary process (gravity flow and contour current; Xie et al., 2008; Han et al., 2010; Xu, 2013). Tectonic dynamic shapes the topography of continental margins from shelf to slope, and provides favorable topographic conditions for the development of submarine canyons (Normandeau et al., 2015). Especially, the faults break the bedrock and induce gravity flow to preferentially erode the fractured zone, which ultimately affects the canyon path (Chiang & Yu, 2006; Xu et al., 2014). Although accidental earthquakes and volcanic activities cannot exert continuous influence on submarine canyons, they provide abundant pyroclastic sources for gravity flow and are one of the main factors that induce mass flow and turbidity erosion in the canyon (Wu & Sakamoto, 2001; de Stigter et al., 2011). The erosion of mass-flow or turbidity current on shelf and slope are considered as the most important mechanisms for the formation and evolution of submarine canyons (Xu, & Noble, 2009; Harris & Whiteway, 2011; Xu et al., 2013; Lo Iacono et al., 2014; Su et al., 2014). Additionally, the numerical simulation also proves that the headward erosion of gravity flow plays a key role in the formation of submarine canyons (Harris & Whiteway, 2011; Xu, 2013; Lo Iacono et al., 2014). Notably, the global sea-level fall caused by the Quaternary glacial cycle is of great significance to the development of submarine canyons (Harris & Whiteway, 2011; Gong et al., 2011; Su et al., 2014; Xu et al., 2014; Tubau et al., 2015). For example, along with the ancient sea level dropped to the current water depth of 120–150 m during the LGM (Lambeck & Chappell, 2001; Li et al., 2014), the East China Sea continental shelf was exposed and eroded extensively, and subsequently, terrestrial rivers extended and carried a large amount of sediment directly to the shelf edge (Li et al., 2004, 2014). The rapid supply of sediment induced mass instability and formed an erosive turbidity flow downward along the continental slope, which caused canyon downcutting (Gao & Collins, 2014; Lo Iacono et al., 2014; Li et al., 2014; Xu et al., 2014; Yin et al., 2015). However, for the slope rich in gas hydrates, it is more important that the changes of temperature and pressure caused by sea-level fall will induce the large-scale decomposition of hydrates (Song et al., 2003; Wu et al., 2009; Nakajima et al., 2014). And the subsequent escape and leakage of methane-bearing fluid to the seabed can trigger slope instability and induce turbidity currents, which promotes the formation of submarine canyons, even leading to large-scale submarine landslides (Wu et al., 2011; Nakajima et al., 2014; Li et al., 2016). Some researchers believe that methane fluid leakage is the main cause of the formation of blind canyons (Orange & Breen, 1992).

Submarine canyons and methane seepages associated with gas hydrates are the most important geological features of the Okinawa Trough (Luan & Qin, 2005; Liu et al., 2005; Li, 2008). The submarine canyons are mainly developed on the central and southern continental slopes of the Okinawa Trough, all of which are shelf-incising canyons (whose heads are not connected to a terrestrial river) or slope-confined canyons (blind or headless canyons) (Li, 2008; Zhao et al., 2011; Wu et al., 2014). Liu et al. (2005), Li (2008), and Zhao et al. (2011) believed that faults are the dominant factor that control the formation and distribution of submarine canyons on the continental slope of the Okinawa Trough, which explains the genesis of submarine canyons associated with fault. However, the submarine canyons unrelated to faults and the discovery of gravity flow deposition inside the canyons show that the role of gravity flow in the formation and evolution of submarine canyons cannot be ignored (Li et al., 2001; Liu et al., 2005; Zhao et al., 2009; Li et al., 2019). Many geological and geophysical indicators for methane-bearing fluid seepage related to gas hydrate in the Okinawa Trough have been reported, such as methane leakage and associated cold seep carbonate (Luan & Qin, 2005; Sun et al., 2015; Li et al., 2018a; Guan et al., 2019; Wang et al., 2019; Zhang et al., 2020; Cao et al., 2020; Li et al. 2021a, 2021b), mud diapir and volcano (Zhao et al., 2006; Xu et al., 2009), methane anomaly in pore water, water column and even sediments (Lu et al., 2003; Li, 2008; Wang et al., 2015b; Li et al. 2015; Xu et al., 2018, 2020; Zhang et al., 2020), and bottom simulating reflectors (BSRs; Luan et al., 2008; Xu et al., 2009, 2012; Chen, 2014; Li et al., 2019). Notably, some methane seep sites and associated cold seep carbonates had been successfully discovered on the northern slope of the Okinawa Trough using remotely operated underwater vehicle (ROV; Wang et al., 2019; Cao et al., 2020; Zhang et al., 2020; Li et al., 2021a). The extremely negative carbon isotopic and positive oxygen isotopic compositions of the cold seep carbonates suggest that the carbon in the carbonates was mainly derived from biogenic methane coupled with sulfate-dependent anaerobic oxidation of methane and the fluid flow from which carbonate precipitated is sourced from dissociation of gas hydrates (Wang et al., 2019; Cao et al., 2020). Cao et al. (2020) proposed that during sea level fall in the late Pleistocene (22.8–55.7 ka BP), gas hydrate decomposed and released extensive methane, resulting in the precipitation of cold seep carbonate. Nakajima et al. (2014) linked the origin of the Joetsu Knoll submarine canyon in the Sea of Japan to the pockmark formed by the decomposition of gas hydrates during the LGM and believed that the submarine canyon formation is the result of turbidity erosion caused by the overflow of methane-bearing sand or mud fluid during the formation of the pockmark. For the submarine canyons developed on the continent slope of the Okinawa Trough, which are far from the estuary of continental rivers, when and why they started to form will be the focus of this paper. Furthermore, whether the formation and evolution of submarine canyons are related to the methane-bearing fluid activity associated with gas hydrate, is also an issue that we attempt to clarify. However, so far, the lack of observation data and drilling sample are still the biggest obstacle to understand this scientific problem.

In this paper, we have carried out a detailed study of seismic stratigraphy, geomorphology, and seismosedimentology using reflection seismic profiles, well logging, and topographic data. The sequence stratigraphic framework in the continental slope of the Okinawa Trough was established, and consequently, the startup times of the submarine canyons was determined. Through the analysis of seismosedimentological characteristics and controlling factors of submarine canyons on the continental slope of the Okinawa Trough, we boldly gave a new and potential genetic model of submarine canyons related to gas hydrate dynamic accumulation due to the Quaternary glacial-interglacial cycle. Our work is not only useful for understanding the genetic mechanism of submarine canyons, but also of great significance to the prediction and exploitation of gas hydrate in the future.

2 Geological setting

The Okinawa Trough is located to the east of the continental shelf of East China Sea and in the west of the Ryukyu Island Arc. It connects with Yilan County of Taiwan in the southwest and Kyushu Islands of Japan in the northeast. The Okinawa Trough and East China Sea Shelf Basin (ECSSB) are separated by the Diaoyu Islands uplift-fold belt. The Okinawa Trough is an important part of the trench–arc–basin system in the western Pacific active continental margin and is still an active back-arc extensional basin (Figure 1). Separated by the NW-trending Tokara and Miyako faults, the trough is divided into three segments: northern, central, and southern parts, which show the “wide”, “hot”, and “deep” features, respectively (Hao et al., 2004; Luan & Qin, 2005; Xu et al., 2012; Wu et al., 2014). The northern section of the Okinawa Trough is NNE-trending, with a width of 230 km and water depth of 200–1000 m (Wu et al., 2014), and filled with thick Miocene–Quaternary strata (Li et al., 2004, 2019). The central section is NE-trending, with a water depth of 1000–2000 m (Wu et al., 2014), and is characterized by high heat flow, high geothermal gradient, and strong hydrothermal and earthquake activities (Luan et al., 2008; Xu et al., 2012). Its average heat flow is 590 mW/m^2 (Xu et al., 2009, 2012). The southern section is NEE–EW-trending, with the deepest water depth over 2000 m (Wu et al., 2014), and has the highest degree of crust extension, with crust thickness of only 15 km in the Yaeyama Graben (Hao et al., 2004; Zhang & Shang, 2014). Submarine magnetic anomaly belts and polarity events, such as the Brunhes, Jaramillo, and Olduvai polarity reversals, indicate that the southern trough has entered the stage of sea-floor spreading and oceanic crust forming (Zhang & Shang, 2014).

For the East China Sea Shelf Basin with abundant hydrocarbon resources, petroleum geologists had determined the stratigraphic sequence of the basin (formations of Yueguifeng, Lingfeng, Mingyuefeng, Oujiang, Wenzhou, Pinghu, Huagang, Longjing, Yuquan, Liulang, Santan, and Donghai; Figure 2; Zhang et al., 2014; Zhang & Zhang, 2015; Liu et al., 2020) and defined the corresponding seismic reflection interfaces (T_0, T_{10}, T_{12}, T_{16}, T_{20}, T_{30}, T_{40}, T_{50}, T_{80}, T_{85}, T_{90}, and T_{100}; Figure 2) among which T_0, T_{12}, T_{20}, T_{30}, T_{80}, T_{85}, and T_{100} were all regional unconformities (Zhang et al., 2014; Zhang & Zhang, 2015; Liu et al., 2020), comprehensively using seismic and well data. This provided an important basis for stratigraphic tracking in the continental slope of the Okinawa Trough (Li et al., 2019). Li et al. (2004) and Li (2008) identified two regional unconformities (equivalent to the Quaternary bottom boundary (T_0) and the Pliocene bottom boundary (T_{10}) in the East China Sea Shelf, respectively) and divided five seismic sequences (Ua, Ub, Uc, Ud, and Ue) in the Okinawa Trough using seismic and shallow seismic profiles. Moreover, they interpreted the sedimentary strata from top to bottom as: the argillaceous silt, semi-deep-sea turbidite, and clay of Holocene; shallow marine terrigenous sand, semi-deep-sea mud, and tuffaceous mud of Pleistocene; dolomitic mudstone, sandstone, and volcanic rocks of Pliocene; and transitional sandstone, mudstone, and tuff of Miocene (Li et al., 2004; Li, 2008). However, Luan et al. (2008) only used reflection seismic to divide the sedimentary strata in the continental slope of the Okinawa Trough into five seismostratigraphic units (A–E) which were speculated as the sedimentary formations of Late Miocene–Quaternary (A), Oligocene–Miocene (B–C), Eocene (D), and Paleocene (F), respectively. Li et al. (2019) tracked the stratigraphic distribution from the East China Sea Shelf Basin to the continental slope using sequence stratigraphic and well-seismic calibration technologies. They identified six sequence boundaries and finally determined that the oldest strata deposited in the continental slope of the Okinawa Trough was the Lower Miocene formation, or even earlier (Li et al., 2019).

The Okinawa Trough is the result of the interaction of subduction, collision, back-arc spreading between the Pacific–Philippine Sea Plate and the Eurasian Plate, and the far-field effect of convergence, collision, and wedging between the Indian–Australian plate and the Eurasian plate (Li et al., 2007, 2013; Hall, 2012). In the Late Cretaceous, the Pacific Plate subducted under the Eurasian Plate in the NNW- direction, and the subduction angle gradually increased to 80° (Li & Zhou, 1999). The high-angle subduction and rollback of the plate made the Pacific subduction zone retreat and jump eastward (Li et al., 2007, 2013; Hall, 2012). Then, the East China Sea Shelf rifted into a NE-trending half-graben (Liu et al., 2004; Zhang et al., 2014; Liu et al., 2020), forming the prototype of the ECSSB. In the Cenozoic, with the retreat of the Pacific Plate and the uplift of the Qinghai-Tibetan Plateau, the ECSSB continuously back-arc rifted until the end of Oligocene and was filled with thick Paleogene strata (Li et al., 2013; Zhang et al., 2014; Liu et al., 2020). After the formation of the Shikoku–Parece Vela Basin in the Middle Miocene, the Pacific subduction zone jumped from the Ryukyu Island Arc to the Izu–Bonin–Mariana Trench, and the Okinawa Trough began to back-arc spreading, which caused the Ryukyu Island Arc to break away from the East Asia continental margin (Li et al., 2013). At this time, the ECSSB had entered depression stage. Since then, the Okinawa Trough continuously back-arc rifted. The discovery of pillow basalt in the central and southern trough indicates that the mantle-derived material has been directly exposed to the seabed (Hao et al., 2004; Zhang & Shang, 2014).

3 Data set and method

Six 2D reflection seismic profiles (inline L1–L5 and crossline L6) across the continental shelf and slope of the East China Sea, logging data of Well A (located on the seismic line L1), digital elevation model (DEM), seabed temperature, heat flow, and paleontological chronostratigraphic data of the ECSSB constitute the data set of this study. The total length of 2D seismic lines is about 2390 km, and the dominant frequency ranges from 20 HZ to 30 HZ. The resolution of these seismic data used for submarine canyons is between 12–18 m. Well A is located in the ECSSB and reveals Oligocene–Quaternary strata sequence (Huagang, Longjing, Yuquan, Liulang, Santan, and Donghai formations, from bottom to top). Although we published the sequence stratigraphic results of seismic line L1 (Li et al., 2019), based on seismogram synthesizing and horizon calibrating, we further revised and tracked the sequence stratigraphic boundaries on seismic line L1–L5 from the East China Sea Shelf to the Okinawa Trough. Sequentially, we established the isochronous stratigraphic framework of the study area and determined the age of stratigraphic boundaries on the seismic profiles, based on the comparison and revision of the biostratigraphic data of the East China Sea Shelf Basin (Wu et al., 1998a, 1998b; Zhong et al., 2006), the 2009 geologic time scale (Walker & Geissman, 2009), the updated international chronostratigraphic chart (v2017/02; Cohen et al., 2013), and magnetostratigraphic–biostratigraphic–chronostratigraphic sequence stratigraphic results (Haq et al., 1987).

As the age and magnetic chronology of the stratigraphic boundaries were slightly different in the chronostratigraphic tables published in different years or by different researchers, and the international chronostratigraphic chart (v2017/02; Cohen et al., 2013) did not provide the magnetic chronology, we firstly assumed that the magnetic chronology in the 2009 geologic time scale (Walker & Geissman, 2009) is consistent with the stratigraphic division in the International Chronostratigraphic Chart (v2017/02; Cohen et al., 2013). Then, based on the sparse stratigraphic ages provided by the international chronostratigraphic chart (v2017/02; Cohen et al., 2013), the ages of magnetic polarity zones in the 2009 Geologic Time Scale (Walker & Geissman, 2009) were determined using interpolation method. Sequentially, the ages of stratigraphic boundaries, sequence boundaries, and biostratigraphic zones provided by Haq et al. (1987) were revised using the new ages of magnetic polarity zones calculated from the previous step. Finally, based on the paleontological and lithostratigraphic data of the ECSSB (Wu et al., 1998a, 1998b; Zhong et al., 2006; Xie et al., 2014) and its revision with the result of Haq et al. (1987), we established the Cenozoic chronostratigraphic table applicable to the East China Sea region (Figure 2). The ages of stratigraphic boundaries and sequence boundaries in Haq's eustatic curve were also determined.

The principle and method implemented for sequence stratigraphy analysis were as follows: (1) By comparing the lithostratigraphic, paleontological, and logging data of Well A with the chronostratigraphic table of the East China Sea, we firstly determined the ages of the stratigraphic boundaries of Well A; (2) Using the density and acoustic logging data of Well A, a synthetic seismogram that used for the seismic horizon calibration on line L1 was made. Then, based on our previous research results (Li et al., 2019) and the Cenozoic chronostratigraphic table (Figure 2), we further revised and redetermined the geological horizons and ages of the seismic reflection interfaces (e.g., seafloor, T_0, T_{10}, T_{12}, T_{16}, T_{20}, T_{30}) on the line L1. And finally, the isochronal seismic stratigraphic framework on line L1 was established (Figure 3). In addition, the T_{LGM} interface [the maximum regressive surface formed by the rapid sea level fall in the East China Sea during the LGM (23 kyr B.P.)] was determined by the identification of a set of regressive parasequence groups and a series of backstepping onlap points on the seismic profiles due to the sea level rise after the LGM (Figure 4); (3) The seafloor, T_{LGM}, T_0, T_{10}, T_{12}, T_{16}, T_{20}, T_{30}, and T_g on the inline L1 were tracked from shelf to slope by using seismic wave parameters, such as frequency, amplitude, seismic event continuity, reflection termination styles, internal structure, and external geometry of seismic reflection units. Then, the seismic horizons on the inline L1 were tracked to the L2, L3, L4, and L5 inlines through the crossline L6. And finally, the isochronal stratigraphic framework of the Okinawa Trough was established. Notably, the T_{12}, T_{16}, T_{20}, T_{30}, and T_g interfaces on the seismic profiles could not be tracked continuously from the shelf to the slope due to the Diaoyu Island Uplift. These seismic interfaces were identified based on the theory and method of sequence stratigraphy. They were comprehensively determined by identifying the unconformities (or its corresponding correlative conformities) and reflection termination symbols (onlap, downlap, toplap, truncation, offlap, progradation, retrogradation, incision, and marine erosion) of the 4^{th}-order sequence boundaries, such as maximum regressive surface, basal surface of forced regression, and maximum flooding surface, as well as the spatial characteristics and superimposed styles of lowstand systems tract (LST), transgressive systems tract (TST), highstand systems tract (HST), and falling stage systems tract (FSST; Figure 4). The terminology of sequence stratigraphy and sedimentology used in this study mainly refers to the concepts and principles of Haq et al. (1987), Hunt & Tucker (1995), and Catuneanu (2002).

The spatial resolution of DEM was 1 . The geomorphological factors, such as elevation, slope, and aspect ratio, were calculated using the ArcGIS software. Considering the low resolution of the DEM, the multi-beam sounding data and topographic maps obtained from Liu et al. (2005), Li (2008), and Wu et al. (2014) were referenced to analyze the geomorphological characteristics of submarine canyons on the slope of the Okinawa Trough. The sea floor heat flow and temperature data are derived from the global heat flow database (http://www.ihfc-iugg.org/products/global-heat-flow-database/data) issued by the International Heal Flow Commission. In addition, partial sea floor temperature data are derived from Luan et al. (2008) and Xu et al. (2012).

4 Results

4.1 Sequence stratigraphy

Based on previous research results (Li et al., 2004; 2019; Luan et al., 2008; Li, 2008) and the Cenozoic chronostratigraphic table of the East China Sea (Figure 2), nine unconformities and sequence boundaries, such as Seafloor, T_{LGM} (23 kyr B.P.; Mix et al., 2001; Li et al., 2014), T_0 (1.8 Ma), T_{10} (6.0 Ma), T_{12} (11.02 Ma), T_{16} (16.12 Ma), T_{20} (23.03 Ma), T_{30} (33.9 Ma), and T_g were finally determined on the seismic profiles (Figure 3) across the East China Sea Shelf and Slope comprehensively using the horizon calibration of a synthetic seismogram of Well A, seismic boundaries tracking, and identification of sequence structure style. Six sequence boundaries, such as Seafloor, T_{LGM}, T_0, T_{10}, T_{12}, and T_{16} were developed on the slope of the Okinawa Trough (Figures. 4a and 4b). The filling strata were divided into five 3^{rd}-order sequences (SQIII 1–SQIII 5). The sequence SQIII 4 consisted of four parasequence units (systems tract), such as LST, TST, HST, and FSST, while the SQIII 5 consisted of only LST and TST. The FSST at the top of SQIII 4 was characterized by a wedge-shaped and stepping-down progradation reflection unit towards the trough basin, which reflected the sedimentary migration stages controlled by sea-level fall. Thus, a regressive unconformity (T_{LGM}) which can be tracked in the whole region was formed (Figure 4). The lower Miocene strata may also have deposited on the slope, but its reflection characteristics were fuzzy, discontinuous, and difficult to track.

Tracking from L1 to L2, L3, L4, and L5 lines, we found that the Diaoyu Island fold-uplift had an increasing influence on the sedimentary structure of the slope from north to south. Only three unconformities and sequence boundaries, such as Seafloor, T_{LGM} (23 kyr B.P.), and T_0 (1.8 Ma) were effectively determined on the southernmost seismic line L5. The T_{10} (6.0 Ma), T_{12} (11.02 Ma), and T_{16} (16.12 Ma) surfaces were further determined using the sequence scale, grade, and growth cycle by compared with other seismic lines. Stratigraphic sequence tracking from north to south showed that the Okinawa Trough started to be rifted in the Early Miocene affected by the subduction of the Philippine Sea Plate (Li et al., 2013). The northern trough was firstly rifted and therefore, filled by thick Miocene–Quaternary strata. Until the Late Miocene–Pliocene, as the rifting center migrating to the southern trough, the Okinawa Trough evolved into a unified basin. The southern trough was only filled by the Pliocene and Quaternary strata (Li et al., 2004; Wu et al., 2014).

Seismic interpretation showed that line L2 extends across submarine canyon C4, which has developed since the Early Pleistocene (<1.8 Ma). Along with the progradation of the continental slope, the canyon channel gradually migrated to the SE (Figure 4b), and then, moved to the present location after the LGM. It can be inferred that, during the LGM, the ancient river channel on the East China Sea Shelf transported a large amount of clastic materials to the submarine canyon C4. Following the deposition of the clastic materials, the downcutting rate of the canyon decreased, resulting in channel filling.

The stratigraphic sequence of line L5 indicated that the submarine canyon C6 started to develop during the LGM (Figures 5a, 5b, 5e, and 5f). Its formation and evolution were mainly controlled by the syndepositional fault developed in the SE-wing wall of the canyon. Line L3 extends across the head of the submarine canyon C5 and its branch C5-1 (Figures 5c and 5d), while line L4 extends across the branch C5-2 (Figures 5g and 5h). The stratigraphic sequence of lines L3 and L4 shows that the canyon system C5 was formed during the LGM, or even earlier (Middle Pleistocene). In addition, two juvenile submarine canyons were seen on line L4 (Figure 5e) which are mainly controlled by the active faults that cut through the seafloor.

In conclusion, submarine canyons on the continental slopes of the central and southern Okinawa Trough began to develop in the Early Pleistocene (< 1.8 Ma) and further evolved after the LGM. The canyon survival time spans two sequence cycles of SQIII 4 (1.8–0.023 Ma) and SQIII 5 (0.023–0 Ma) (Figure 4). Some submarine canyons may have migrated or even disappeared due to the climate changes during the glacial-interglacial cycle.

4.2 Geomorphological features of submarine canyons

There are many submarine canyons and valleys of different scales and shapes on the central and southern slopes of the Okinawa Trough (Liu et al., 2005; Li, 2008; Li et al., 2019; Wu et al., 2014). As mentioned above, the canyons were mainly formed in the Quaternary period. During the LGM, the sea-level in the East China Sea dropped to the current water depth of 135–150 m, which caused the continental shelf to be completely exposed and denuded, and finally led to the formation of the regional unconformity interfaces (T_{LGM}). This also provided favorable provenance and hydrodynamic conditions for the development of submarine canyons (Gao & Collins, 2014; Li et al., 2014; Wu et al., 2014). The submarine canyon showed typical erosional–depositional structures, with obvious down-cutting truncation at the bottom on reflection seismic profiles. It was characterized by irregular V-shaped or U-shaped with different terrain height. Small secondary-sequence surfaces developed in the interior of these canyons (Wu et al., 2011; Su et al., 2015).

The slope gradient map extracted from the DEM (Figure 6) indicates that the average slope gradient of the Okinawa Trough gradually increases from north to south. The slope gradient of the northern slope ranged from 0.5° to 2°, and the slope gradient of the central slope was mainly between 0.5–10°. The slope gradient of the transition zone between the central and the southern slopes increased to 2–15°. However, the slope gradient of the southern slope decreased to 0.5–10°. On the map, ten large-scale submarine canyons (C1–C10) was identified.

In this study, two large-scale submarine canyons (C5 and C6) in the central slope of the Okinawa Trough were selected for geomorphological analysis (Figure 7). The submarine canyons C5 and C6 were separated by a submarine plateau on the slope. The lengths of canyons C5 and C6 from the shelf break (water depth 180–200 m) to the bottom of the Okinawa Trough (water depth 1800 m) were about 90 km and 73 km, respectively. Their structures can be divided into three parts: head, upstream, and downstream (Figures 7c and 7e). From the head to downstream area, the canyon gradually changes from near SN-trending to NW-trending or NWW-trending. The submarine plateau partly affected the extension direction of submarine canyons. The canyon head is V-shaped and gradually transits to an irregular V-shaped or U-shaped structure with a wider canyon shoulder or a U-shaped structure with a wider canyon floor. The canyon downstream was mostly dish-shaped or dustpan-shaped (Figures 7d and 7f). The submarine canyons C5 and C6 are the meandering shelf-incising canyons not connected with a river whose heads have retrogressively eroded into the East China Sea Shelf. Branching channels were common at the head and upstream of the canyons (Figures 7a and 7b).

On the topographic profile along the thalweg of canyon C6, the bottom configuration slope presents two steps (Figure 7c). The maximum shoulder width of C6 ranged from 9 km–20 km (Figure 7d), and the maximum undercutting depth at the transition zone between the head and the upstream reached 900 m. The slope gradient of the side wall at the canyon head ranged from 0.5° to 7.4°, and the slope gradient of the upstream was between 1.5–9.1°. The slope gradient of the downstream gradually decreased, mostly to less than 3°. Notably, there was a long and narrow natural levee (of 35 km length) on the NE-side in the downstream channel of canyon C6. The topographic height difference was 100–170 m across the channel, and the slope gradient of the NE-side wall was higher than that of the SW-side wall (Figures 7b and 7d). The seismic profile indicated a parallel–subparallel reflection structure with medium–high continuity and medium–strong amplitude (Zhao et al., 2008), reflecting the characteristics of fine-grained overbank sediments at the end of the canyon. The reason that the overbank sediments formed on the NE-side of the channel is speculated to be the combined effects of Coriolis force and the Kuroshio movement from south to north (Li et al., 2014, 2019), which preserved the turbidity sediments effectively in the NE-side of the channel.

The submarine canyon C5 has many branches (e.g. C5-1 and C5-2). However, the connectivity between the branch channel and the main channel was still unclear (Figures 7a and 7b). The maximum shoulder width of canyon C5 was 7–19 km (Figure 7f), and the incised depth was 40–430 m. The slope gradient at the canyon head ranged from 0.1° to 6.4°. The slope gradient at the canyon upstream was 0.3°–4.8°, while the slope gradient at the canyon downstream was less than 2°. The thalweg profile showed that the bottom configuration descended in three steps (water depths were 180–610 m, 610–1200 m, and 1200–1800 m, respectively; Figure 7e).

4.3 Erosional–depositional texture in submarine canyons

On the seismic line L4, the canyon head of C6 is V-shaped. The seismic reflection with medium amplitude and medium continuity at the canyon bottom represents turbidite channels, while the seismic reflection with weak amplitude, low continuity at the middle part represents the mass transport deposits (MTD) (Figures 5e and 5f). The ancient sea-level in the East China Sea dropped to the current water depth of 120–150 m during the LGM, which caused the East China Sea Shelf to be exposed and eroded. Affected by the rejuvenation of the rivers, many incised channels developed on the shelf edge (Li et al., 2004, 2019). According to the morphological structure of the canyon and its downcutting position, the head of the canyon C6 justly developed from these channels.

The seismic line L5 shows that the canyon C6 is dustpan-shaped, with steep SE-side-wall and gentle NW-side-wall. The morphological structure of the canyon is obviously controlled by a normal fault paralleling or obliquing to the canyon strike (Figures 5a and 5b). Within the canyon, only two complexes of turbidity current channels could be identified, which are mainly characterized by layered seismic reflections with medium–strong amplitude and medium continuity. The maximum downcutting depth of the canyon was found to be consistent with the T_{LGM} surface (Figures. 5a and 5b). However, five–six large-scale MTDs were identified in the canyon, which were characterized by layered or progradation reflections with weak amplitude and medium continuity. Besides, imbricated seismic reflections due to gravitational sliding and compressional deformation were also observed (Figures. 5a and 5b). The dustpan-shape and internal structure of the canyon C6 indicated that it was jointly controlled by gravity flow and seabed subsidence caused by the syndepositional fault dragging on the SE-wing (Liu et al., 2005; Li, 2008; Zhao et al., 2011). Therefore, the bottom boundary of the canyon C6 was not exactly the downcutting surface of the gravity flow. Based on the comprehensive interpretation and analysis of seismic stratigraphy, we believe that the maximum regressive surface (T_{LGM}) formed at the LGM is the bottom boundary of the submarine canyon C6.

The seismic line L3 extends across the head of the canyon C5 and its branch C5-1. The seismic profile shows that there are one or two ancient, incised valleys buried under the canyon C5 (Figures 5c and 5d). According to the superimposed relationship, it can be inferred that the rapid sea-level fall in the East China Sea during the LGM caused the continental shelf to be exposed and downcut due to river rejuvenation. The ancient, incised valleys now buried under the head of canyon C5 were thus formed. After LGM, the rivers gradually retreated to the continent due to sea-level rise, and the ancient channels on the continental shelf were filled and buried (Li et al., 2004). However, it still retained the negative topography which became the prototype of the canyon head.

The seismic profile showed that the channel of canyon C5-1 was about 6 km wide and undercut close to the surface T_0. Eroded by the mass flow transportation, the bottom surface of the canyon was undulating (Figures 5c and 5d). In the canyon, three MTD units are identified, which indicated that the submarine canyon has entered the shrinking and filling stage (Reading & Richards, 1994; Wu & Qin, 2009). The NW-side wall of the canyon is one MTD unit formed by slump, which presents chaotic or continuous reflection with medium–weak amplitude. The toe of the slump body was strongly folded. The sedimentary layer was broken to form an imbricated structure, in which many compressional deformation structures developed. All of these indicated that the side wall of the canyon may further slide or slump (Figures 5c and 5d). The SE-side wall of the canyon was composed of two MTD units. The interface between these two MTDs was interpreted as one detachment fault for sediment decoupling. The detachment surface formed the bottom boundary of the canyon. The lower part of the MTDs showed layered seismic reflection with medium amplitude and medium–weak continuity, while the upper part presented imbricated or chaotic reflections with medium–low amplitude and medium–low continuity (Figures 5c and 5d).

The seismic profile L4 indicated that the canyon C5-2 underwent obvious lateral migration and diversion (Figures 5g and 5h). We believe that the SE-migration of canyon C5-2 was mainly caused by the rapid sea-level fall and the rightward deflection of Coriolis force during the LGM (Li et al., 2014, 2019). The buried canyon channel was U-shaped, or even dish-shaped, with wide canyon floor. Its interior was characterized by progradational-filling reflections with weak amplitude and medium continuity. The canyon was mainly filled by multi-stage turbidite deposits characterized by the medium–strong amplitude, medium–high continuous, and layered-filling reflection complexes (Figures 5g and 5h).

Seismic profile L2 showed that the canyon C4 underwent 3–4 stages of SE-migration and diversion, during which two ancient channels now buried under the continental slope seabed were formed (Figure 4b). The first ancient channel presented an irregular U-shaped and undercut to the bottom of the Quaternary strata. Its channel was about 3 km wide. The lower channel presents waving reflection with weak-amplitude and medium–low continuity, which reflects the sedimentary characteristics of high-density debris flow. The central channel shows layered-filling reflection with strong amplitude and medium continuity, which represents turbidite channel deposits. The upper part is characterized by mounded or chaotic reflection with weak amplitude and medium–low continuity, which represent the MTDs (Figure 4b). The other ancient channel was U-shaped, with a channel width of 2.5 km, characterized by the layered reflection with medium–strong amplitude and medium–low continuity (Figure 4b). The head of canyon C4 had two branches. The branch channel width ranged 2–2.5 km and represented an irregular U-shaped or V-shaped. The channels were filled by layered sediments characterized by weak amplitude and medium continuous reflections. The syndepositional deformation structures were also developed in the channels (Figure 4b).

In addition, on the seismic profile L3, eight ancient, incised channels were identified on the shelf edge (Figures 5c and 5d). These channels were small with widths of 0.7–1.5 km, respectively and presented chaotic-filling, onlap-filling, progradational-filling, or complex-filling reflections. The ancient channels were mainly distributed near the T_{LGM} and migrated frequently, indicating that its formation was closely related to the river rejuvenation during the LGM (Figure 5c). On one hand, these small-scale channel systems could carry turbidity sources for the erosion of submarine canyon, while on the other hand, under the action of the retrogressive erosion, they could connect with the slope-confined canyons (blind canyon or headless canyon) and transformed into the canyon head (Li et al., 2014; Wu et al., 2014).

4.4 Seismic reflection mark of methane-bearing fluid activity

Methane leakage and gas-bearing fluid activities at the bottom of the Okinawa Trough have been confirmed by the seabed gas leakage and associated cold seep carbonates (Luan & Qin 2005; Sun et al., 2015; Wang et al., 2019; Guan et al., 2019; Zhang et al., 2020; Cao et al., 2020; Li et al., 2018a, 2021b), pore water geochemistry in shallow sediments (Wang et al., 2015b, 2019; Li et al., 2015; Xu et al., 2018, 2020), mud diapir and volcano (Zhao et al., 2006; Xu et al., 2009) and abnormal methane flux in water column (Luan & Qin 2005; Zhang et al., 2020).

The arched, imbricated reflections on seismic profiles L3, L4, and L5 may indicate the upward escape and diffusion of methane-bearing fluids caused by gas hydrate decomposition (Figures 4d, 5a, 5c and 5e; Wu et al., 2011; Davies, et al., 2012; Su et al., 2015). On the SE- and NW-side walls of canyon C6, well preserved fluid migration channels had been found and identified (Figure 5a). The gas-bearing fluid leakage through these channels only cut the seismic events and formed gaps on the seabed, which did not cause large-scale stratigraphic disturbance. Therefore, the intact escape channels were preserved on the seismic profiles (Figure 5a). The location of canyon C6 is exactly close to the mud volcano or diapir associated with gas hydrate reported by Xu et al. (2009), which confirms the judgment that fluid escape and leakage has occurred and participated in the evolution of canyon C6.

The gap on the side wall of canyon C5-1 and the adjacent slope indicated the traces left by the escaping gas after hydrate decomposition (Figures 5c and 5d). We believed that the detachment fault on the SE-side wall of canyon C5-1 was also further shaped by MTD sliding from the fluid escape channel. However, when the fluid could not be effectively discharged, the liquefied deformation of sediments will present distorted, chaotic or twisty reflections on the seismic profiles (Figures 4d, 5a, and 5c). The ridge of canyon C5-1 are composed of several wedgy or triangular slope fans which are characterized by weak amplitude, chaotic-filling reflections or medium amplitude, medium–low continuous, oblique-filling reflections. The liquefaction-induced deformation exactly developed at the fan end (Figure 5c). Therefore, we believed that the SE-wing of canyon C5-1 was an active methane seep area, which could be confirmed by methane flux observation (Zhang et al., 2020). Coincidentally, the gaps, imbricated structures, and internal chaotic-twisty reflection marks caused by strong methane-bearing fluid seepage were also identified at the end of seismic line L3 (Figure 8c).

On the seismic line L4, we identified a cold seep site which is exactly close to the seabed gas spring (Luan & Qin 2005; Zhang et al., 2020) and an active CH_4 emission area (Xu et al., 2018; Zhang et al., 2020). We believed that the liquefaction deformation due to strong methane-bearing fluid leakage and disturbance caused some gap structures and arched, imbricated reflection units on the seismic profile (Figure 4d). The interior units were characterized by chaotic or twisty reflections (Figure 4d). The reflection seismic, seabed gas spring (Luan & Qin 2005), pore water geochemistry in sediments (Xu et al., 2018), and the highest sea-to-air flux of methane (Zhang et al., 2020) all confirmed the universality of methane-bearing fluid activity in this area of Okinawa Trough.

5 Discussion

5.1 Dynamic accumulation of hydrate indicated by BSRs and its relationship with methane seepage

Since the discovery of the BSRs (Yang et al., 2004; Luan et al., 2008; Xu et al., 2009; Xu et al., 2012; Chen et al., 2014; Li et al., 2019), many evidences for gas hydrate, such as seabed methane seepage and associated carbonate (Luan & Qin, 2005; Sun et al., 2015; Li et al., 2018a; Guan et al., 2019; Wang et al., 2019; Zhang et al., 2020; Cao et al., 2020; Li et al. 2021a, 2021b), pyrite associated with methane leakage (Wang et al., 2015b), mud diapir or volcanoes (Zhao et al., 2006; Xu et al., 2009), and methane anomaly in pore water, water column and even sediments (Lu et al., 2003; Li, 2008; Wang et al., 2015b; Li et al. 2015; Xu et al., 2018, 2020; Zhang et al., 2020), were revealed in the Okinawa Trough (Figure 1). The hydrate phase equilibrium simulation showed that the hydrate resource in the Okinawa Trough can be as high as 24×10^{12} m^3 (Chen, 2014). In this study, based on the measured temperature–depth (pressure) data in the Okinawa Trough (Xu et al., 2012; Li et al., 2019), the phase equilibrium model of gas hydrates was also established, according to the 4^{th}-order equation of temperature-pressure (depth) proposed for the stable existence of gas hydrates

(Miles, 1995; Xu et al., 2009). The results show that the minimum pressure required for gas hydrate formation in the Okinawa Trough is 630 m in water depth, which is very close to the result of 500–600 m calculated by Fan & Yang (2004), and the results of 600 m calculated by Luan et al. (2008). All this show that the continental slope of the Okinawa Trough has favorable thermodynamic geological conditions for gas hydrate accumulation.

On the seismic profile L5, two intermittent BSRs with different buried depth were found on the NW-side wall of the canyon C6 (Figure 8a). The distribution horizon of the lower BSR was consistent with the T_{LGM}, distributed across or parallel to the sedimentary strata. The reflection polarity of the BSR was opposite to that of the seafloor, showing strong amplitude and negative seismic polarity clamped by positive polarity (Figure 8a). The blank reflection unit above the lower BSR indicated that the hydrate reservoir thickness was about 150–300 ms (two-way reflection time). The residual discontinuous reflections inside the seismic unit reflected the spatial heterogeneity of the gas hydrates. The upper BSR was distributed intermittently from the side wall slope to the canyon floor, with a cumulative extended distance of 10 km. The BSR trend was basically consistent with the seabed topography (Figure 8a). The thickness of the blank reflection zone above the BSRs on the side wall was about 50–150 ms (two-way reflection time). At the canyon floor, the thickness of the blank reflection zone above the BSR was 100–300 ms (two-way reflection time). Therefore, we believe that there were already gas hydrates in the submarine sediments of the East China Sea Slope during the Pleistocene.

On the seismic profile L4 (Figure 8b), the BSR was located under the NW-side wall of canyon C5-2. The blank reflection zone was characterized by weak amplitude, chaotic-filling or low continuous, oblique-filling reflections, with thickness of 50–150 ms (two-way reflection time). The BSR extended about 4.5 km in the SE-direction and was cut off by the canyon channel, indicating that the submarine canyon has an important influence on the GHSZ (Figure 8b). In the maturity stage, the canyon underwent strong erosion, and the seafloor was downcut into V-shaped or U-shaped structures. Influenced by the cooling effects of seawater (Bangs et al., 2010; Davies et al., 2012), the GHSZ under the canyon floor will gradually migrate deeper. While in the old stage, the submarine canyons are strongly filled, and the MTDs and turbidite channel sand in these canyons can become gas hydrate reservoirs again.

After the last glacial period, owing to the pressure release and rise in the seafloor temperature caused by the rapid sea-level fall, the gas hydrate stable zone (GHSZ) gradually drifted upward and moved towards the seafloor during the LGM, resulting in the overlapping of the lower BSR and the T_{LGM} surface. The leakage of methane-bearing fluid released from hydrate decomposition due to GHSZ migration caused gap structures and fluid escape channels on the seismic profile (Figure 5a). During this period, jointly controlled by sediment slumping (Figure 8a; large wedge-shaped and blank reflection unit above the lower BSR) induced by gas hydrate decomposition and seafloor subsidence caused by contemporaneous faulting on the SE-side wall, the submarine canyon C6 grew rapidly and suffered turbidity flow erosion, which ended the SE-extension of the lower BSR. After the LGM, along with the sea-level rose, the turbidity sediments filled in the canyon once again hosted gas hydrates, forming a 10-km long BSR across the side wall and subchannel floor in the canyon C6 (Figure 8a). Mass flow sediments constituted the main body of the blank reflection zone above the BSR (Figure 8a), indicating that deep water turbidites, such as canyon channel and MTD, were the dominant gas hydrate reservoirs in these canyons (Noguchi et al., 2011; Boswell et al., 2012; Wu et al., 2011; Su et al., 2015; Suzuki et al., 2015). The detachment surface of the shallow MTDs inside the canyon C6 completely coincided with the BSRs (Figure 8a), indicating an inseparable connection between gas hydrate decomposition and the erosive turbidity current that dominates the development of the canyon.

Although we did not identify enough BSRs on the seismic profiles, a lot of gap structures and fluid transport channels caused by gas escaping, and imbricated, chaotic or twisty seismic reflections caused by gas-bearing fluid liquefaction associated with methane leakage were found (Figures 4d, 5a, 5c, and 8c). Notably, the petrological, mineralogical, and geochemical analysis of carbonate associated with methane seepage in the Okinawa Trough, show that the leakage of biogenic methane and intense anaerobic oxidation of methane (AOM) resulted in the formation of abundant authigenic carbonates, which represented extremely negative carbon isotopic and positive oxygen isotopic compositions (Wang et al., 2019; Cao et al., 2020). Moreover, isotopes have confirmed that the fluid required for carbonates precipitation in the Okinawa Trough comes from decomposition of gas hydrate (Cao et al., 2020), which just approves our understanding that the methane-bearing fluid activity caused by hydrate dynamic decomposition affects the origin and evolution of submarine canyons.

5.2 Factors controlling the formation and evolution of submarine canyons

The submarine canyons on the continental slope of Okinawa Trough began to form in the early Pleistocene (<1.8 Ma), which was strongly controlled by the climate and environment changes due to the glacial-interglacial cycle in the Quaternary (Gao & Collins, 2014). The origin and evolution of these submarine canyons are mainly related to the gravity transportation (small-scale landslides and sediment gravity flows; Li et al., 2001; Liu et al., 2005; Zhao et al., 2009; Li et al., 2019), the rifting settlement of syndepositional faults (Liu et al., 2005; Li, 2008; Zhao et al., 2011), and the sea-level eustacy, river rejuvenation and methane-bearing fluid leakage due to dynamic evolution of GHSZ caused by climate change in the Quaternary glacial-interglacial cycles (Li et al., 2019; Cao et al., 2020). In addition, the strong submarine volcanic activities in the Okinawa Trough may also affect the development of submarine canyons.

The seabed topography shows that the trend of the submarine canyons on the continental slope of Okinawa Trough is basically perpendicular to the isobaths, reflecting that the extension of canyons is controlled by gravitational process. The MTDs associated with slide or slump and characterized by imbricated, twisty or chaotic seismic reflections, the channel-lag deposits (high density debris flow) characterized by chaotic-filling reflections, and turbidity channel deposits characterized by progradational-filling, parallel onlap-filling or divergent-filling reflections indicate that gravity flow plays a key role in shaping the submarine canyons (Wu & Sakamoto, 2001; Wu et al., 2011; Xu et al., 2014; Su et al., 2014, 2015; Yin et al., 2015). Published cases of submarine fans outside the canyon mouths and the natural levees and fine-grained overflow deposits of the Chiwei canyon-fan system also illustrate the frequent turbidity current activities in the Okinawa Trough (Li et al., 2001; Liu et al., 2005; Li, 2008; Zhao et al., 2009, 2011). Especially since the Holocene, after the Kuroshio warm current strengthened (Xiang et al., 2003; Gao & Collins, 2014), it intruded into the Okinawa Trough again and would induce the frequent activities of seabed turbidity current to a certain extent.

The dustpan-shaped structure with NE-wing faulting and SW-wing overlapping and its associated relationship with syndepositional faults show that some submarine canyons on the continental slope of Okinawa Trough are dominated by active faults. Canyon embryos controlled by these syndepositional faults were also found on the seismic line L4. The dragging subsidence of active faults can not only form canyon negative topography, but also induce erosive activities of turbidity current, and instability and slump of canyon side-walls, thus leading the evolution process of this kind of submarine canyons. Since the late Miocene, under the control of back-arc tension, two groups of NE-SW trending (approximately E-W trending in the southern part of the trough) and NW-SE trending fault systems have developed in the Okinawa Trough (Liu et al., 2005; Li, 2008; Zhao et al., 2011). The NE-SW trending faults control the topographic division from continental shelf to slope. While the secondary NW-SE trending faults and its branch faults cut the continental shelf and slope from west to east and break the bedrocks providing good geological conditions for the formation of submarine canyons.

The formation time of the submarine canyons (< 1.8 Ma) on the continental slope of the Okinawa Trough is equivalent to the starting time of the oldest glacial epoch (Shishapangma epoch) in China, the Eburonian epoch recorded in the European Alps, and pre-Illinoian H epoch recorded in the Great Lakes (Shi & Liu, 1964; Zhang et al., 2002; Mutton et al., 2003; Ehlers & Gibbard, 2007; Cui et al., 2011) reflecting that the formation of submarine canyons is closely related to the Quaternary glacial-interglacial cycle (Nakajima et al., 2014; Xu et al., 2014; Su et al., 2014, 2015; Yin et al., 2015; Li et al., 2019; Cao et al., 2020). During the LGM, the sea-level of the East China Sea dropped to the present-day water depth of 120–150 m (Lambeck & Chappell, 2001; Li et al., 2014) and the continental shelf was exposed. The terrestrial rivers advanced rapidly toward the ocean and eroded the shelf margin, thus forming many incised channels (Li et al., 2004, 2014). The heads of submarine canyons C5 and C6 was inherited from these ancient incised channels. At the same time, these ancient channels also transported a large amount of clastic materials for the downcutting of canyons due to gravity flow. For the Okinawa Trough, another important influence of the Quaternary sea-level eustacy was the variation of the temperature and pressure conditions of gas hydrate (Song, 2003; Yu et al., 2014; Maslin et al., 2004). The periodic decomposition of hydrate and methane leakage caused by GHSZ migration due to the temperature and pressure change, weakened the stability of seabed sediments on the continental slope, which had seriously affected the development and evolution of submarine canyons in the forms of landslides and sediment gravity flows. In return, the continuously downcutting and lateral erosion of canyons would also cause the spatial migration of GHSZ (Bangs et al., 2010; Davies et al., 2012; Su et al., 2015). The MTDs characterized by imbricated, twisty or chaotic seismic reflections, the gaps that indicate gas escaping on the canyon side-walls, the liquefaction deformation structures on the canyon ridge, and the truncated relationship between BSRs' reflectors and canyon channels on the seismic profiles all proved the interaction between gas hydrate and submarine canyons. In addition to the gravity flow, the sea-level and climate changes caused by the Quaternary glacial-interglacial cycle are the main factors for the origin and evolution of submarine canyons in the Okinawa Trough.

5.3 Submarine canyon evolution model coupling with methane seepage associated with hydrate

The temperature and pressure conditions of the GHSZ can be destroyed by the alternating cold and warm events caused by climate change or sea-level eustacy (Song, 2003; Maslin et al., 2004; Wu et al., 2009; Bangs et al., 2010; Nakajima et al., 2014). The most remarkable is the global sea-level fluctuation caused by glacial-interglacial cycle in the Quaternary controlled by the Milankovich cycle. For example, during the LGM, the sea level of the East China Sea dropped to the present-day water depth of 120–150 m and reached the continental slope edge of the Okinawa Trough (Lambeck & Chappell, 2001; Li et al., 2014; Gao & Collins, 2014). During this period, the intense climate change and sea-level fall played a key role in the formation, decomposition, and accumulation of gas hydrates in the Okinawa Trough. In turn, the methane released from hydrate decomposition could also contributed to climate change (Maslin et al., 2004; Wang et al., 2015a).

Many submarine canyons have developed on the central and southern slope of the Okinawa Trough (Li et al., 2001; Liu et al., 2005; Liu et al., 2005; Li, 2008; Wu et al., 2014). The formation of these canyons began in the early Pleistocene (< 1.8 Ma), and they continue to develop even today. During this period, the submarine canyons underwent multi-stages of channel migration and erosional–depositional evolution. Some submarine canyons had even disappeared and were buried. The submarine canyons on the slope of the Okinawa Trough were formed earlier than the oldest Shishapangma Glaciation (1.17–0.8 Ma) discovered in Western China (Shi & Liu, 1964; Zhang et al., 2002; Cui et al., 2011) and the age of the seep carbonates [31.54–34.1 ka B.P. from Sun et al. (2015) and 22.8–55.7 ka B.P. from Cao et al. (2020), respectively] in the Okinawa Trough. However, its formation time is consistent with the starting time of the Eburonian epoch in and pre-Illinoian H epoch (Mutton et al., 2003; Ehlers & Gibbard, 2007; Cui et al., 2011). Moreover, the rapid sea-level fall during the LGM in the East China Sea Shelf are confirmed by many sedimentary records (Gao & Collins, 2014; Li et al., 2014, 2019). Therefore, the formation, development, and evolution of submarine canyon in the study area are closely related to the global glacial–interglacial cycle during the Quaternary period (Nakajima et al., 2014; Xu et al., 2014; Su et al., 2014, 2015; Yin et al., 2015).

Since the LGM, the coupling evolution process of submarine canyon and gas hydrate system in the Okinawa Trough were clearly preserved in the canyon sediment records, such as the MTD characterized by imbricated, twisty or chaotic seismic reflections, fluid transport channels and the gaps that indicate gas escaping on the side walls of the C6 and C5-1 submarine canyons (Figures 5a and 5c). Additionally, a truncated relationship between the BSRs reflector and the submarine canyon on seismic lines L5 and L4 (Figure 8) was also observed. All these indicate that there is a complex relationship between the erosional–depositional evolution of submarine canyons and the development of gas hydrates on the continental slope of the Okinawa Trough. On one hand, strong downcutting and retrogressive erosion of submarine canyons will steepen the canyon sidewall, which can easily induce sediments instability on the canyon sidewall. The channel downcutting and sediment instability will destroy the GHSZ. Therefore, the methane released by hydrate decomposition will leak out through the gap formed by the sediment instability on the side walls and seabed gas seepage (Luan & Qin, 2005; Wu et al., 2011; Davies et al., 2012; Su et al., 2015; Cao et al., 2020); On the other hand, the sea-level eustacy caused by the glacial–interglacial cycles will lead to frequent changes of temperature and pressure in the GHSZ. Therefore, the hydrates can form or decompose dynamically and repeatedly, that promotes the escape and leakage of methane-bearing fluids. This methane-bearing fluid activity can, in turn, induce sediment instability and deformation, and then, influence the formation and erosion processes of the submarine canyon (Nakajima et al., 2014; He et al., 2014; Li et al., 2017, 2018b) and even cause the occurrence of submarine landslide. However, the channel sand inside the submarine canyon and the submarine fan outside the canyon mouth can often be used as the high-quality reservoirs for hydrate. We believe that erosion and deposition in the submarine canyon and the dynamic accumulation of gas hydrate are interdependent and reciprocal.

Based on the influence of sea-level fall caused by Quaternary glaciation on the gas hydrate dynamic accumulation system in the continental slope of the Okinawa Trough and the interaction between the gas hydrate decomposition and the formation of submarine canyons, a coupling evolution model of submarine canyon erosion and gas hydrate dynamic accumulation on the continental slope of the Okinawa Trough was established (Figure 9): The stage of sea-level fall, hydrate decomposition, and submarine canyon forming. The formation time (<1.8 Ma) of submarine canyon on the continental slope of the Okinawa Trough is consistent with the glacier onset time in the Northern Europe and Northern America (Mutton et al., 2003; Ehlers & Gibbard, 2007; Cui et al., 2011), which indirectly proves the genetic relationship between submarine canyons and the sea-level fall during the glacial epoch. During the glacial epoch in the Middle Pleistocene, the sea-level fall led to pressure release and seabed temperature rise and the upward migration of GHSZ resulted in the decomposition of hydrate layers between the old and new stable zones (Wu et al., 2011; Nakajima et al., 2014; He et al., 2014). The released methane migrated and seeped rapidly upward to the seabed and accumulated beneath the seafloor, forming hydrate mounds on the continental slope. With the continuous hydrate accumulation, the stress reached the critical condition, which resulted in the collapse of the hydrate mound. The scarp formed by the instability of hydrate mounds became the rudiment of the valley, which opened the development process of the submarine canyon (Figures 9a and 9b). Notably, the formation of submarine canyon C6 is also controlled by contemporaneous faulting (Figure 5a). In other words, faulting is also one factor affecting the initiation of submarine canyons. Active faults break the bedrocks of the seabed to form a negative terrain, inducing gravity flow to preferentially erode the broken strata and ultimately, affected the canyon path. Faulting can be combined with the decomposition of gas hydrate to control the development and evolution of the submarine canyon;

The stage of submarine canyon continuously downcutting, canyon retrogressive erosion, and gas hydrate stable zone (GHSZ) dynamic migrating. After the rudiment formation of the submarine canyons, the scour and retrogressive erosion of gravity flow (e.g., MTDs and turbidity flow) became the main factor to shape the canyon structure. In this stage, the seabed continuously suffered downcutting and erosion, forming V-shaped or U-shaped canyon channels. Affected by the cooling effects of seawater (Bangs et al., 2010; Davies et al., 2012), the GHSZ under the canyon floor gradually migrated deeper (Figure 9c). The free methane under the previous GHSZ then combined with water molecules to form new gas hydrates (Sun et al., 2017). The BSRs were truncated by the MTDs on the side wall of the submarine canyons C6 and C5-2, which proved the influence of canyon downcutting on the GHSZ migration. At the same time, the reason why multiple BSRs have developed in the canyon development area is explained reasonably (Wu et al., 2009; Davies et al., 2012; Su et al., 2015).

The mutual promotion stage of sediment instability and the collapse of the canyon wall, along with methane leakage. The gap from which the gas escaped, imbricated deformation structures on the side wall of the C6 and C5-1 canyons, and the liquefaction deformation structures on the canyon ridge (Figure 5) all indicated that, in the trough, gas escape interacted with mass sliding. When the slope gradient of the canyon wall increased to the critical conditions under the erosion of turbidity flow, the sediments on the head and flank of the canyon channel became instable and collapsed. Thus, the hydrate layers on the canyon wall decomposed, resulting in the methane escaping and a gap was formed where the gas seeped through. Similarly, the escape of methane-bearing fluid will also aggravate the sediment deformation and induce new mass sliding events. With the retrogressive erosion of the canyon, the ancient, incised channels formed on the edge of the outer shelf during the LGM may be connected to the canyon, forming the head of the current submarine canyon (Figure 9d).

The stage of the wakening of canyon erosion, filling of the sandy channel, and hydrate reaccumulating. With the weakening of canyon downcutting, the submarine canyon entered the main filling stage (Wu & Qin, 2009; Walsh et al., 2007). The coarse-grained channel sand with high porosity and permeability or re-transported MTDs started to develop in the canyon. If the methane supply is enough, the hydrates will be reaccumulated in these high-quality reservoirs. Of course, most of the submarine canyons on the continental slope of the Okinawa Trough are in their youth. It is possible that only a few submarine canyons filled and buried by clastic sediments have experienced this stage.

6 Conclusions

According to the theory of sequence stratigraphy, six seismic sequence boundaries have been identified on the central and southern slopes of the Okinawa Trough. Their geological ages have been determined as Seafloor (0 Ma), T_{LGM} (23kyr B. P.), T_0 (1.8 Ma), T_{10} (6.0 Ma), T_{12} (11.02 Ma), and T_{16} (16.12 Ma). The isochronous chronostratigraphic framework in the central and southern slopes of the Okinawa Trough was established and the sedimentary strata were divided into five 3rd-order sequences. The central and northern slopes of the Okinawa Trough were characterized by thick Miocene–Quaternary strata, while the southern slope was mainly filled with Pliocene–Quaternary strata. The submarine canyons on the central and southern slopes of the Okinawa Trough began to develop in the early Pleistocene (< 1.8 Ma) and continued to develop even today.

The geomorphological features of submarine canyons on the central and slopes of the Okinawa Trough (e.g., C5 and C6) were found to be segmented: The head was V-shaped; the upstream was gradually transformed into V-shaped or U-shaped with wider shoulder and deeper downcutting depth; and the downstream region consisted as dish-shaped or dustpan-shaped structure with a wide canyon floor. These canyons were meandering canyons not connected to a river. The heads of the C5 and C6 submarine canyons were evolved from the ancient, incised channels formed in the LGM. The canyon C5-1 was filled by three MTD units related to side-wall sliding. The canyon C5-2 migrated southeastward, and the interior was mainly filled by turbidite channel complex. There were two turbidite scouring–depositional layers and five–six MTDs in the canyon C6. The maximum downcutting position of the C6 coincided with the T_{LGM} surface. The dustpan-shape and internal filling structures of the canyon C6 indicated that it was formed by turbidity current erosion and unstable collapse of the canyon walls under the control of the seabed subsidence caused by the SE-wing synsedimentary faulting.

The gas hydrate phase equilibrium simulation predicts that the minimum water depth required for gas hydrate is 630 m, which shows that the Okinawa Trough has favorable thermodynamic geological conditions for gas hydrate accumulation. Three BSRs were identified on the seismic profiles L5 and L4, of which the profile L5 had double-BSRs structure. The trend of the BSRs was consistent with the seabed topography, which was inclined across or parallel to the sedimentary strata, showing strong amplitude, negative polarity, and continuous reflections. The blank reflection zone above the BSRs showed that the thickness of the GHSZ ranged between 50 ms and 300 ms (two-way reflection time).(4) The origin and evolution of submarine canyons on the continental slope of Okinawa Trough are mainly related to the gravity transportation of continental slope, the rifting settlement of syndepositional faults, and the sea-level eustacy, river rejuvenation and methane seepage due to dynamic evolution of GHSZ caused by climate change due in the Quaternary glacial-interglacial cycle. The formation time of submarine canyons on the continental slope of the Okinawa Trough was found to overlap with the start of the Eburonian epoch in North Europe and pre-Illinoian H epoch in North America. Especially, the seismogeologic characteristics, including MTDs associated with the BSRs, the gaps and fluid channels on the side-walls (through which gas could escape), the liquefaction deformation structures and the truncated relationship between the BSRs reflector and the submarine canyons all indicate that there is a complex relationship between the submarine canyons and the methane seepage associated with hydrate dynamic decomposition on the continental slope of the Okinawa Trough. Finally, a coupled model with four evolutional stages for the submarine canyons associated with gas hydrate was established.

Acknowledgments

This work is supported by the National Natural Science Foundation of China (Grant No. 41806073), the Fundamental Research Funds for the Central Universities (Grant No. 201964016), the Opening Foundation of Key Lab of Submarine Geosciences and Prospecting Techniques, MOE, Ocean University of China (Grant No. SGPT-2020OF-06) and the Natural Science Foundation of Shandong Province (Grant No. ZR2017BD014). We would like to thank professors San-Zhong Li of Ocean University of China and Zheng-Xiang Li of Curtin University, Australia for their scientific guidance and help during the article preparing process.

Data Availability

Datasets related to this article can be found at https://www.bodc.ac.uk/data//hosted_data_systems/gebco_gridded_bathymetry_data/ and http://www.ihfc-iugg.org/products/global-heat-flow-database/data, the open-source online data repositories hosted by British Oceanographic Data Centre and the International Heat Flow Commission, respectively. The original seismic images are included in the article.

References

Bangs, N.L., Hornbach, M.J., Moore, G.F., & Park, J.D. (2010). Massive methane release triggered by seafloor erosion offshore southwest Japan. *Geology*, *38*, 1019-1022.

Boswell, R. Frye, M., Shelander, D., Shedd, W., McConnell, D., & Cook, A. (2012). Architecture of gas-hydrate-bearing sands from Walker Ridge 313, Green

Canyon 955, and Alaminos Canyon 21: Northern deepwater Gulf of Mexico. *Marine and Petroleum Geology*, *34*, 134-149.

Bozzano, G., Cerredo, M.E., Remesal, M., Steinmann, L., Hanebuth, T.J.J., Schwenk, T., Baqués, M., Hebbeln, D., Spoltore, D., Silvestri, O., Acevedo, R.D., Spiess, V., Violante, R.A., & Kasten, S. (2020). Dropstones in the Mar del Plata Canyon area (SW Atlantic): evidence for provenance, transport, distribution, and oceanographic implications. *Geochemistry*, *Geophysics*, *Geosystems*, *22*, e2020GC009333. https://doi.org/10.1029/2020GC009333

Cao, H., Sun, Z.L., Wu, N.Y., Liu, W.L., Liu, C.L., Jiang, Z.K., Geng, W., Zhang, X.L., Wang, L.B., Zhai, B., Jiang, X.J., Liu, L.P., & Li, X. (2020). Mineralogical and geochemical records of seafloor cold seepage history in the northern Okinawa Trough, East China Sea. *Deep-Sea Research I*, *155*, 103165.

Catuneanu, O. (2002). Sequence stragraphy of clastic systems: concepts merits, and pitfalls. *Journal of African Earth Sciences*, *35*, 1-43.

Chen, J. W. (2014). Formation Conditions and Resources Potential of Gas Hydrate in the Okinawa Trough of the East China. *Acta Geoscientica Sinica*, *35(6)*, 726-732.

Cohen, K.M., Finney, S.C., Gibbard, P.L., & Fan, J.X. (2013). The ICS International Chronostratigraphic Chart. *Episodes*, *36*, 199-204.

Cui, Z.J., Chen, Y.X., Zhang, W., Zhou, S.Z., Zhou, L.P., Zhang, M., & Li, C.C. (2011). Research history, glacial chronology and origins of Quaternary glaciations in China. *Quaternary Sciences*, *31(5)*, 749-764.

Chiang, C. S., & Yu, H.S. (2006). Morphotectonics and incision of the Kaoping submarine canyon, SW Taiwan orogenic wedge. *Geomorphology*, *80*, 199-213.

Davies, R.J., Thatcher, K.E., Mathisa, S.A., & Yang, J. (2012). Deepwater canyons: An escape route for methane sealed by methane hydrate. *Earth and Planetary Science Letters*, *323-324*, 72-78.

de Stigter, H.C., Jesus, C.C., Boer, W., Richter, T.O., Costa, A., & van Weering, T.C.E. (2011). Recent sediment transport and deposition in the Lisbon-Setúbal and Cascais submarine canyons, Portuguese continental margin. *Deep-Sea Research II*, *58*, 2321-2344.

Ding, W. W., Li, J.B., Li J., & Han, X. B. (2013). Formation process and controlling factors of the Pearl River Canyon in the South China Sea. *Journal of Tropical Oceanography*, *32(6)*, 63-72.

Ehlers, J., & Gibbard, P.L. (2007). The extent and chronology of Cenozoic global glaciation. *Quaternary International*, *164-165*, 6-20.

Fan, D.J., & Yang, Z.S. (2004). Development and distribution of natural gas hydrate in the Okinawa trough. *Acta Petrolei Sinica*, *25(3)*, 11-18.

Gao, S., & Collins, M.B. (2014). Holocene sedimentary systems on continental shelves. *Marine Geology*, *352*, 268-294.

Gong, C.L., Wang, Y.M., Zhu, W.L., Li, W.G., Xu, Qiang, & Zhang, J.M. (2011). The Central Submarine Canyon in the Qiongdongnan Basin, northwestern South China Sea: Architecture, sequence stratigraphy, and depositional process. *Marine and Petroleum Geology*, *28*, 1690-1702.

Gong, C.L., Steel, R.J., & Wang, Y.M. (2020). Channel-levee evolution in combined contour current-turbidity current flows from flume-tank experiments: Comment. *Geology*, DOI: 10.1130/G47508C.1.

Guan, H.X., Sun, Z.L., Mao, S.Y., Xu, L.F., Cao, H., Geng, W., Xu, C.L., Zhang, X.R., & Wu, N.Y. (2019). Authigenic carbonate formation revealed by lipid biomarker inventory at hydrocarbon seeps: a case study from the Okinawa Trough. *Marine and Petroleum Geology*, *101*, 502-511.

Hall, R. (2012). Late Jurassic-Cenozoic reconstructions of Indonesian region and the Indian Ocean. *Tectonopyhsics*, *570-571*, 1-41.

Han, W.C., Liu, C.S., Chi, W.C., Chen, L.W., Lin, C.C., & Chen, S.C. (2017). Westward advance of the deformation front and evolution of submarine canyons offshore of southwestern Taiwan. *Journal of Asian Earth Sciences*, *149*, 6-19.

Han, X.B., Li, J.B., Long, J.P., Chu, F.Y., Ding, W.W., Zhang, S.Y., Xu, D., & Yang, H.L. (2010). Development of research on submarine canyon in China. *Marine Geology Letters*, *26(2)*, 41-48.

Hao, T.Y., Liu, J.H., Guo, F., Huang, Z.X., Xu, Y., Dai, M.G., Li, A.C., & Fu, Y.T. (2004). Research on crustal structure and lithosphere property in the Okinawa Trough area. *Chinese Journal of Geophysics*, *47(3)*, 462-468.

Haq, B.U., Hardenbol, J., & Vail, P.R. (1987). Chronology of fluctuating sea levels since the Triassic. *Science*, *235*, 1156-1166.

Harris, P.T., & Whiteway, T. (2011). Global distribution of large submarine canyons: Geomorphic differences between active and passive continental margins. *Marine Geology*, *285*, 69-86.

He, Y., Zhong, G.F., Wang, L.L., & Kuang, Z.G. (2014). Characteristics and occurrence of submarine canyon-associated landslides in the middle of the northern continental slope, South China Sea. *Marine and Petroleum Geology*, *57*, 546-560.

Huh, C.A., Liu, J.T., Lin, H.L., & Xu, J.P. (2009). Tidal and flood signatures of settling particles in the Gaoping submarine canyon (SW Taiwan) revealed from radionuclide and flow measurements. *Marine Geology*, *267*, 8-17.

Hunt, D., & Tucker, M.E. (1995). Stranded parasequences and the forced regressive wedge systems tract: deposition during base-level fall-reply. *Sedimentary Geology*, *95*, 147-160.

Kopper, A.A.P., & Staudigel, H. (2005). Asynchronous bends in Pacific seamont trails: a case for extensional volcanism. *Science*, *307*, 904-907.

Lambeck, K., & Chappell, J. (2001). Sea level change through the last glacial cycle. *Science*, *292*, 679-686.

Li, A., Davies, R., & Yang, J.S. (2016). Gas trapped below hydrate as a primer for submarine slope failures. *Marine Geology*, *380*, 264-271.

Li, A., Li, Q., Xu, C.L., Cai, F., & Wang, H.B. (2021a). Review of Methane Seepages in the Okinawa Trough: Progress and Outlook. *Geofluids*, https://doi.org/10.1155/2021/5539893.

Li, A., Cai, F., Wu, N.Y., Li, Q., Yan, G.J., Sun, Y.B., Dong, G., Luo, D., & Wang, X.X. (2021b). Gas emissions in a transtensile regime along the western slope of the Mid-Okinawa Trough. *Frontiers in Earth Science*, *9*, 557634.

Li, D.Y., Chen, H.Y., Xu, S.J., Xing, J.H., Cheng, H.G., & Wang, J.K. (2019). Stratigraphic sequence and sedimentary systems in the Middle-Southern Continental Slope of the East China Sea from seismic reflection data: exploration prospects of gas hydrate. *Journal of Ocean University of China*, *18*, 1302-1316.

Li, G.X., Lin, P., Liu, Y., Qiao, L.L., Ma, Y.Y., Xu, J.S., & Yang, Z.G. (2014). Sedimentary system response to the global sea level change in the East China Seas since the last glacial maximum. *Earth-Science Reviews*, *139*, 390-405.

Li, G.X., Liu, Y., Yang, Z.G., Yue, S.H., Yang, W.D., & Han, X.B. (2004). Ancient Changjiang channel system in the East China Sea continental shelf during the last glaciation. *Science China D*, *35 (3)*, 284-289.

Li, J.B. (2008). *East China Sea regional geology.* Beijing: Ocean Press,

Li, J.W., Peng, X.T., Bai, S.J., Chen, Z.Y., & Nostrand, J.D.V. (2018a). Biogeochemical processes controlling authigenic carbonate formation within the sediment column from the Okinawa Trough. *Geochimica et Cosmochimica Acta*, *222*, 363-382.

Li, J.Z., Liu, S.S., Zhang, J.L., Fan, Z.L., Sun, Z.Q., Zhang, M., Yuan, Y., & Zhang, P.H. (2015). Architecture and facies model in a non-marine to shallow-marine setting with continuous base-level rise: An example from the Cretaceous Denglouku Formation in the Changling Depression, Songliao Basin, China. *Marine & Petroleum Geology*, *68*, 381-393.

Li, Q., Cai, F., Liang, J., Shao, H.B., Dong, G., Wang, F., Yang, C.S., & Hu, G.W. 2015. Geochemical sonstraints on the methane seep activity in western slope of the middle Okinawa Trough, the East China Sea. *Science China: Earth Sciences*, *45(5)*, 676-687.

Li, S.Z., Yu, S., Zhao, S.J., Liu, X., Gong, S.Y., Suo, Y.H., Dai, L.M., Ma, Y., Xu, L.Q., Cao, X.Z., Wang, P.C., Sun, W.J., Yang, C., & Zhu, J.J. (2013). Tectonic transition and plate reconstructions of the East Asian continental margin. *Marine Geology and Quaternary Geology*, *33*, 65-94.

Li, W., Alves, T.M., Urlaub, M., Georgiopoulou, A., Klaucke, I., Wynn, R.B., Gross, F., Meyer, M., Repschäger, J., Berndt, C., & Krastel, S. (2017). Morphology, age and sediment dynamics of the upper headwall of the Sahara Slide Complex, Northwest Africa: Evidence for a large Late Holocene failure. *Marine Geology*, *393*, 109-123.

Li, W., Krastel, S., Alves, T.M., Urlaub, M., Mehringer, L., Schürer, A., Feldens, P., Gross, F., Stevenson, C.J., & Wynn, R.B. (2018b). The Agadir Slide offshore NW Africa: Morphology, emplacement dynamics, and potential contribution to the Moroccan Turbidite System. *Earth and Planetary Science Letters*, *498*, 436-449.

Li, W.R., Yang, Z.S., Wang, Q., Cao, L.H., Wang, Y.J., & Wang, X.L. (2001). Sedimentation of submarine fan in the Okinawa Trough. *Oceanologia et Limnologia Sinica*, *32(4)*, 371-380.

Li, W.X., & Zhou, X.M. (1999_. Late Mesozoic subduction zone of Southeastern China. *Geological Journal of China Universities*, *5*, 164-169.

Li, X.S., Liu, B.H., Wu, J.L., Zhao, Y.X., & Wang, K.Y. (2004). Seismic reflection facies and deposit systems in the west slope of the Okinawa Trough. *Oceanologia et Limnologia Sinica*, *35(2)*, 120-129.

Li, Z.X., & Li, X.H. (2007). Formation of the 1300-km-wide intracontinental orogen and postorogenic magmatic province in Mesozoic South China: A flat-slab subduction model. *Geology*, *35*, 179-182.

Liu, M., Cui X.J., & Liu F.T. (2004). Cenozoic rifting and volcanism in eastern China: a mantle dynamic link to the Indo–Asian collision? *Tectonophysics*, *393*, 29-42.

Liu, B.H., Li, X.S., Zhao, Y.X., Zheng, Y.P., & Wu, J.L. (2005). Debris transport on the western continental slope of the Okinawa Trough: slumping and gravity flowing. *Oceanologia et Limnologia Sinica*, *36(1)*, 1-9.

Liu, J.P., Kuehl, S.A., Pierce, A.C., Williams, J., Blair, N.E., Harris, C., Aung, D.W., Aye, Y.Y. (2020). Fate of Ayeyarwady and Thanlwin rivers sediments in the Andaman Sea and Bay of Bengal. *Marine Geology*, *423*, 106137.

Liu, J.P., DeMaster, D.J., Nittrouer, C.A., Eidam, E.F., Nguyen, T.T. (2017). A sesmic study of the Mekong subaqueous delta: Proximal versus distal sediment accumulation. *Continental Shelf Research*, *147*, 197-212.

Liu, J.S., Xu, H.Z., Jiang, Y.M., Wang, J., & He, X.J. (2020). Mesozoic and Cenozoic basin structure and tectonic evolution in the East China Sea basin. *Acta Geologica Sinica*, *94(3)*, 675-691.

Liu, Z.C., Liu, B.H., Huang, Z.Z., Zhu, B.D., Fu, M.Z., Yan, J., Zhang, X.H., & Zheng, Y.P. (2005). *Topography of China offshore and adjacent Sea.* Beijing: Ocean Press.

Lo Iacono, C., Sulli, A., & Agate, M. (2014). Submarine canyons of northwestern Sicily (Southern Tyrrhenian Sea): Variability in morphology, sedimentary processes and evolution on a tectonically active margin. *Deep-Sea Research II*, *104*, 93-105.

Lu, Z.Q., Gong, J.M., Wu, B.H., Chen, J.W., & Deng, J. (2003). Geochemical perspective of gas hydrate in the East China Sea. *Marine Geology and Quaternary Geology*, *23(3)*, 77-81.

Luan, X.W., Lu, Y.T., Zhao, K.B., Sun, D.S., & Li, J. (2008). Geological factors for the development and newly advance in exploration of gas hydrate in East China Sea Slope and Okinawa Trough. *Geoscience*, *22(3)*, 342-355.

Luan, X.W., & Qin, Y.S. (2005). Discovery of the gas spring at the seabed of the Miyako segment in the Okinawa Trough. *Chinese Science Bulletin*, *50(8)*, 802-810.

Maslin, M., Owen, M., Day, S. & Long, D. (2004). Linking continental-slope failures and climate change: testing the clathrate gun hypothesis. *Geology*, *32*, 53-56.

Miles, P.R. (1995). Potential distribution of methane hydrate beneath the European continental margin. *Geophysical Research Letters*, *22*, 3179-3182.

Mix, A.C., Bard, E., & Schneider, R. (2001). Environmental processes of the ice age: Land, oceans, glaciers (EPILOG). *Quaternary Science Reviews*, *20*, 627-657.

Muttoni, G., Carcano, C., Garzanti, E., Ghielmi, M., Piccin, A., Pini, R., Rogledi, S., & Sciunnach, D. (2003). Onset of major Pleistocene glaciations in the Alps. *Geology*, *31(11)*, 1574-1578.

Nakajima, T., Kakuwa, Y., Yasudomi, Y., Itaki, T., Motoyama, I., Tomiyama, T., Machiyama, H., Katayama, H., Okitsu, O., Morita, S., Tanahashi, M., & Matsumoto, R. (2014). Formation of pockmarks and submarine canyons associated with dissociation of gas hydrates on the Joetsu Knoll, eastern margin of the Sea of Japan. *Journal of Asian Earth Sciences*, *90*, 228-242.

Nazarian, R.H., Burns, C.M., Legg, S., Buijsman, M.C., Kaur, H., & Arbic, B.K. (2021). On the Magnitude of Canyon-Induced Mixing. *Journal of Geophysical Research: Oceans*, *126*, e2021JC017671. https://doi.org/10.1029/2021JC017671

Noguchi, S., Shimoda, N., Takano, O., Oikawa, N., Inamorim, T., Saeki, T., & Fujii,T. (2011). 3-D internal architecture of methane hydrate-bearing turbidite channels in the Eastern Nankai Trough, Japan. *Marine and Petroleum Geology*, *28*, 1817-1828.

Normandeau, A., Lajeunesse, P., & St-Onge, G. (2015). Submarine canyons and channels in the Lower St.Lawrence Estuary (Eastern Canada): Morphology, classification and recent sediment dynamics. *Geomorphology*, *241*, 1-18.

Orange, D.L., & Breen, N.A. (1992). The effects of fluid escape on accretionary wedges 2: Seepage force, slope failure, headless submarine canyons, and vents. *Journal of Geophysical Research*, *97*, 9277–9295.

Reading, H.G., & Richards, M. (1994). Turbidite systems in deep-water basin margins classified by grain size and feeder system. *AAPG Bulletin*, *78*, 792-822.

Shepard, F.P. (1981). Submarine canyons: Multiple causes and long-time persistence. *AAPG Bulletin*, *65*, 1062-1077.

Song, H.B. (2003). Researches on dynamic evolution of gas hydrate system (I): Its development in geological history. *Progress in Geophysics*, *18(2)*, 188-196.

Shi, Y.F., & Liu, D.S. (1964). Preliminary report of scientific expedition in the region of Mount Shishapangma. *Chinese Science Bulletin*, *10*, 928-938.

Su, M., Sha, Z.B., Kuang, Z.G., Qiao, S.H., Liang, J.Q., Yang, R., Wu, N.Y., & Cong, X.R. (2015). Erosion and sedimentation of the submarine canyons and the relationship with gas hydrate accumulation. *Geoscience*, *29(1)*, 155-162.

Su, M., Zhang, C., Xie, X.N., Wang, Z.F., Jiang, T., He, Y.L, & Zhang, C.M. (2014). Controlling factors on the submarine canyon systems: a case study of the central canyon system in the Qiongdongnan Basin, northern South China Sea. *Science China: Earth Sciences*, *44(8)*, 1807-1820.

Sun, Q.L., Alves T., Xie, X.N., He, J.X., Li, W., & Ni, X.L. (2017). Free gas accumulations in basal shear zones of mass-transport deposits (Pearl River Mouth Basin, South China Sea): An important geohazard on continental slope basins. *Marine and Petroleum Geology*, *81*, 17-32.

Sun, Q.L., Cartwright, J., Xie, X.N., Lu, X.Y., Yuan, S.Q., & Chen, C.X. (2018). Reconstruction of repeated Quaternary slope failures in the northern South China Sea. *Marine Geology*, *401*, 17-35.

Sun, Z.L., Wei, H.L., Zhang, X.H., Shang, L.N., Yin, X.J., Sun, Y.B., Xu, L., Huang, W., Zhang, X.R., 2015. A unique Fe-rich carbonate chimney associated with cold seeps in the Northern Okinawa Trough, East China Sea. *Deep-Sea Research Part I*, *95*, 37-53.

Suzuki, K., Schultheiss, P., Nakatsuka, Y., Ito, T., Egawa, K., Holland, M., & Yamamoto, K. (2015). Physical properties and sedimentological features of hydrate-bearing samples recovered from the first gas hydrate production test site on Daini-Atsumi Knoll around eastern Nankai Trough. *Marine and Petroleum Geology*, *66*, 346-375.

Tubau, X., Paull, C.K., Lastras, G., Caress, D.W., Canals, M., Lundsten, E., Anderson, K., Gwiazda, R., & Amblas, D. (2015). Submarine canyons of Santa Monica Bay, Southern California: Variability in morphology and sedimentary processes. *Marine Geology*, *365*, 61-79.

Voigt, I., Henrich, R., Preu, B.M., Piola, A.R., Hanebuth, T.J.J., Schwenk, T., & Chiessi, C.M., (2013). A submarine canyon as a climate archive-Interaction of the Antarctic Intermediate Water with the Mar del Plata Canyon (Southwest Atlantic). *Marine Geology*, *341*, 46-57.

Walker, J.D., & Geissman, J.W., compilers, (2009). Geologic Time Scale: Geological Society of America, doi: 10.1130/2009.CTS004R2C

Walsh, J.P., Alexander, C.R., Gerber, T., Orpin, A.R., & Sumners, B.W. (2007). Demise of a submarine canyon? Evidence for highstand infilling on the Waipaoa River continental margin, New Zealand. *Geophysical Research Letters*, *34*, L20606. doi:10.1029/2007GL031142, 2007

Wang, D.W., Wu, S.G., Yao, G.S., & Wang, W.W., (2015a). Architecture and evolution of deep-water cyclic deposits in the Qiongdongnan Basin, South China Sea: Relationship with the Pleistocene climate events. *Marine Geology*, *370*, 43-54.

Wang, M., Cai, F., Li, Q., Liang, J., Yan, H.J., Dong, G., Wang, F., Shao, H.B., & Hu, G.W. (2015b). Characteristics of authigenic pyrite and its sulfur isotopes influenced by methane seep at core A, site 79 of the middle Okinawa Trough. *Science China: Earth Sciences*, *45(12)*, 1819-1828.

Wang, M., Li, Q., Cai, F., Liang, J., Yan, G.J., Wang, Z., Sun, Y.B., Luo, D., Dong, G., & Cao, Y.M. (2019). Formation of authigenic carbonates at a methane seep site in the middle Okinawa Trough, East China Sea. *Journal of Asian Earth Sciences*, *185*, 104028.

Wang, Y.M., Xu, Q., Li, D., Han, J.H., Lv, M., Wang, Y.F., Li, W.G., & Wang, H.R. (2011). Late Miocene Red River submarine fan, northwestern South China Sea. *Chinese Science Bulletin*, *56(10)*, 781-787.

Webster, J.M., Beaman, R.J., Bernabéu, Á. P., Ludman, D., Renema, W., Wust, R.A.J., George, N.P.J., Reimer, P.J., Jacobsen, G.E., & Moss, P. (2012). Late Pleistocene history of turbidite sedimentation in a submarine canyon off the northern Great Barrier Reef, Australia. *Palaeogeography*, *Palaeoclimatology*, *Palaeoecology*, *331-332*, 75-89.

Wu, F.D., Li, S.T., Lu, Y.C., Li, P.L., Zhou, P., & Zhao, J.H. (1998a). The Tertiary sea-level changes in the East China Sea Shelf Basin. *Scientia Geologica Sinica*, *33(2)*, 214-221.

Wu, F.D., Lu, Y.C., Li, S.T., Xie, X.n., Li, P.L., Zhou, P., & Zhao, J.H. (1998b). Tertiary sequence stratigraphic framework and sea-level changes in the East China Sea Shelf Basin. *Earth Science-Journal of China University of Geosciences*, *23(1)*, 13-20.

Wu, S.G., & Qin, Y.S. (2009). The research of deepwater depositional system in the northern South China Sea. *Acta Sedimentologica Sinica*, *27(5)*, 922-930.

Wu, S.G., Dong, D.D., Yang, S.X., Zhang, G.X., Wang, Z.J., Li, Q.P., Liang, J.Q., Gong, Y.H., & Sun, Y.B. (2009). Genetic model of the hydrate system in the fine grain sediments in the northern continental slope of South China Sea. *Chinese Journal of Geophysics*, *52(7)*, 1849-1857.

Wu, S.G., Qin, Z.L., Wang, D.W., Peng, X.C., Wang, Z.J., & Yao, G.S. (2011). Seismic characteristics and triggering mechanism analysis of mass transport deposits in the northern slope of the South China Sea. *Chinese Journal of Geophysics*, *54(12)*, 3181-3195.

Wu, S.G., & Sakamoto. (2001). Sedimentation and development of the Qianzhou Deep Sea Canyon in Philippines Sea. *Chinese Science Bulletin*, *46(supplement)*, 84-88.

Wu, Z.Y., Li, J.B., Jin, X.L., Shang, J.H., Li, S.J., & Jin, X.B. (2014). Distribution, features, and influence of the submarine topographic boundaries of the Okinawa Trough. *Science China: Earth Sciences*, *44(7)*, 1477-1487.

Xiang, R., Li, T.G., Yang, Z.S., Li, A.C., Jiang, F.Q., Yan, J., & Cao, Q.Y. (2003). Geological records of marine environmental changes in the southern Okinawa Trough. *Chinese Science Bulletin*, *48(1)*, 78-82.

Xie, H., Zhou, D., Li, Y.P., Pang, X., Li, P.C., Chen, G.H., Li, F.C., & Cao, J.H. (2014). Cenozoic tectonic subsidence in deepwater sags in the Pearl River Mouth Basin, northern South China Sea. *Tectonophysics*, *615-616*, 182-198.

Xie, X.N., Chen, Z.H., Sun, Z.P., Jiang, T., & He, Y.L. (2012). Depositional architecture characteristics of deepwater depositional systems on the continental margins of northwestern South China Sea. *Earth Science-Journal of China Univeristy of Geosciences*, *37(4)*, 627-634.

Xie, X.N., Müller, R.D., Ren, J.Y., Jiang, T., & Zhang, C. (2008). Stratigraphic architecture and evolution of the continental slope system in offshore Hainan, northern South China Sea. *Marine Geology*, *247*, 129-144.

Xu, C.L., Wu, N.Y., Sun, Z.L., Zhang, X.R., Geng, W., Cao, H., Wang, L.B., Zhang, X.L., & Xu, G.Q. (2018). Methane seepage inferred from pore water geochemistry in shallow sediments in the western slope of the Mid-Okinawa Trough. *Marine and Petroleum Geology*, *98*, 306-315.

Xu, C.L., Wu, N.Y., Sun, Z.L., Zhang, X.R., Geng, W., Cao, H., Wang, L.B., Zhang, X.L., & Zhai, B. (2020). Assessing methane cycling in the seep sediments of the mid-Okinawa Trough: insights from pore-water geochemistry and numerical modeling. *Ore Geology Reviews*, *129*, 103909.

Xu, H., Cai, Y., Sun, H.Q., Yan, G.J., Wei, K., Zhao, X.W., Zhu, Y.R., Shi, J., Dong, G., & Li, Q. (2012). The survey status and geological conditions of accumulation of gas hydrate resource in the East China Sea. *Journal of Tropical Oceanography*, *32(4)*, 22-29.

Xu, J.P. (2013). Accomplishments and challenges in measuring turbidity currents in submarine canyons. *Advances in Earth Science*, *28(5)*, 552-558.

Xu, J.P., & Noble, M.A. (2009). Currents in Monterey Submarine Canyon. *Journal of Geophysical Research*, *114*, C03004. doi:10.1029/2008JC004992

Xu, N., Wu, S.G., Shi, B.Q., Lu, B., Xue, L.Q., Wang, X.J., & Jia, Y. (2009). Gas hydrate associated with mud diapirs in southern Okinawa Trough. *Marine and Petroleum Geology*, *26*, 1413-1418.

Xu, S., Wang, Y.M., Peng, X.C., Zhou, H.Y., Qiu, Y., Gong, C.L., & Zuo H.T. (2014). Origin of Taiwan Canyon and its effects on deepwater sediment. *Science China: Earth Sciences*, *44(9)*, 1913-1924.

Yang, R.C., & Van Loon, A.J. (2016). Early Cretaceous slumps and turbidites with peculiar soft-sedimentart deformation structures on Lingshan Island (Qingdao, China) indicating a tensional tectonic regime. *Journal of Asian Earth Sciences*, *129*, 206-219.

Yang, W.D., Zeng, J.L., & Wang, Z.Y. (2004). Prospect of gas hydrate resources in the continental slope of the East China Sea. *Offshore Oil*, *24(2)*, 1-8.

Yin, S.R., Wang, L.L., Guo, Y.Q., & Zhong, G.F. (2015). Morphology, sedimentary characteristics, and origin of the Dongsha submarine canyon in the northeastern continental slope of the South China Sea. *Science China: Earth Sciences*, *45(3)*, 275-289.

Yu, H.S., & Hong, E. (2006). Shifting submarine canyons and development of a foreland basin in SW Taiwan: Controls of foreland sedimentation and longitudinal sediment transport. *Journal of Asian Earth Sciences*, *27*, 922-932.

Zhang, B.X., Xu, Q.Q., & Shen, Y.P. (2002). The relationship between climate change and Quaternary glacial cycles on the Qinghai-Tibetan Plateau: review and speculation. *Quaternary International*, *97-98*, 93-101.

Zhang, G.H., & Zhang, J.P. (2015). A discussion on the tectonic inversion and its genetic mechanism in the East China Sea Shelf Basin. *Earth Science Frontiers*, *22(1)*, 260-270.

Zhang, J.P., Zhang, T., & Tang, X.J. (2014). Basin type and dynamic environment in the East China Sea Shelf Basin. *Acta Geologica Sinica*, *88(11)*, 2033-2042.

Zhang, X.H., & Shang, L.N. (2014). Study on crustal structure and nature of the Okinawa Trough. *Periodical of Ocean University of China*, *44(6)*, 72-80.

Zhang, X.R., Sun, Z.L., Wang, L.B., Zhang, X.L., Zhai, B., Xu, C.L., Geng, W., Cao, H., Yin, X.J., & Wu, N.Y. (2020). Distribution and discharge of dissolved methane in the middle Okinawa Trough, East China Sea. *Frontiers in Earth Science*, *8*, 333.

Zhao, H.Q., Wu, S.G., Xu, N., Wang, X.J., & Zhang, G.X. (2006). The elementary research of gas hydrate associated with mud diapir structure in the East China Sea. *Geoscience*, *20(1)*, 115-122.

Zhao, Y.X., Liu, B.H., Li, X.S., Cui, A.J., Han, G.Z., Hua, Q.F., & Hu, G.H. (2011). Sedimentary characters and material transportation of submarine canyon-fan systems in slope of the East China Sea. *Journal of Palaeogeography, 13(1)*, 119-126.

Zhao, Y.X., Liu, B.H., Li, X.S., Liu, C.G., Pei, Y.L., Wu, J.L., & Zheng, Y.P. (2009). Distributions of different submarine canyon on the East China Sea Slope and their tectonic response. *Advances in Marine Science*, *27(4)*, 460-468.

Zhong, S.L., Jiang, L., Li, B.H., & Wang, J.P. (2006). *Paleogene high-resolution biostratigraphy and sequence stratigraphy of the Taibei Depression in the East China Sea Shelf.* Beijing: Petroleum Industry Press.

Figure 1. Geographic location of the study area and the distribution of seismic reflection lines and well and heat flow stations. Seafloor temperature and heat flow data are from the global heal flow database (http://www.ihfc-iugg.org/products/global-heat-flow-database/data) published by the International Heal Flow Commission. Location of methane seeping points is derived from Wang et al. (2015b) and Li et al. (2015). Location of bottom simulating reflectors (BSRs) is derived from Luan et al. (2008). Location of mud diapirs associated with hydrates is derived from Xu et al. (2009). Location of submarine gas seepage is from Luan & Qi (2005). Location of methane seepages are from Sun et al. (2015), Li et al. (2015), Wang et al. (2015, 2019), Li et al. (2018a), Xu et al. (2018, 2020), Guan et al. (2019), Zhang et al. (2020), Cao et al. (2020), and Li et al. (2021b)

Figure 2. Cenozoic stratigraphic sequence in the East China Sea (Wu et al., 1998a, 1998b; Zhong et al., 2006; Xie et al., 2014; Zhang et al., 2014; Zhang & Zhang, 2015; Liu et al., 2020) and its sequence boundary age. The magnetostratigraphic data is derived from the 2009 Geologic Time Scale (Walker & Geissman, 2009). The global sea level curve and biostratigraphic data are modified from Haq et al. (1987), where the sequence boundary and biostratigraphic zone age are revised using the International Chronostratigraphic Chart (v2017/02; Cohen et al., 2013) and the 2009 Geologic Time Scale (Walker & Geissman, 2009).

Figure 3. Cenozoic stratigraphic sequence framework in the East China Sea established by reflection seismic line

Figure 4. Chronostratigraphic framework, stratigraphic structure, and surface identification marks of lines L1 (a) and L2 (b) on the central and southern slope of the Okinawa Trough (see Figure 1 for seismic line location). (c) and (d) provide zoomed images of the regressive unconformity and backstepped onlap formed by sea-level fall at the Last Glacial Maximum (LGM). The gap structures and chaotic, twisty, or imbricated reflections in (d) also indicate the leakage of methane-bearing fluid. LST: Lowstand systems tract; TST: Transgressive systems tract; HST: Highstand systems tract; and FSST: Falling stage systems tract.

Figure 5. Morphological structure, growth time, and erosional–depositional characteristics of submarine canyons in the central and southern slopes of the Okinawa Trough (see Figure 1. for seismic line location and Figure 4. for legend). MTD Mass transport deposit; BSRs Bottom simulating reflections.

Figure 6. Topographic slope map of Okinawa Trough and its adjacent area based on the digital elevation model (https://www.bodc.ac.uk/data//hosted_data_systems/gebco_gridded_bathymetry_data/) and submarine canyons identification.

Figure 7. Submarine topographic map (a; modified from Wu et al., 2014) and multi-beam geomorphologic map (b; modified from Li, 2008) of submarine canyons C5 and C6 in the Okinawa Trough continental slope (see Figure 1 for location). (c) and (d) are thalweg and transverse topographic profiles based on digital elevation model (DEM) of submarine canyon C6, respectively. (e) and (f) are thalweg and transverse topographic profiles based on digital elevation model (DEM) of submarine canyons C5, respectively.

Figure 8. Seismic reflection characteristics of Bottom Simulating Reflectors (BSRs) and methane leakage on variable density and variable area profiles (see Figure 5 and Figure 1 for seismic line location).

Figure 9. Coupling evolution model of submarine canyon and gas hydrate in Okinawa Trough slope. BGHSZ: bottom of gas hydrate stability zone. (a) During the interglacial period in the Quaternary, the sea level was at a high-water stage. Under suitable temperature and pressure in the continental slope of the Okinawa Trough, the thermogenic or biogenic methane combined with water molecules to form hydrates. Of course, methane can also be leaked to the seabed through a fault. (b) Entering the glacial epoch, the sea level fell rapidly. With the change of seafloor temperature and pressure due to the sea level fall, the original hydrates decomposed and released extensive methane. Due to the rapid accumulation of methane-bearing fluid under the seabed, the sediments on the slope lost stability and slumped to form the prototype of the submarine canyons. (c) As the continuously sea level fall, under the influence of scour and retrogressive erosion of gravity flow that partly associated with hydrate decomposition, the submarine canyons strongly downcut the slope to form V-shaped or U-shaped channels. The gas hydrate stability zone also migrated to the deep. (d) During the low sea level stage, although the gas hydrate stability zone remained relatively stable, the canyon sidewalls continued to slump due to the erosion of turbidity current and the methane continuously leaked. The submarine canyons can even be connected to the channels formed by syndepositional faults or the ancient incised valleys to form a new canyon system.